MOLECULAR MECHANISMS GOVERNING DEVELOPMENT OF THE HYPOTHALAMUS

By

Elizabeth A. Newman

A dissertation submitted to Johns Hopkins University in conformity with the requirements for the degree of Doctor of Philosophy.

Baltimore, Maryland

August, 2017

ABSTRACT

The hypothalamus is a small, but anatomically and functionally complex, region of the brain. Due in part to its anatomical complexity, its development is not well understood. Here, we have explored its development by studying two different patterning mechanisms: intrinsic factors, in the form of the transcription factor Foxd1, and extrinsic factors, via the canonical Wnt signaling pathway. *Foxd1* is expressed broadly throughout the hypothalamus and prethalamus early in development, but its function was unknown. We generated *Foxd1*$^{-/-}$ mice and used a panel of *in situ* hybridization markers to study their development. These mice have a very selective defect in the anterior hypothalamus, specifically the suprachiasmatic

nucleus, periventricular nucleus and paraventricular nucleus. RNA-Seq analysis suggests that *Foxd1* may be controlling anterior hypothalamic development through regulation of the transcription factors *Six3* and *Vax1*. We also studied the role of canonical Wnt signaling in the patterning of the hypothalamus and prethalamus by manipulating its effector protein, β-catenin by using *Foxd1-Cre*, which is expressed in both the hypothalamus and prethalamus. Loss of β-catenin resulted in an anteriorization of the hypothalamus. Posterior structures were lost or reduced, and anterior structures were expanded. We also generated a mouse with constitutively active β-catenin through excision of its autoinhibitory domain. *In situ* hybridization analysis of these mice revealed a complex phenotype where there was a general loss of most, but not all, markers of regional and nuclear identity. However, the posterior hypothalamus was not only preserved, but potentially expanded. In neither the loss- or gain-of-function mice was the patterning of the prethalamus affected. However, in the gain-of-function mice, the prethalamus was only partially differentiated. We next manipulated the Shh signaling pathway by generating a constitutively active form of its effector protein, Smo, which had no effect on patterning in the hypothalamus or prethalamus. However, by crossing the constitutively active Smo mice to our constitutively active β-catenin mice, we were able to rescue the defects observed in the constitutively active β-catenin single mutant mice. Thus, we have revealed an important interaction between two major signaling pathways in the development of the hypothalamus. We have identified multiple novel mechanisms controlling

development of the hypothalamus, although further research will need to be done to determine the exact methods by which they are directing patterning and differentiation.

Readers: Seth Blackshaw and Jeremy Nathans

Thesis Committee: Shan Sockanathan, Angelika Doetzlhofer, Jeremy Nathans

ACKNOWLEDGEMENTS

I first would like to thank everyone who helped with the technical aspects of my thesis, especially Dan Wu (in the laboratory of Jiangyang Zhang), for performing the MRI experiments, Jonathan Augustin for his assistance with the GO analysis, and Jie Wang and Jun Wan (in the laboratory of Jiang Qian) for performing the differential RNA-seq analysis. I would also like to thank the members of my lab who have assisted me over the years, especially our amazing technicians, Hong and Lizhi, and my rotation mentor, Joe.

Thanks to my PI, Seth, for being an incredibly supportive mentor over the past 7 years. He's allowed me the space to grow both personally and professionally as a scientist, and has been very understanding about the importance of work-life balance. Thanks as well to all the

members of the Blackshaw lab, past and present, for creating such a fun and supportive work environment, especially Thuzar, Brian, Dan, Sooyeon, Kai, and Thomas.

I would like to thank my parents and my best friend, Jonathan, for their love and encouragement over the many years it has taken me to finish my PhD. I could not have weathered grad school without having their guidance and support to keep me going during all the low times.

Thanks to my incredible fiancé Scott for being such a patient and understanding "grad school widower" over the past couple of years. Thank you for taking care of me during all those late nights, picking up the slack at home and bringing me endless cups of tea.

Lastly, I would like to dedicate this thesis in memory of my beloved grandfather, Dr. Mario Stefanini. I had always hoped that he could be alive to see me complete my PhD, but the desire to make him proud has fueled me to finish even in his absence. He fostered my love of science at an early age, and I would not be here today without him.

ABBREVIATIONS

AH: anterior hypothalamus
AP: anterior-posterior
ArcN: arcuate nucleus
BP: basal plate
dlAH: dorsolateral anterior hypothalamus
DMH: dorsomedial hypothalamus
DTJ: diencephalic-telencephalic junction
DV: dorso-ventral
E[x]: embryonic date [x] in mouse
HH: Hamburger-Hamilton developmental stage in chick
ID: intrahypothalamic diagonal
LH: lateral hypothalamus
MM: medial mammillary
p[x]: prosomere x
PCP: prechordal plate
PeVN: periventricular nucleus
PH=posterior hypothalamus
PMN: premammillary nucleus

POA: preoptic area
PrTH: prethalamus
PVN: paraventricular nucleus
SON: supraoptic nucleus
SCN: suprachiasmatic nucleus
SMM: supramammillary nucleus
TH: tuberal hypothalamus
TT: tuberomammillary terminal
vAH: ventral anterior hypothalamus
VMH: ventromedial hypothalamus
ZI: zona incerta
ZLI: zona limitans intrathalamica

CONTENTS

TABLE OF FIGURES

TABLE OF TABLES

1. INTRODUCTION[1]

The hypothalamus controls a wide range of homeostatic processes essential for life, including feeding, thirst, sleep, circadian rhythms, reproductive behavior, and more. This brain region, derived from the rostral diencephalon of the forebrain, is enormously anatomically complex. Where other brain regions like the cortex or hippocampus have a clear overall structure of columns and parallel feed-forward loops, respectively, the hypothalamus has a densely interconnected patchwork of often quite ill-defined nuclei. Partially for this reason, the study of hypothalamic development has lagged behind that of many other brain regions, whose simpler

[1] A modified version of this introduction was previously published (Bedont, Newman, Blackshaw, 2015)

anatomy facilitated the identification of factors that pattern them. However, as determinants of hypothalamic identity were studied in recent years, it has become increasingly clear that many of the same factors implicated in development of the cortex, retina and other CNS regions play similar roles in the hypothalamus.

Shortly after the neural plate forms following gastrulation, diffusible morphogens begin patterning the developing nervous system, including the hypothalamus. In the beginning, these factors are generated outside of neural tissues, in mesodermal domains including the axial notochord and more anterior prechordal plate (PCP), as well as other more lateral tissues. Often, production of these same cues is later induced in neural tissue near or within the nascent hypothalamus, where dynamically shifting sources of morphogen production create ever-finer concentration gradients within the region. Sharp boundaries are translated from these gradients through induction of distinct and often mutually repressive sets of cell-autonomous transcription factors, progressively defining the fate of neural progenitors and emerging hypothalamic nuclei (Wilson and Houart, 2004; Hoch et al., 2009).

1.1 HYPOTHALAMIC INDUCTION AND SPATIAL PATTERNING

1.1.1 Wingless Family (Wnt) Signaling

The Wnts are a large family of secreted, lipid-modified glycoproteins long known to be involved in patterning during development, having originally been implicated in developmental segmentation by their homology to the Drosophila *Wingless* gene. Anterior-posterior (AP) patterning of newly induced neural plate is initiated by the posteriorizing morphogen Wnt8, secreted by lateral mesodermal precursors. Its effect is enhanced and sustained by nodal signaling in the posterior neural plate. Conversely, Wnt inhibition is necessary for anterior patterning, including the region that eventually gives rise to the hypothalamus. A variety of Wnt inhibitors are expressed in spatially and temporally dynamic patterns, first in the PCP (Figure 1) and later in the developing anterior brain. These inhibitors include sFRP1, sFRP2, sFRP3/Frzb1, Crescent/Frzb2, Dickkopf1 and Cerberus (Chapman et al., 2004; Erter et al., 2001).

After initial AP patterning, Wnt signaling in turn subdivides the forebrain. The domain receiving lower Wnt signaling gives rise to the telencephalon, which includes the cerebral cortex, hippocampus, striatum, amygdala and associated structures. Higher Wnt signaling induces development of the diencephalon, including a more rostral domain that gives rise to the hypothalamus and prethalamus, and a more caudal domain that gives rise to the thalamus (Chatterjee and Li, 2012). Telencephalic and rostral diencephalic neuroepithelium are hereafter distinguished by expression of the forkhead domain transcription factors FOXG1 and FOXD1, respectively (Hatini et al., 1994; Shimogori et al., 2010).

However, despite relatively high Wnt signaling in the diencephalon early on, inhibition of canonical Wnt signaling by Axin1 is essential for initial hypothalamic specification. In *Axin1*$^{-/-}$ mice, the ventral midline cells of the hypothalamus fail to develop, instead assuming a caudal floor plate identity (Kapsimali et al., 2004). Later roles of Wnts in hypothalamic development explain this seeming paradox. During the late gastrula stage in zebrafish, Wnt8b and Wnt1 secreted from the midbrain-hindbrain boundary pattern the forebrain and induce specification of posterior diencephalon, including the sensory thalamus and habenula. Overexpression of these Wnts or their receptors, or loss of the Wnt inhibitor *Axin1*, induce expanded expression of posterior hypothalamic markers such as *Emx2* at the expense of anterotuberal hypothalamic markers such as *Rx3*, suggesting a posteriorization of hypothalamic neuroepithelium (Kapsimali et al., 2004; Kim et al., 2002).

Consistent with this finding, *Wnt8b* is expressed in the mouse posterior hypothalamus beginning at ~E8.5 (Shimogori et al., 2010; Garda et al., 2002), consistent with a role in patterning, but its function has not been directly explored in this context (Figure 2E). By E12.5, *Wnt8b* becomes restricted to the mammillary region, suggesting it may act to impart posterior hypothalamic identity in mammals as it does in zebrafish (Shimogori et al., 2010) (Figure 2F). WNT7a/7b become expressed selectively in prethalamic and hypothalamic GABAergic neuronal progenitors around the same time, suggesting a role in interneuron development, but

their function is even less well characterized than WNT8b (Shimogori et al., 2010) (Figure 2F).

Meanwhile, a gradient of WNT3 signaling further patterns the developing forebrain, including the hypothalamus (Figure 2F). High levels of WNT3 induce *Irx3* expression in the sensory thalamus, while low WNT3 signaling is permissive for more anterior *Six3* expression in the hypothalamus and prethalamus (Braun et al., 2003). Mutual cross-repression of SIX3 and IRX3 demarcates the border between these regions, an effect that is reinforced by SIX3-mediated dampening of WNT responsiveness. Confirming the importance of these interactions, *Six3*$^{-/-}$ mice show a rostral expansion of caudal diencephalic markers at the expense of the hypothalamus and telencephalon, largely due to an anterior expansion of WNT1 expression in the roof plate of the forebrain (Wilson and Houart, 2004; Lagutin et al., 2003).

1.1.2 Sonic Hedgehog (SHH) Signaling

Concurrent with Wnts' central role in early AP patterning of the developing neural tube, the lipid-linked polypeptide signal SHH is a key secreted morphogen controlling neural dorso-ventral (DV) patterning. SHH is first expressed in the PCP (Figure 1), and is necessary for initial induction of the hypothalamus (Chiang et al., 1996; Mathieu et al., 2002). The ventral midline cells initially have a quasi-caudal floor plate identity,

including expression of HNF3β but not the floor plate markers FP3 and FP4 (Dale et al, 1997) (Figure 1). PCP-derived SHH goes on to induce transient *Shh* expression in the ventral diencephalic midline (and much of the rest of the developing hypothalamus) through a GLI-mediated signaling cascade that activates expression of transcription factors including SIX3, SOX2, and SOX3 (Braun et al., 2003; Zhao et al., 2012). SOX2 and SOX3, members of the SOXB1 transcription factor family, directly activate and maintain *Shh* transcription in hypothalamic neuroepithelium (Zhao et al., 2012). SIX3 likewise targets the *Shh brain enhancer-2* to directly activate *Shh* transcription there (Geng et al., 2008; Jeong et al., 2008).

A subsequent down-regulation of *Shh* expression is important for hypothalamic patterning. Indeed, early patterning of the ventral hypothalamus along the AP axis is achieved in part through down-regulation of *Shh* expression in ventral tuberomammillary hypothalamus (Mathieu et al., 2002; Ohyama et al., 2008; Manning et al., 2006) (Figure 2B). For instance, studies in chick demonstrate cells giving rise to this region must down-regulate *Shh* to adopt their proper fate through induction of Tbx2 expression, which in turn triggers Shh downregulation by upregulation of Bmp7 in the tuberomammillary hypothalamic neuroepithelium (see next section).

In contrast to the ventral tuberomammillary hypothalamus, *Shh* expression in the basal plate, which is initially induced by PCP Shh and additional feed-forward Shh signaling from the ventral midline, is maintained through E14.5 (Zeltser 2005; Vieira and Martinez, 2006) (Figure 2B-D). This more dorsally located hypothalamic region

begins immediately posterior and ventral to the presumptive suprachiasmatic nucleus (SCN) and terminates in the mammillary region (Shimogori et al., 2010; Alvarez-Bolado et al., 2012) (Figure 2B-D). *Shh*-positive cells of the basal plate originate at the diencephalic/mesencephalic border, then migrate to their final destination in the hypothalamus (Manning et al., 2006). Basal plate SHH plays a critical role in hypothalamic patterning. Several studies have looked at loss of function mutants in which *Shh* is deleted from the basal plate. In these studies, the hypothalamus is still specified, but neurons fail to undergo further differentiation, resulting in the loss or reduction of several nuclear markers. In all mutant lines examined, both AP and DV patterning is disrupted, although the reported phenotypes are not identical among these studies, most likely because they used *Cre*-drivers with different spatial and temporal patterns of activity (Shimogori et al., 2010; Zhao et al., 2012; Szabo et al., 2009; Blackshaw et al., 2010).

Basal plate Shh is also necessary to initiate sustained Shh expression in the zona limitans incerta (ZLI), a secondary *Shh*-positive organizer dividing the prethalamus and thalamus (Beccari et al., 2013; Scholpp et al., 2006). ZLI-derived Shh plays a central role in patterning the sensory thalamus, and is required for proliferation and differentiation of prethalamic progenitors (Zeltser, 2005; Vieira and Martinez, 2006; Vieira et al., 2010) (Figure 2B-D). Importantly, ZLI *Shh* expression is preserved in Cre/lox studies where *Shh* was deleted in the basal plate, showing that the hypothalamic patterning roles of basal plate- and ZLI-derived Shh are distinct.

1.1.3 Bone-Morphogenetic Protein (Bmp) Signaling

BMP7 is the primary member of this family of TGF-beta superfamily members that has been studied in the context of hypothalamic development. Surprisingly given the classical physical separation and antagonistic effects of BMPs and SHH in spinal DV patterning, many known actions of BMP7 in the hypothalamus revolve around cooperative interactions with SHH. For instance, during gastrulation, PCP-derived BMP7 and SHH cooperate to induce expression of early general hypothalamic markers such as *Nkx2.1* in the ventral diencephalic midline, distinct from more caudal midline gene expression induced by notochord-derived SHH alone (Figure 1) (Dale et al., 1997).

During later stages of hypothalamic patterning, both *Bmp7* and *Shh* are transiently coexpressed in ventral tuberomammillary hypothalamus (Manning et al., 2006) (Figure 1). BMP7 swiftly down-regulates *Shh* expression here by activating expression of first *Tbx2* and subsequently *Gli3*, although it's unclear if TBX2 directly activates *Gli3* expression (Ohyama et al., 2008; Manning et al., 2006). In chick this process begins around Hamburger and Hamilton (HH) stage 10, inducing complete elimination of *Shh* by HH stage 16 (roughly equivalent to E9.5-10.5 in mouse) (Alvarez-Bolado et al., 2012). *Tbx2* itself is in turn down-regulated during stages 16-22; toward the end of this period, ventral tuberomammillary markers such as *Fgf10*

and *Emx2* begin to be expressed in these now *Shh*-negative subdomains of the developing hypothalamus.

BMP7 signaling is also required for induction of *Pax7* expression in more dorsally located tuberomammillary progenitors, which occurs by HH stage 30. BMP7 accomplishes this by both down-regulating *Shh* expression in ventral tuberomammillary hypothalamus, and by directly activating *Pax7* transcription via induction of Smad5 phosphorylation (Ohyama et al., 2008). Interestingly, widespread expression of the Bmp antagonist *Chrdl1* is detected in chick hypothalamus at HH stage 13, with expression restricted to the anterioventral hypothalamic neuroepithelium by HH15 as Bmp expression becomes restricted to posterioventral hypothalamus. *Chrdl1* expression is upregulated in response to inhibition of Notch signaling, suggesting that Notch may play a role in early hypothalamic development by modulating BMP signaling (Ratié et al., 2013), although this has not yet been shown directly.

1.1.4 Nodal Signaling

Nodal proteins are other members of the TGF beta superfamily that play an important role in hypothalamic patterning. PCP-derived Nodal signaling, most notably by cyclops, plays an essential role in initial hypothalamic specification in zebrafish

(Machluf et al., 2011) (Figure 1). Together with Shh and Bmp7, nodal signaling is essential for induction of early hypothalamic markers such as *Nkx2.1*; however, unlike in the telencephalon, Shh is not able to restore initial expression of the *Nkx2.1* homolog in zebrafish diencephalon in the absence of nodal, suggesting a separable role for nodal in early hypothalamic induction (Rohr et al., 2001).

On the other hand, cells defective in both Nodal and Shh signaling are unable to give rise to hypothalamic cells following transplantation into wildtype zebrafish, and Shh can restore some *nkx2.1* expression in the zebrafish ventral posterior hypothalamus (vPH) during early stages of hypothalamic development (Mathieu et al., 2002; Rohr et al., 2001). Together, these data suggest a cooperative role for Nodal and Shh in later stages of hypothalamic development, with Nodal enhancing the ability of cells to respond to Shh.

There also appears to be cross-talk between Nodals and Wnts in hypothalamic development, as the Wnt inhibitor Axin1 facilitates Nodal signaling (Kapsimali et al., 2004). Axin1 may thus alter the competence of hypothalamic progenitors to respond to both Nodal and indirectly, to Shh signaling, likely explaining the non-cell-autonomous requirement for Nodal signaling in patterning of the dorsal anterior hypothalamus (dAH) by Shh (Mathieu et al., 2002). Conversely, cells of the zebrafish vPH require Nodal signaling cell-autonomously in order to activate *emx2* expression, while excessive Shh signaling inhibits *emx2* expression. Thus, Nodal must cooperate with Bmp7 to induce *emx2* in vPH—while Nodal acts as a cell-autonomous factor

conferring competence to activate *emx2* expression, Bmp7 inhibits local *shh* to prevent Shh signaling from becoming excessive. Thus, Axin1 sits at the nexus of Wnt, Shh, Nodal, and Bmp signaling, from which it serves as a critical, integrative determinant of anterior-posterior identity.

1.1.5 Fibroblast Growth Factor (FGF) Signaling

FGF family members do not appear to play a critical role in early stages of hypothalamic patterning. Irx3 is required for competence to respond to Fgf8 signaling, but is excluded from the hypothalamus during this time by its cross-repressive interaction with Six3. The ZLI lies between the *Six3*-positive rostral diencephalon and *Irx3*-positive caudal diencephalon, demarcating the boundary of competence to Fgf8 signaling from the isthmic organizer and telencephalic roof plate (Kobayashi et al., 2002). That said, FGF family members do regulate cell proliferation at later stages of hypothalamic development.

1.2 HYPOTHALAMIC NEUROGENESIS AND LATE PATTERNING

Hypothalamic neurogenesis occurs from ~E10.5-16.5 in mice, with the great majority of hypothalamic neurons being generated between E12.5 and E14.5 (Ratié et al., 2013; Byerly and Blackshaw, 2009; Shimada and Nakamura, 1973). Birthdating studies using tritiated thymidine and BrdU indicated that neurons in lateral hypothalamic nuclei are typically born before medial nuclei, resulting in an "outside-in" pattern of birth in the hypothalamus (Shimada and Nakamura, 1973). However, later research has contradicted this model. Looking at different parvocellular neuronal cell types within the neurosecretory dorsolateral anterior hypothalamus (dlAH), all were found to be born during the same approximate interval, despite occupying different medial-lateral locations within the hypothalamus (Markakis and Swanson, 1997). Similar results have been reported for different neuronal subtypes in the arcuate nucleus (ARC) (Padilla et al., 2010), suggesting that for progenitors in at least some regions of the hypothalamus, this "outside-in" order of cell generation may not hold.

Growth and differentiation factors that pattern the developing hypothalamus also play important roles in later stages of hypothalamic cell fate specification. For example, while SHH is required for both early and late neurogenesis in much of the hypothalamus (Shimogori et al., 2010; Ishibashi and McMahon, 2002), *Shh* down-regulation is necessary for proliferation and expansion of the ventral tuberomammillary progenitor pool (Manning et al, 2006). Meanwhile, canonical Wnt signaling, through its effector Lef1, plays an important role in both progenitor maintenance and in driving progenitor differentiation in the posterior hypothalamus

(Lee et al., 2006; Wang et al., 2009). Notch signaling is also involved in progenitor maintenance in the hypothalamus, as it is elsewhere in the developing nervous system, but the specifics of its role in different parts of the hypothalamus has only recently begun to be understood (Ratié et al., 2013; Aujla et al., 2013). In the rostral hypothalamus, Notch signaling works through lateral inhibition to regulate the progenitor population and generate new neurons. High levels of Notch signaling in AH upregulate Hes and Hey family genes, while downregulating proneural genes such as *Ascl1* and *Nhlh1*. The genes *Tagln3*, *Chga*, *Robo2*, *Slit1*, and *Chrdl1* are then needed for terminal neural differentiation once precursor cells have exited mitosis.

Expression of a diverse assortment of transcription factors are induced by the intricate spatiotemporal code of exposure to morphogens discussed previously, which in turn confer intrinsic spatial identity upon hypothalamic progenitor cells. Patterning processes establish the anatomical DV and AP axes within the hypothalamus, limiting which nuclei can develop at any given set of coordinates. Consequently, many markers ubiquitously expressed in early hypothalamic progenitors become more restricted once neurogenesis begins. For instance, *Six3* and *Lhx2* are expressed in the anterior and tuberal hypothalamus (AH and TH), but not the PH. Meanwhile, *Rax* and *Nkx2.1* are expressed in the TH and PH, but only in limited regions of the AH (http://www.brain-map.org).

However, these still relatively broad domains of transcription factor expression become even more regionalized as neurogenesis progresses. Continuing with the

previous examples, *Lhx2* becomes restricted to the dorsolateral aspects of AH (dlAH) while *Six3* becomes restricted to the ventral AH (vAH). Meanwhile, *Rax* expression is rapidly downregulated everywhere except the ventral TH, though *Nkx2.1* remains comparatively broadly expressed in the TH and PH (Shimogori et al., 2010; http://www.brain-map.org; Lu et al., 2013; Roy et al., 2013; VanDunk et al., 2011). By mouse E12.5, progressive restriction of expression of these and assorted other genes has already defined many nuclei found in the adult hypothalamus (Figure 3).

Developmental expression of over a thousand such mouse genes were documented in an extensive screen published by Shimogori et al. in 2010. Among other findings, this study identified the intrahypothalamic diagonal/tuberomammillary terminal (ID/TT) complex, an excellent example of progressive regionalization in the hypothalamus. This region traverses most of the hypothalamus in the sagittal plane starting at E12.5 (Figure 3) and is characterized by uniform expression of *Arx* and patterned expression of Lim homeodomain factors *Lhx1*, *Lhx6*, *Lhx8*, and *Lhx9*. This largely non-overlapping pattern of LIM homeodomain factor expression appears to define a number of hypothalamic nuclei involved in control of circadian rhythms and sleep homeostasis, such as the SCN, DMH, and parts of the LH (Figure 4). In at least two cases, these genes are required for proper development of the hypothalamic cell types in which they are expressed (Bedont et al., 2014; Dalal et al., 2013). Such findings have already begun to facilitate the study of the development of individual hypothalamic nuclei.

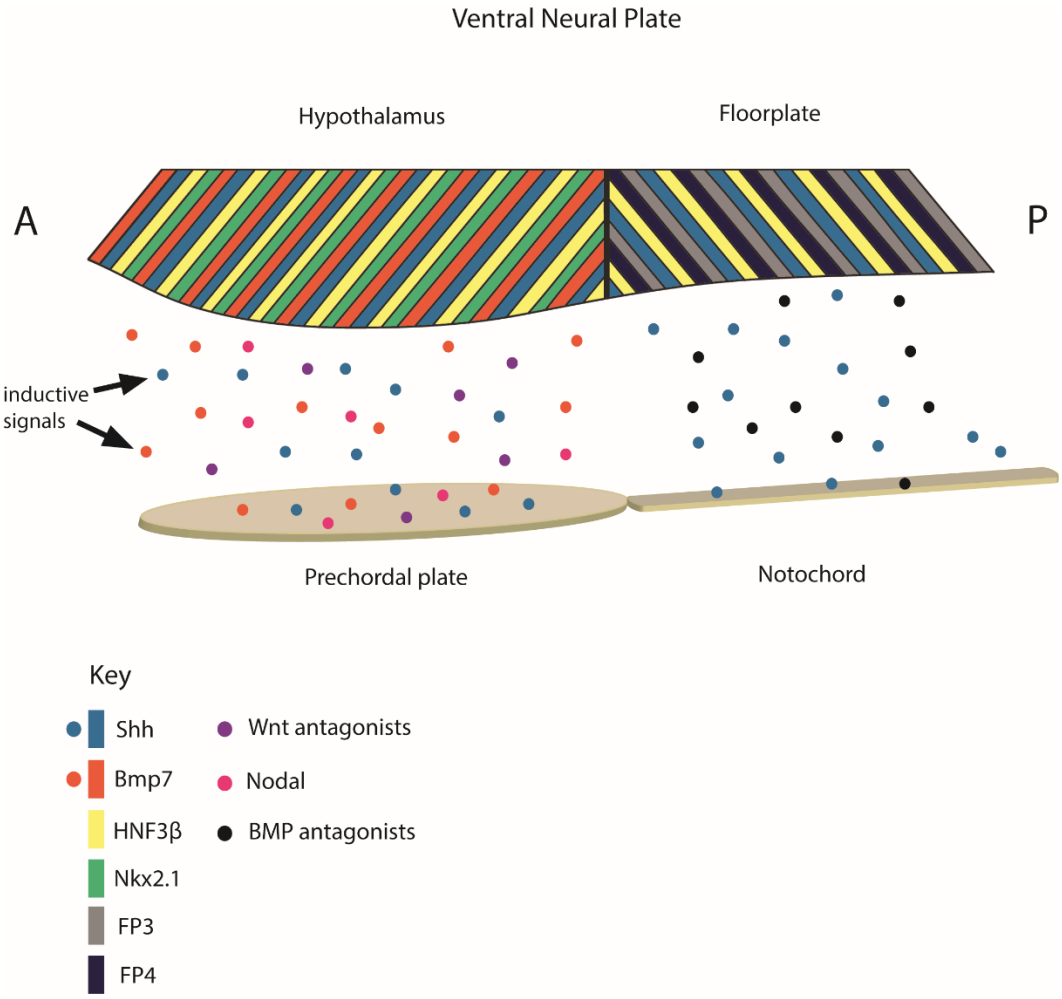

Figure 1-1: Schematic showing the inductive signals that act on the ventral neural plate. The posterior neural plate receives inductive signals from the notochord to become floor plate, whereas the more anterior neural plate that goes on to become the hypothalamus receives a different set of inductive signals from the prechordal plate. Circles represent signaling from the prechordal plate/notochord, whereas the

diagonal bars in the neural plate represent local gene expression. It should be noted that the juxtaposition of the prechordal plate and the hypothalamic neural plate is transient. These structures migrate out of register with each other. The prechordal plate reaches its final rostral position in advance of the hypothalamic neural plate, which migrates over and rostrally past the prechordal plate. Thus by the time the floor plate and the hypothalamic neural plate are specified, the prechordal plate actually resides caudal to the hypothalamic neural plate (Dale et al., 1999). A, anterior; P, posterior

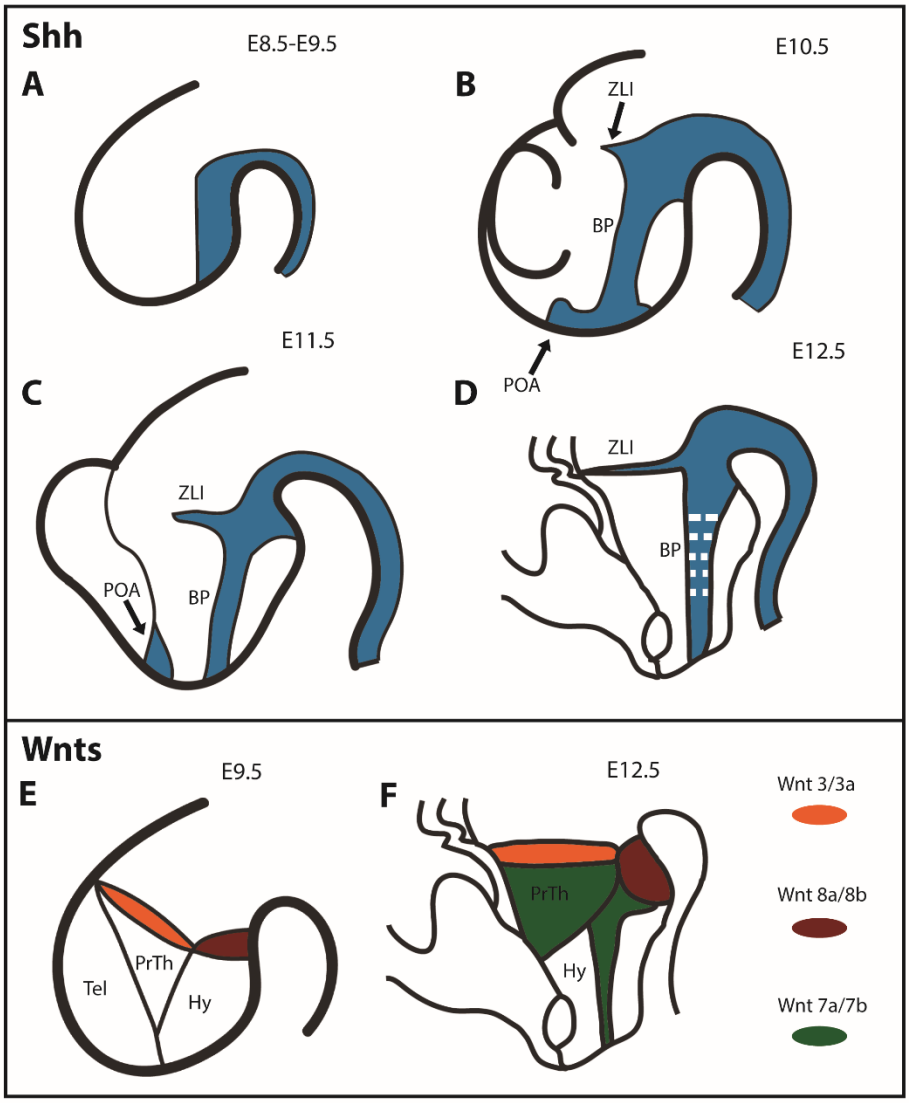
Shh
A
E8.5-E9.5
B
E10.5
ZLI
BP
POA
C
E11.5
ZLI
POA
BP
D
E12.5
ZLI
BP
Wnts
E
E9.5
Tel
PrTh
Hy
F
E12.5
PrTh
Hy
Wnt 3/3a
Wnt 8a/8b
Wnt 7a/7b

Figure 1-2: Sagittal view of morphogen expression over the course of development in the mouse forebrain, emphasizing the hypothalamus. (a–c). Forebrain *Shh* expression from E8.5 through E11.5. (d). Hypothalamic *Shh* expression at E12.5. White bars represent areas of diffuse *Shh*expression. (e) Wnt expression in the forebrain at E9.5. (f). Wnt expression in the hypothalamus at E12.5. *Wnt 7a/7b* is expressed in interneuron progenitors only while *Wnt 3/3a* and *Wnt 8a/8b* are expressed more broadly. BP, basal plate; ZLI, zona limitans intrathalamica; POA, preoptic area; Tel, telencephalon; PrTh, prethalamus; Hy, hypothalamus.

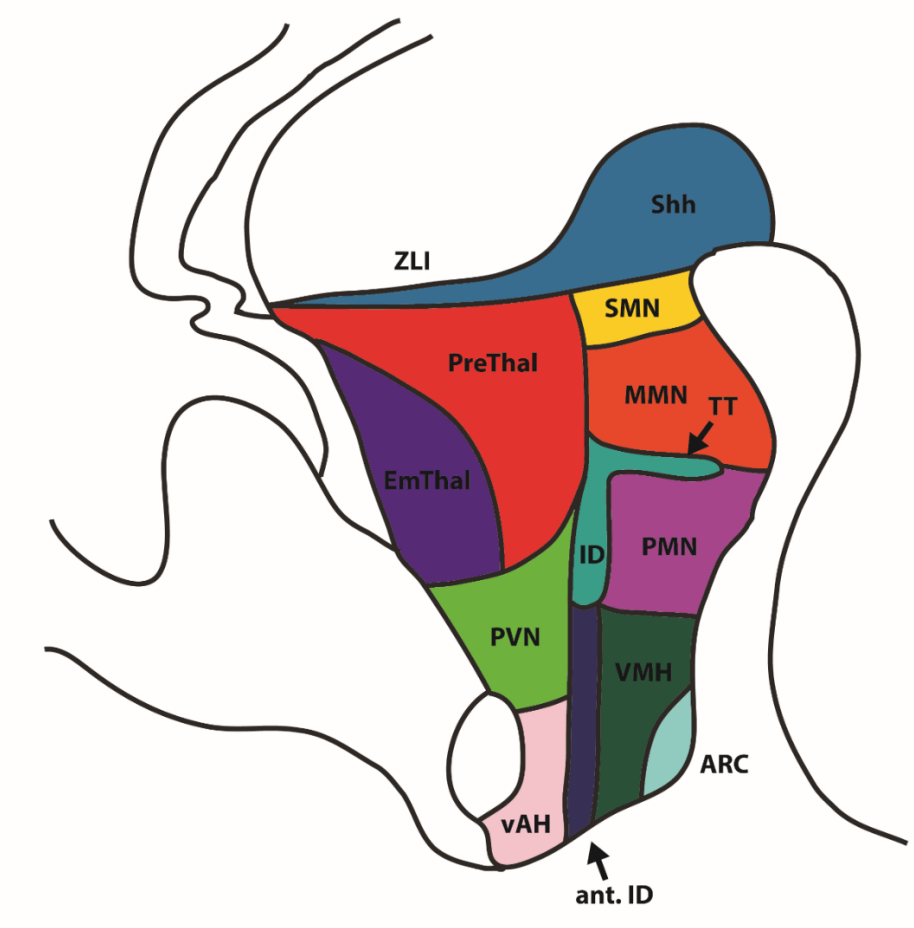

Figure 1-3: Sagittal map of nuclei in the mouse hypothalamus at E12.5 at the level of the third ventricle. ZLI, zona limitans intrathalamica; PreThal, prethalamus; EmThal, thalamic eminence; PVN, paraventricular nucleus; vAH, ventral anterior hypothalamus; ant. ID, anterior intrahypothalamic diagonal; ID, intrahypothalamic diagonal; ARC, arcuate nucleus; VMH, ventromedial hypothalamus; PMN, premammillary nucleus; TT, tuberomammillary terminal; MMN, mammillary nucleus; SMN, supramammillary nucleus.

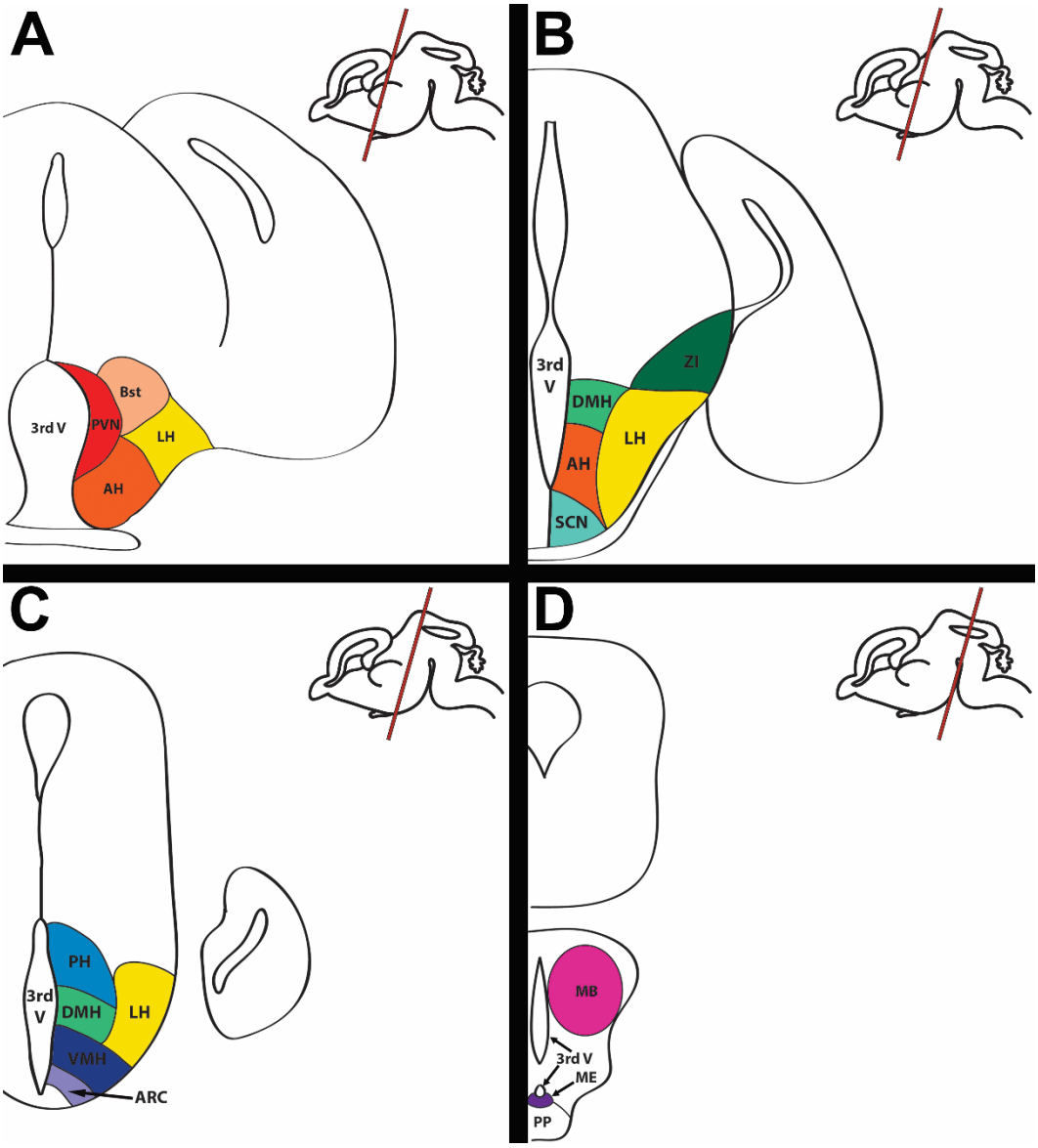

Figure 1-4: (a-d): Coronal diagrams of the nuclei of the developing hypothalamus at ~E15.5. Insets in the upper right-hand corners indicate the approximate position of these coronal sections in the sagittal plane. Note that the angle of the cut shown in the developing hypothalamus sometimes places nuclei normally

present on different coronal planes in typical adult brain sections on the same plane in our diagram (e.g.: SCN and DMH in panel b). SCN, suprachiasmatic nucleus; DMH, dorsomedial hypothalamic; PVN, paraventricular nucleus; AH, anterior hypothalamus; PH, posterior hypothalamus.

2. FOXD1

2.1 RESULTS

2.1.1 Foxd1 Expression in the Hypothalamus

Previous work from our lab has shown that the Forkhead domain transcription factor *Foxd1* is expressed in the ventricular zone of the prethalamus and anterior and dorsal hypothalamus by E11.5, shows reduced expression thereafter, and is almost undetectable by E14.5 except for a small domain near the 3rd ventricle in the prethalamus (Shimogori et al, 2010). Further characterization and fate-mapping of

this gene by our lab showed broad and efficient labeling of cells throughout the prethalamus and hypothalamus in adult mice using a Cre-induced GFP reporter line (Salvatierra et al., 2014). *Foxd1* is known to be involved in the development of the kidneys (Hatini et al., 1996), retina (Carreres et al., 2011), and optic chiasm (Herrera et al., 2004) and is a close homolog of, and cross-inhibitory with, *Foxg1*, which is known to control the competence of cortical progenitors (Siegenthaler et al., 2008). Nothing is known about the role of *Foxd1* in the development of the diencephalon, but given its broad expression throughout the hypothalamus and prethalamus, it may potentially play an important role in the patterning of these structures.

2.1.2 *Foxd1* is Expressed Early and Broadly in Neural Progenitors of the Prethalamus and Hypothalamus

Although previous research had shown that Foxd1 is expressed broadly in hypothalamic and prethalamic progenitors, it was not yet known when Foxd1 is first turned on in the presumptive diencephalon. To determine this, we employed mice in which a Cre-GFP fusion has been inserted into the endogenous Foxd1 locus, simultaneously disrupting expression of *Foxd1* (these mice are hereafter referred to as *Foxd1-Cre* mice). We then crossed these mice to an *Ai9* reporter line in which expression of Tdtomato (under the control of a constitutively active Rosa26 promoter) is activated by *Foxd1-Cre*. In these mice, green cells are currently expressing the *Foxd1-*

Cre while red cells have expressed the *Foxd1-Cre* at some point in their lineage. Analysis of TdTomato expression in an E8.5 *Foxd1-Cre*$^{+/-}$*; Ai9* mouse embryo revealed strong expression in the ventral forebrain (white arrowheads, Figure 1A). Therefore, *Foxd1* is expressed at least as early as E8.5 in the presumptive hypothalamus and prethalamus. Whole-mount *in situ* hybridization against *Foxd1* mRNA at E9.0 (Figure 1C) and E10.0 (Figure 1D) revealed strong expression in the hypothalamus and prethalamus at both ages (white arrowheads, Figure 1 C, D). By E12.5, *Foxd1* expression is limited to the ventricular zone of the prethalamus and anterior hypothalamus (AH), as revealed by immunohistochemistry against GFP in a Foxd1-Cre$^{+/-}$ embryo. However, staining for TdTomato in an E12.5 *Foxd1-Cre*$^{+/-}$*; Ai9* mouse embryo revealed widespread staining throughout the entire hypothalamus (white arrowheads, Figure 1F) and prethalamus (open arrowheads, Figure 1F) at E12.5 (left panel shows efferent and afferent connections). This was further confirmed by analyzing the *Foxd1-Cre*$^{+/-}$*; Ai9* mouse at P0, which labelled all mature nuclei and areas of the hypothalamus and prethalamus (open arrowheads=prethalamus, white arrowheads=SCN, Figure 1D).

2.1.3 Loss of *Foxd1* Leads to a Disruption in Development of the Anterior Hypothalamus by P0

We generated a *Foxd1*-null animal by crossing *Foxd1-Cre*$^{+/-}$ animals to generate *Foxd1-Cre*$^{+/+}$ pups (hereafter referred to as *Foxd1*$^{-/-}$ mice). The Cre used is a knock-in that

disrupts transcription of the endogenous *Foxd1* but operates under the control of the *Foxd1* promoter (Humphreys et al., 2008). *Foxd1*-null mutants die within 24 hrs of birth as shown in previous studies of these animals (Hatini et al., 1996) so the latest time point analyzed was P0. It is not known exactly why these mutants die, but may be related to the fact that Foxd1-deficient animals show severe defects in kidney development and function.

We analyzed *Foxd1*$^{-/-}$ mice at P0 using *in situ* hybridization and ran a large panel of probes to determine which areas of the prethalamus and hypothalamus, if any, would be affected by the loss of *Foxd1* during development. Surprisingly, the only major defect seen was in the nuclei of the anterior hypothalamus. The suprachiasmatic nucleus (SCN) showed a reduction, or in some cases complete loss, in the majority of probes tested. The nuclear markers *Lhx1* and *Vipr2* were completely absent in the *Foxd1*-null mutants (Figure 2 E, F, K, and L). Other nuclear markers were significantly reduced, including *Avp* (Figure 2 A and B), *Rorb* (Figure 2 G and H), *Emx2* (Figure 2 M and N), and *Rora* (Figure 2 Q and R). Surprisingly, *Gad67* expression appeared to be normal in the SCN of the *Foxd1*$^{-/-}$ mice (Figure 2 C and D), and *Th* and *Trh*, which are expressed in cells bordering the SCN but not within it, were normal as well (Figure 2 I, J, U and V). In wild-type mice, the SCN is easily detectable using DAPI staining as a cell-dense tear-drop shaped nucleus on the ventral surface of the anterior hypothalamus (Figure 2W). In most *Foxd1*$^{-/-}$ mice examined, the SCN could not be

identified using DAPI staining (data not shown). Less commonly, the SCN appeared as a large, diffuse, poorly defined area (Figure 2 X).

The loss of *Foxd1* affected other nuclei of the anterior hypothalamus as well. The paraventricular nucleus (PVN) was disrupted, as demonstrated by the reduction in *Avp* expression (black arrowheads, Figure 2 A and B) and complete loss of Sst expression (black arrowhead, Figure 2 S and T). However, *Trh* expression was normal within the PVN (black arrowhead, Figure 4 I and J). *Sst* expression was also completely absent in the periventricular nucleus (PeVN) (open arrowheads, Figure 2 S and T), along with *Emx2*, which is expressed in a small domain of the anteroventral hypothalamus (black arrowhead, Figure 2 M and N). Expression of *Isl1*, which is broadly expressed in the anterior and tuberal hypothalamus, was also reduced but not absent (Figure 2 O and P). The results of the anterior hypothalamic defect are summarized in Figure 3.

Given the dramatic loss of anterior hypothalamic markers, we wanted to determine if loss of *Foxd1* affected progenitor proliferation or cell apoptosis, leading to a loss of these cells. A 2hr EdU pulse was given to pregnant dams on E12.5, and EdU-positive cells within the prethalamus and hypothalamus were counted, but there was no effect seen on numbers of proliferating cells in *Foxd1*$^{-/-}$ mice when averaged relative to area (μm^2) (Figure 5 A-C; n=2 mice). There was also no change seen in a TUNEL assay of cell death in *Foxd1*$^{-/-}$ mice (data not shown).

Foxd1 expression persists longest in progenitors of the anterior hypothalamus and the prethalamus, but surprisingly despite the severe disruption of the development of the anterior hypothalamus, there were no discernible defects in the prethalamus. *Isl1* and *Sst*, whose expression patterns were disrupted in the anterior hypothalamus in *Foxd1*$^{-/-}$ mice, showed unaltered expression in the prethalamus (red arrowheads, Figure 2 O, P, S and T).

In contrast to the strong defect seen in the anterior hypothalamus in *Foxd1*$^{-/-}$ mice, the lateral and posterior hypothalamus developed relatively normally. *Emx2* and *Foxb1* expression were unaffected in the mammillary body (black arrowheads, Figure 4 A and B; data not shown). Markers of the arcuate nucleus (Arc) developed normally as well, including *Th* (black arrowheads, Figure 4 G and H), *Sst* (open arrowheads, Figure 4 E and F), *Npy* and Cart (data not shown). The same was true of the dorsomedial hypothalamus (DMH) (*Sst*: black arrowheads, Figure 4 E and F; *Trh*: black arrowheads; Figure 4 K and L, *Cart*: data not shown), and the lateral hypothalamus (LH) (Trh: open arrowheads; Figure 4 I-L). *Sst* expression in the tuberomammillary (red arrowheads, Figure 4 E and F), and in the border between the DMH and ventromedial hypothalamus (VMH) (yellow arrowheads, Figure 4 E and F) was unaffected. Similarly, *Trh* in the supraoptic nucleus (SON) (red arrowheads, Figure 4 I and J) showed no change in the Foxd1-null mutants. One notable exception was the marker Isl1, whose expression in the DMH (open arrowheads, Figure 4 C and D), arcuate (red arrowheads, Figure 4 C and D) and ventrolateral ventromedial

hypothalamus (VMH) (yellow arrowheads, Figure 4 C and D) was completely absent in the Foxd1-null mutants, with only a small remnant remaining in the most medial portion of its LH domain (black arrowheads, Figure 4 C and D). This may be due to inefficient staining during the *in situ* hybridization, but strong staining in the prethalamus (red arrowhead, Figure 2 P) suggests against this theory.

2.1.4 *Foxd1*$^{-/-}$ Mice Have a Mild Developmental Defect at E12.5 and E16.5

There were two possible scenarios for the developmental dynamics of the disrupted anterior hypothalamus in our mutants: either the anterior hypothalamus failed to be specified early in development, or the anterior hypothalamus was specified correctly, but failed to turn-on and/or maintain expression of the markers of the mature nuclei. To determine which scenario was occurring, we examined *Foxd1*$^{-/-}$ embryos at two stages of development: E12.5, coinciding with the onset of the earliest markers of the anterior hypothalamus, and E16.5 when the first SCN-specific markers are turned on.

At E12.5, ventral anterior hypothalamic markers *Isl1* (open arrowheads, Figure 6 B and C) and *Rax* (Figure 6 D and E) were normal in *Foxd1*$^{-/-}$ mice. *Isl1* expression was also normal within the prethalamus (Figure 6 B and C). *Arx*, which is expressed in a stripe from the prethalamus through the hypothalamus, was expressed normally in both regions (black arrows: prethalamus, open arrow: hypothalamus, Figure 6 H

and I). One of the earliest markers of the PVN, *Sim1*, was similarly normal (Figure 6 L and M). Importantly, *Lhx1*, which is completely absent by P0 in the SCN of *Foxd1*$^{-/-}$ mice, was not affected at E12.5 in either the anterior hypothalamus (open arrowheads, Figure 6 J and K) or the prethalamus (black arrowheads, Figure 6 J and K). However the *Foxd1*$^{-/-}$ mice did not phenocopy wild-type embryos with all markers tested. Both *Six3* (open arrowheads, Figure 6 F and G) and *Vax1* (open arrowheads, Figure 6 N and O) showed moderate-to-strong reductions in the ventral anterior hypothalamus. In addition, the central nuclear portion of *Six3* staining in the prethalamus was absent in *Foxd1*$^{-/-}$ mice (black and red arrowheads, indicating the prethalamus and missing expression domain, respectively, Figure 6 F and G).

By E16.5, *Lhx1*, which in *Foxd1*$^{-/-}$ mice was present and normal at E12.5 and absent at P0, was present but mildly reduced in the SCN (Figure 7 E and F). Similarly, *Rorb*, which was strongly reduced by P0, was mildly reduced in the SCN at E16.5 (Figure 7 C and D). *Sst* expression is not yet initiated in the PeVN at E16.5 (Figure 7 G and H) and *Isl1* expression was normal in the anterior hypothalamus (Figure 7 A and B).

To determine which genes may be under the transcriptional control of Foxd1, RNAseq analysis was performed on RNA extracted from dissected hypothalamic tissue at E12.0, E12.5 and E17.5. The E12.0 and E12.5 data were pooled together for analysis. Genes with a q-value of <0.05 were considered significant. The statistically significant differentially expressed genes are listed in Table 1 (E17.5 data) and Table 2

(E12.0 and E12.5 pooled data). In both data sets, Foxd1 was the most significantly downregulated gene, as expected. Gene ontology (GO) analysis was performed on the statistically significant genes in order to group them within three domains: biological processes (Figure 8), cellular compartments (Figure 9) and molecular function (Figure 10). The genes included in each category within each domain are summarized in Table 3 (E12.0/E12.5 genes), Table 4 (E17.5 data for cellular compartments and molecular function) and Table 5 (E17.5 data for biological processes).

At E12.0/E12.5, one of the significantly downregulated genes was *Six3*, which is confirmed by the E12.5 *in situ* hybridization data; *Six3* was one of only two genes whose expression was lower in *Foxd1*$^{-/-}$ mice at E12.5 (Figure 6 F and G). The other downregulated gene at E12.5 was *Vax1*, which did not reach significance in the E12.0/E12.5 RNA-Seq data, but was significantly downregulated in the E17.5 RNA-seq data set. At E17.5, there were several other anterior hypothalamic genes which were significantly downregulated, including *Avp*, which was also confirmed by our P0 *in situ* hybridization data (Figure 2 A and B), as well as *Crh* (expressed in the PVN), *Zbtb18* (in the ventral AH), *Cdh23* (AH), *Neurod6* (ventral AH), *Slc6a3* (AH and zona incerta (ZI)), *Oxt* (PVN), *4930555G01Rik* (AH), and *Moxd1* (BNST and POA).

There were several genes enriched in the E17.5 RNA-Seq data set that likely represent dissection contaminants (Table 1), most originating from telencephalon and habenula, including *Tbr1*, *Foxg1*, *Irx1*, *Neurod2*, *Pou4f1*, and *Satb2*. There were also

contaminants from the choroid plexus (Ttr), and meninges (*Dcn*, although *Foxd1* is also expressed in the meninges). *Ddx3y* and *Eif2s3y* are Y chromosomal genes, and their inclusion is likely an artifact resulting from the fact that we did not sex the embryos used for the hypothalamic dissection. The female sex-specific gene *Xist* was also found enriched in the E12.0/E12.5 RNAseq data set (Table 2).

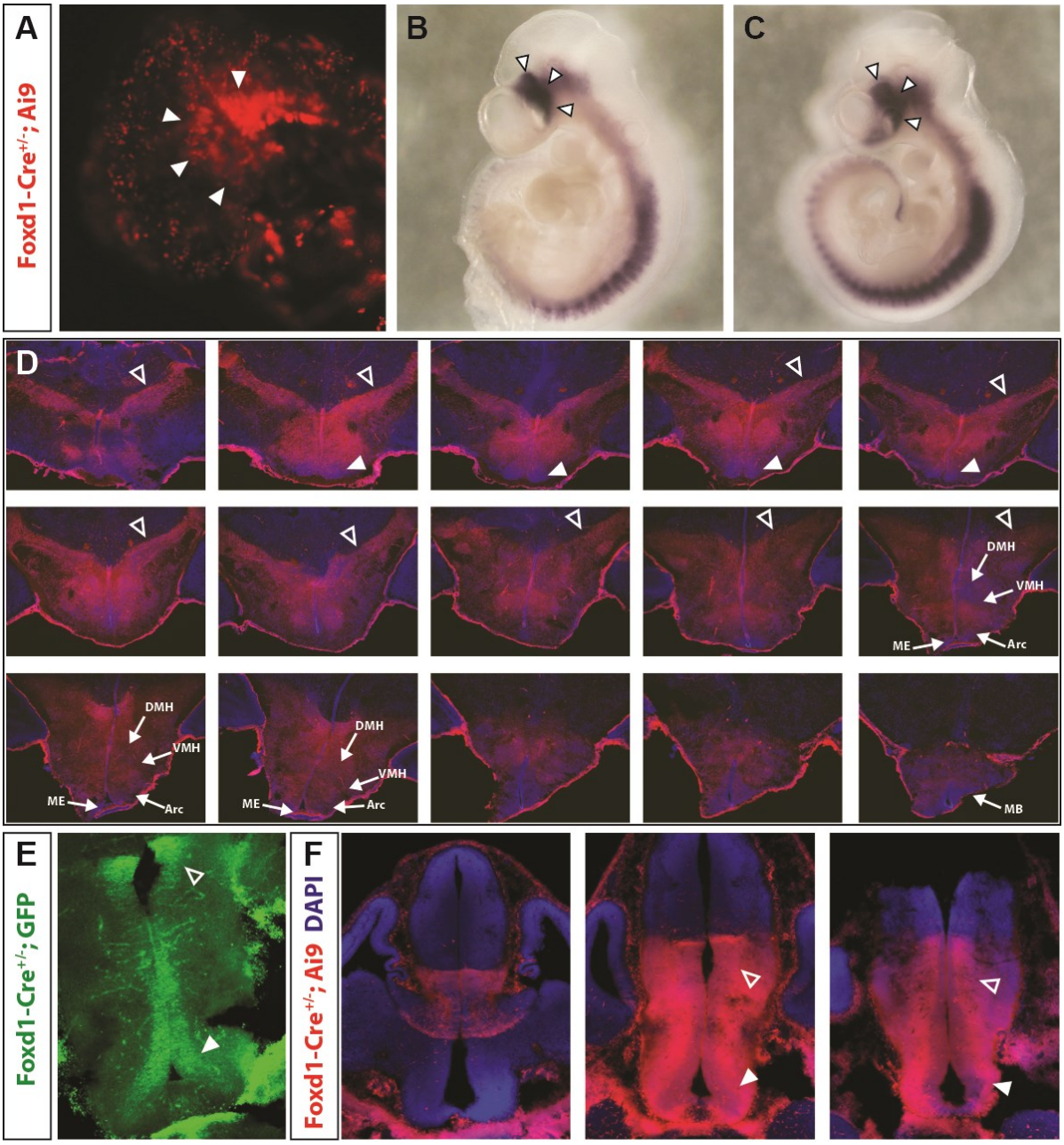
A
Foxd1-Cre+/-; Ai9
B
C
D
DMH
VMH
ME
Arc
MB
E
Foxd1-Cre+/-; GFP
F
Foxd1-Cre+/-; Ai9 DAPI

Figure 2-1: The *Foxd1* lineage encompasses every cell of the hypothalamus and prethalamus, and its expression is turned on early. A: Endogenous staining from a *Foxd1-Cre*$^{+/-}$*; Ai9* E8.5 embryo. White arrowheads indicate the presumptive hypothalamus in the ventral neural tube. B, C: Whole mount *in situ* hybridization of Foxd1 mRNA at E9.0 (B) and E10.0 (C). The hypothalamus is designated by the white arrowheads. D: Lineage tracing via immunohistochemistry staining against dsRed in a *Foxd1-cre*$^{+/-}$*; Ai9*, P0 brain. Red cells have expressed Foxd1-cre at some point in their lineage. Blue=DAPI. Open arrowheads=prethalamus, white arrowheads=SCN. Anterior to posterior goes from left to right and top to bottom. E: Immunohistochemistry staining against GFP in a *Foxd1-cre*$^{+/-}$*:GFP* E12.5 brain. By this age, *Foxd1* is expressed only in the prethalamus (open arrowhead) and the anterior hypothalamus (white arrowhead) along the ventricle. F. Despite the limited *Foxd1* expression at E12.5, lineage tracing in an E12.5 *Foxd1-Cre*$^{+/-}$*; Ai9* brain reveals that every cell in the hypothalamus and prethalamus originates from a *Foxd1*-positive lineage. Open arrowheads=prethalamus, white arrowheads=hypothalamus.

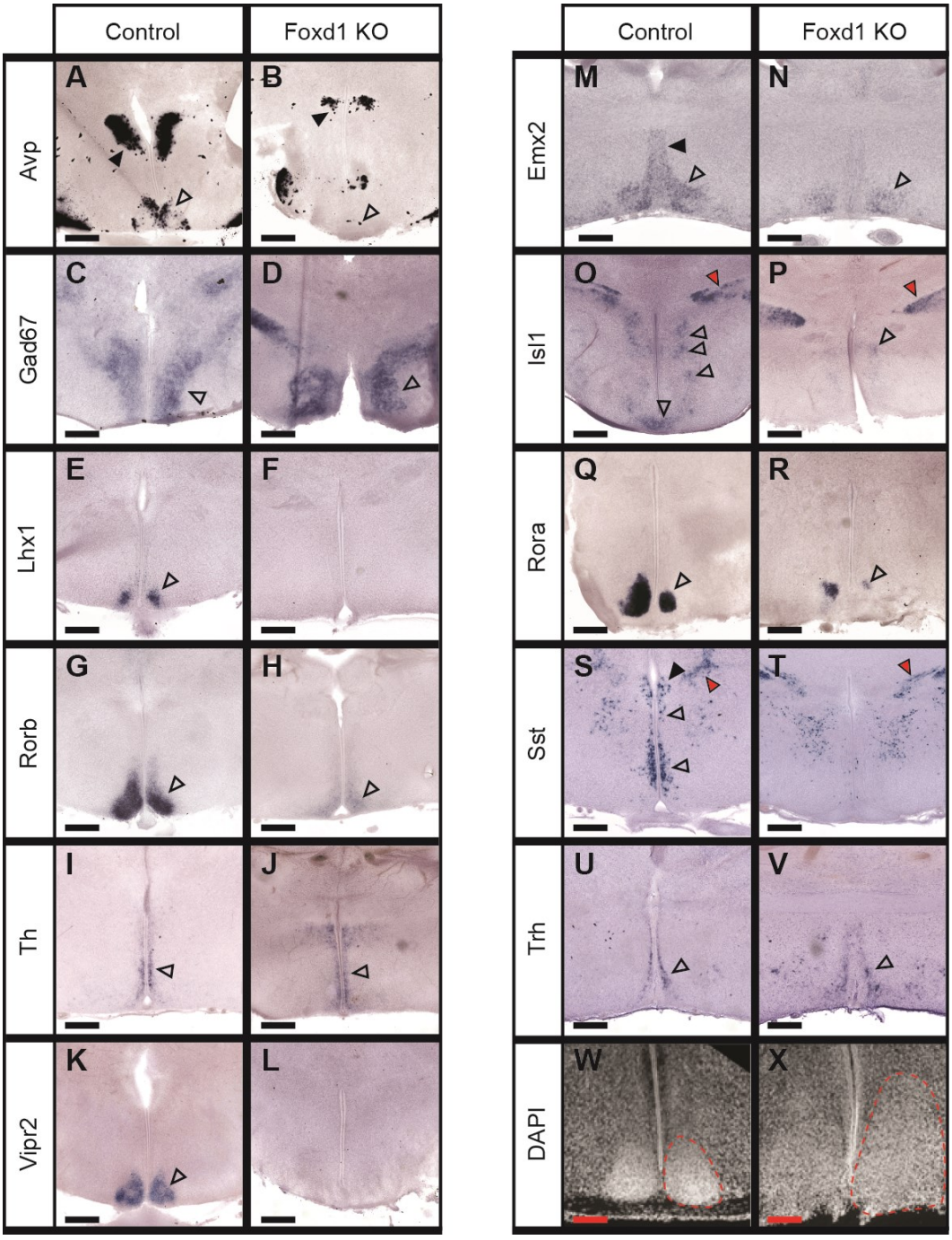
Control
Foxd1 KO
Avp
Gad67
Lhx1
Rorb
Th
Vipr2
A
B
C
D
E
F
G
H
I
J
K
L
Control
Foxd1 KO
Emx2
Isl1
Rora
Sst
Trh
DAPI
M
N
O
P
Q
R
S
T
U
V
W
X

Figure 2-2: Loss of *Foxd1* results in a selective loss of anterior hypothalamic markers at P0. A-V: *In situ* hybridization of P0 wild-type and *Foxd1*$^{-/-}$ coronal brain sections. There was either a complete loss, or a strong reduction, in markers of the SCN (open arrowheads, A-N, Q, R). However, there were exceptions, including *Gad67* (open arrowheads, C, D) and the markers *Th* and *Trh* (open arrowheads, I, J, U, V), which are not expressed in the SCN proper, but rather the cells that border it. Markers of the PVN were also negatively affected by the loss of *Foxd1* (black arrowheads, A, B, S, T), as was *Sst* in the PeVN (open arrowheads, S, T). The general anterior hypothalamic marker *Isl1* was also strongly reduced (open arrowheads, O, P. The prethalamus was unaffected, despite strong *Foxd1* expression in this area (red arrowheads, O, P, S, T). W, X: The SCN is normally identified as a tear-drop shaped, dense nucleus (red dashed outline, W) but in some *Foxd1*$^{-/-}$ brains, it presented as a poorly defined, diffuse area (red dashed outline, X).

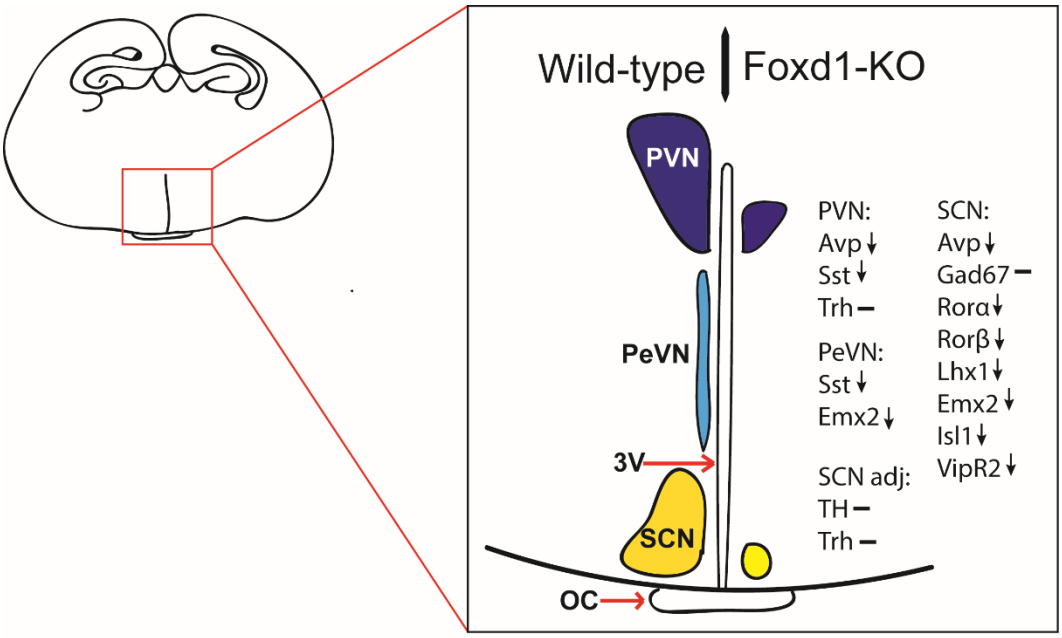

Figure 2-3: A schematic summarizing the developmental defects in the anterior hypothalamus of *Foxd1*$^{-/-}$ brains at P0. Expression of anterior hypothalamic markers was either reduced (down arrow) or unaffected(-).

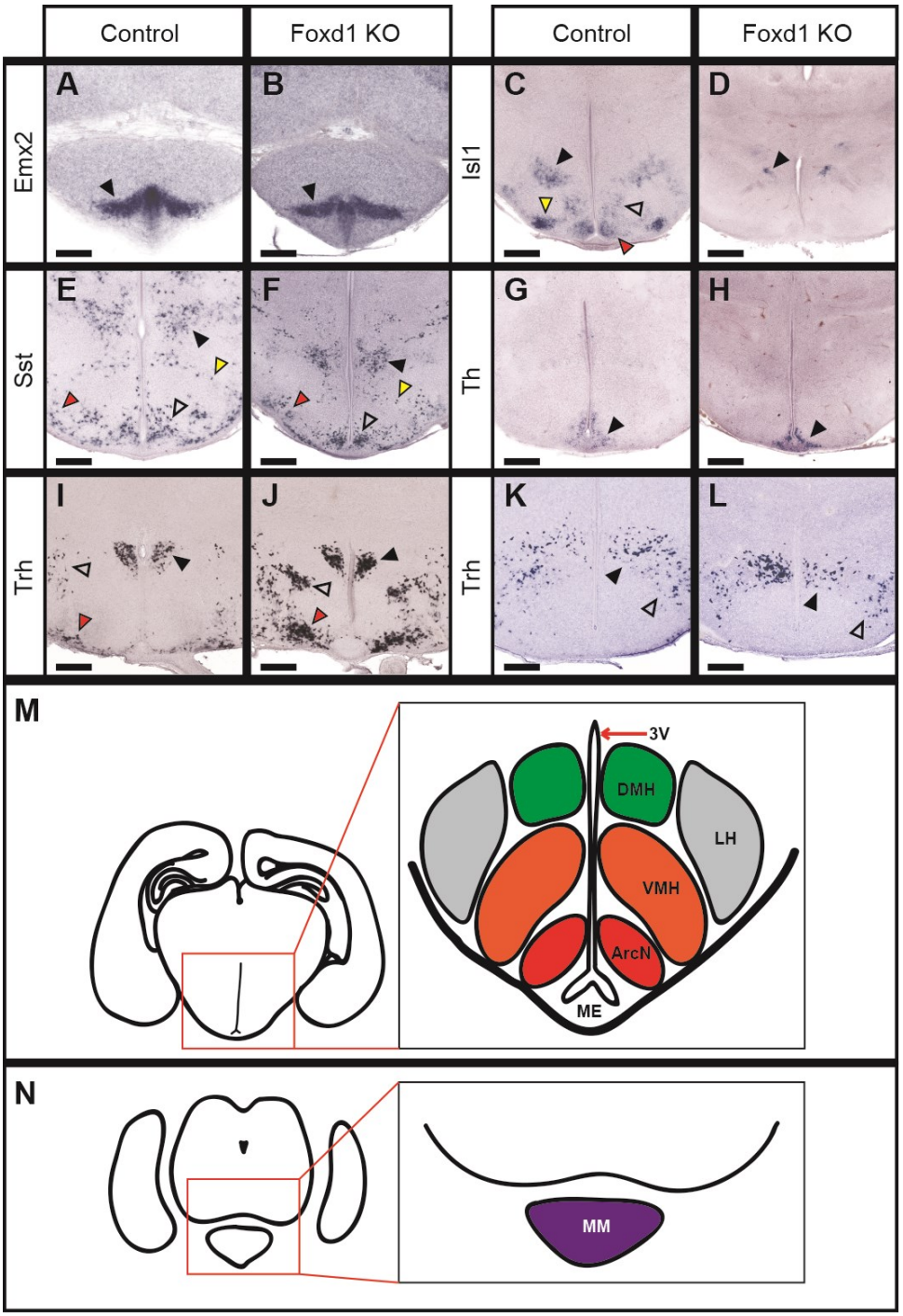
Control
Foxd1 KO
Control
Foxd1 KO
A
B
C
D
Emx2
Isl1
E
F
G
H
Sst
Th
I
J
K
L
Trh
Trh
M
3V
DMH
LH
VMH
ArcN
ME
N
MM

Figure 2-4: Posterior and lateral hypothalamic structures are unaffected in Foxd1-null animals at P0. A-L: *In situ* hybridization on P0 wild-type and *Foxd1*$^{-/-}$ coronal sections. There was no change in markers of the mammillary body (black arrowheads, A, B, K, L). Arcuate expression of *Sst* (open arrowheads, E, F), and *Th* (black arrowheads, G, H) was unchanged in *Foxd1*$^{-/-}$ brains, but Isl1 expression (red arrowheads, C, D) was lost. The DMH was relatively unaffected (black arrowheads, E, F, K, L), but as with the arcuate, it too lost expression of *Isl1* (open arrowheads, C, D). Isl1 expression in the ventrolateral VMH was also lost in *Foxd1*$^{-/-}$ brains (yellow arrowheads, C, D). The lateral hypothalamus had normal *Trh* expression (open arrowheads, I-L), but reduced Isl1 expression (black arrowheads, C, D). Other unaffected brain areas were the tuberomammillary terminal (red arrowheads, E, F) and the supraoptic nucleus (red arrowheads, I, J). M, N: Schematics showing the overall organization of posterior hypothalamic nuclei at two coronal planes. M corresponds to the coronal plane featured in C-H and K, L, and N corresponds to sections A, B.

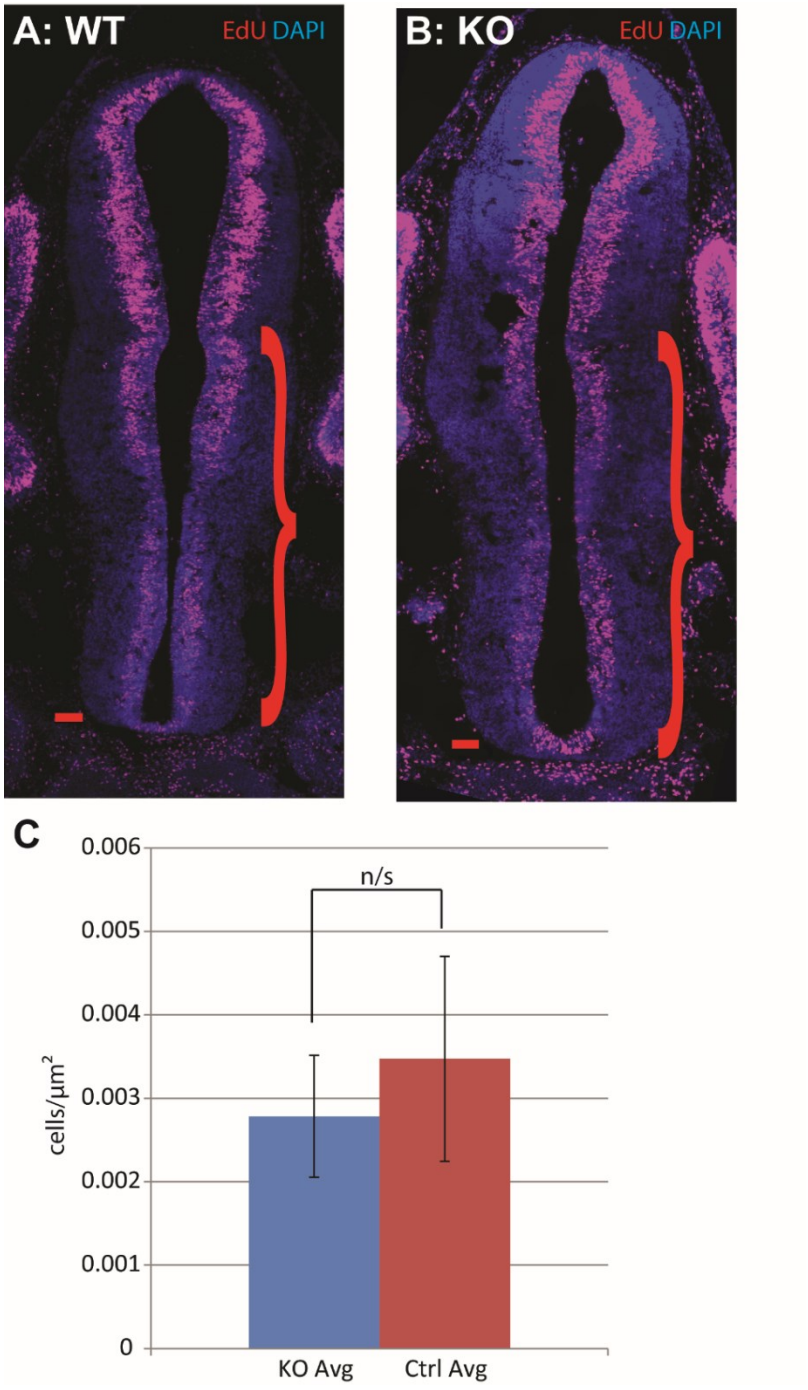
A: WT
EdU DAPI
B: KO
EdU DAPI
C
0.006
0.005
0.004
0.003
0.002
0.001
0
cells/µm²
n/s
KO Avg
Ctrl Avg

Figure 2-5: Proliferation is not affected by loss of *Foxd1*. A-B: Immunohistochemistry staining against EdU (red) and DAPI (blue) on E12.5 wild-type and *Foxd1*$^{-/-}$ coronal sections after a 2hr EdU pulse. Red scroll bars indicate the counted portion of the section containing the prethalamus and hypothalamus. C: Quantification of EdU-positive cells relative to area (μm^2) in control versus *Foxd1*$^{-/-}$ brains (n=2).

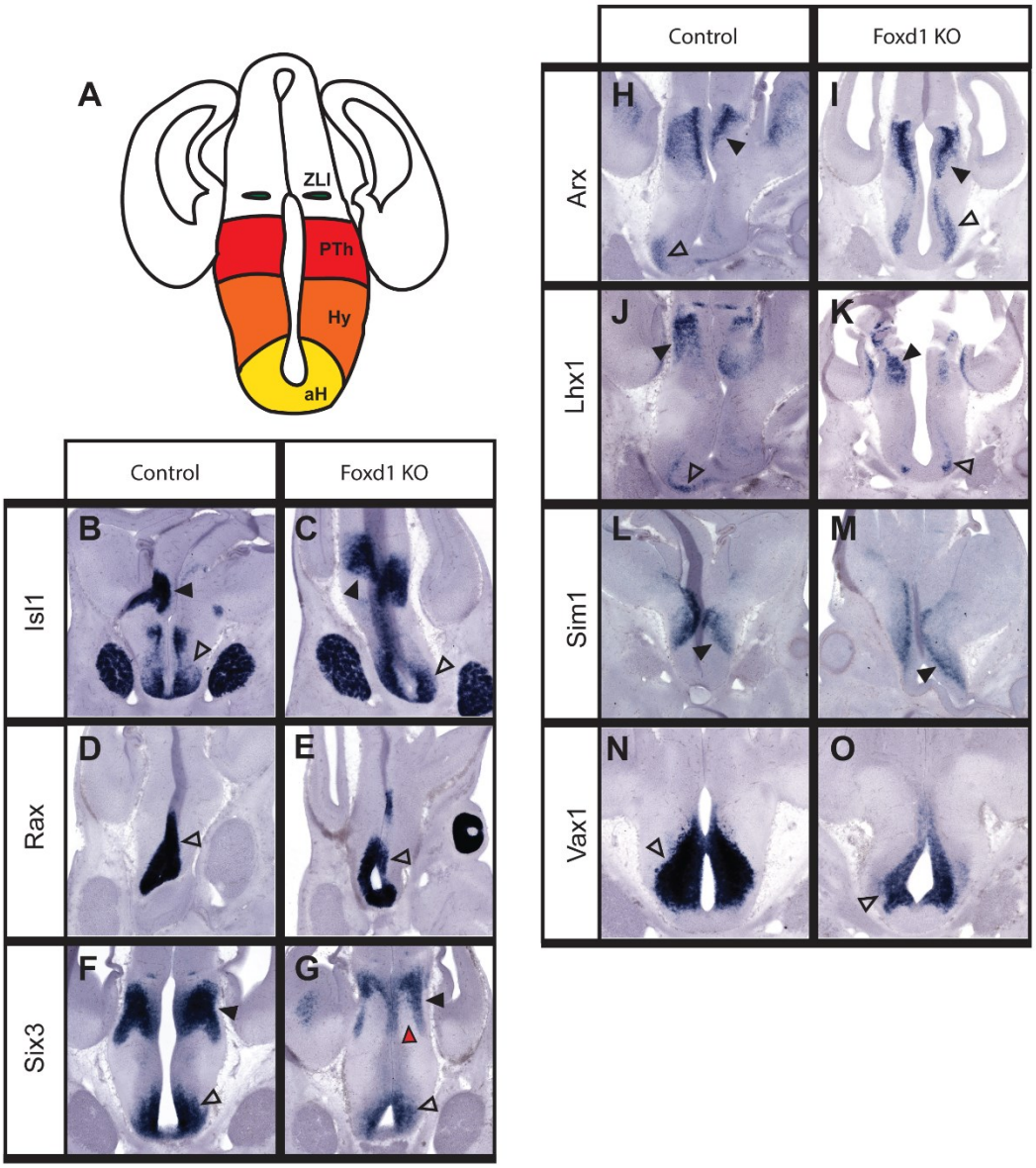

Figure 2-6: At E12.5, when *Foxd1* expression is highest, hypothalamic markers are largely unaffected by loss of *Foxd1*. A: Schematic demonstrating the organization of the hypothalamus and prethalamus at the coronal level depicted in B-

O. B-O: *In situ* hybridization on E12.5 wild-type and *Foxd1*$^{-/-}$ coronal sections. Some markers of the ventral AH (open arrowheads, B-E, H-K), and prethalamus (black arrowheads, B, C, H-K) were unaffected in *Foxd1*$^{-/-}$ brains. However, *Vax1* and *Six3* were both down in the ventral AH (open arrowheads, F, G, N, O) and Six3 expression in the prethalamus was also reduced (black arrowheads indicate the prethalamus, red arrowhead shows missing expression domain, F, G). *Sim1* expression in the presumptive PVN was unaffected (black arrowheads, L, M).

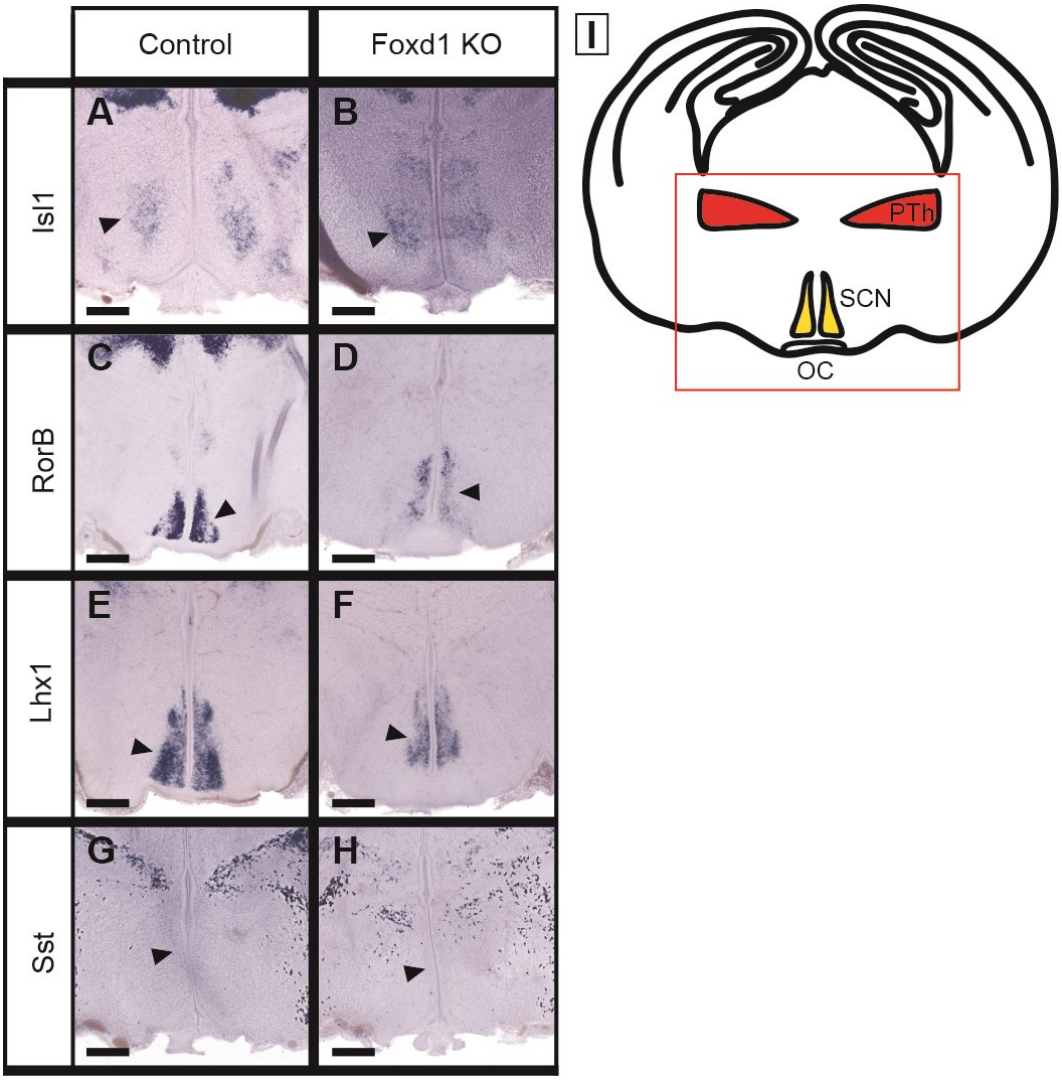

Figure 2-7: Anterior hypothalamic markers are reduced, but not absent, at E16.5. A-H: *In situ* hybridization on E16.5 wild-type and *Foxd1*$^{-/-}$ coronal sections. I: A schematic demonstrating the organization of the hypothalamus and prethalamus at the coronal plane shown in A-H. A-F: Markers of the anterior hypothalamus and SCN that are drastically reduced or lost at P0 are only mildly affected at E16.5 (black

arrowheads in A and B show the anterior hypothalamus, black arrowheads in C-F indicate the SCN). G, H: At E16.5, *Sst* is not yet expressed in the PeVN (black arrowheads).

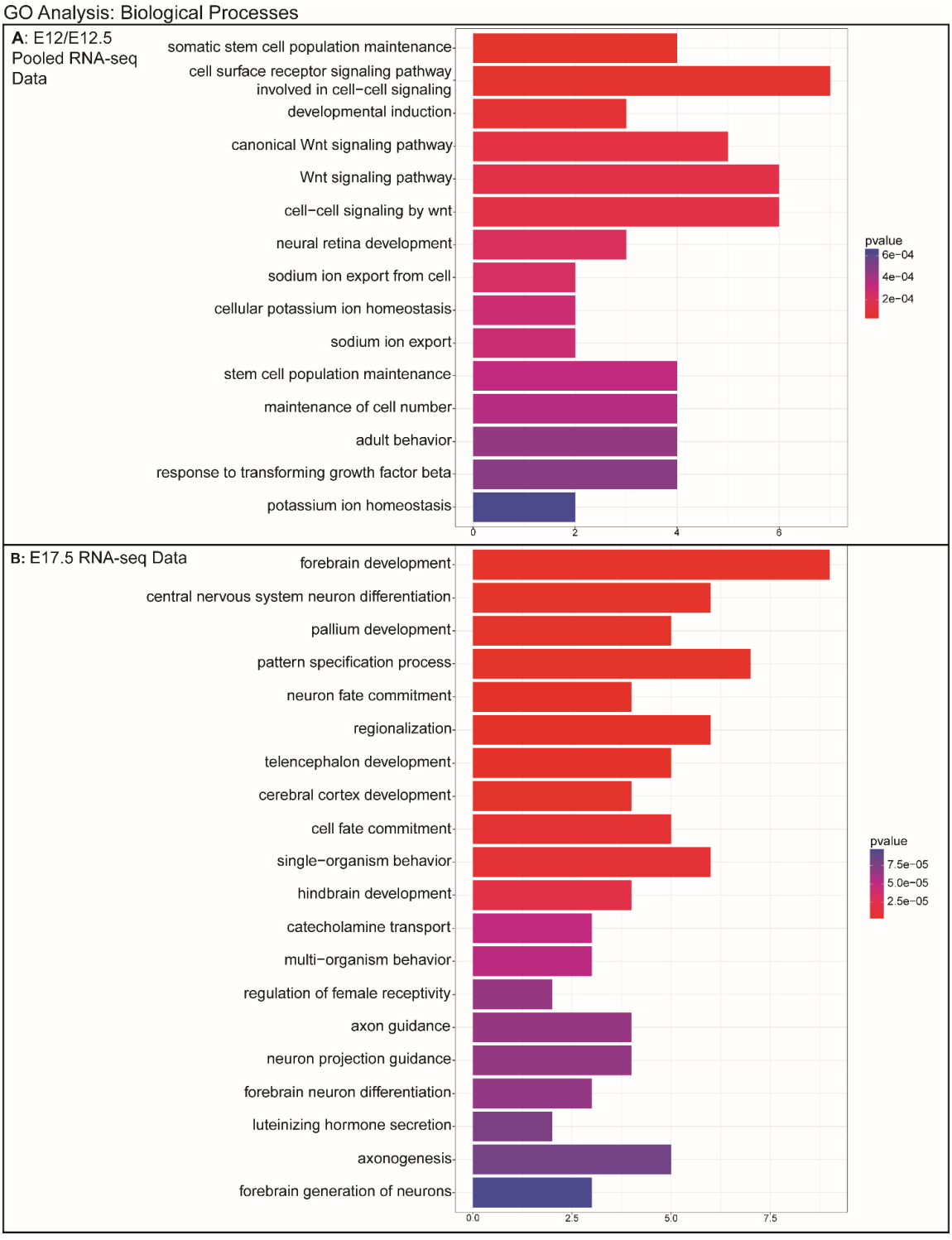

GO Analysis: Biological Processes.

Figure 2-8: GO Analysis: Biological Processes. A, B: Gene ontology analysis of biological processes performed on the significantly differentially expressed genes from RNA-Seq analysis of E12.0/E12.5 (A) and E17.5 (B) wild-type and *Foxd1*$^{-/-}$ data.

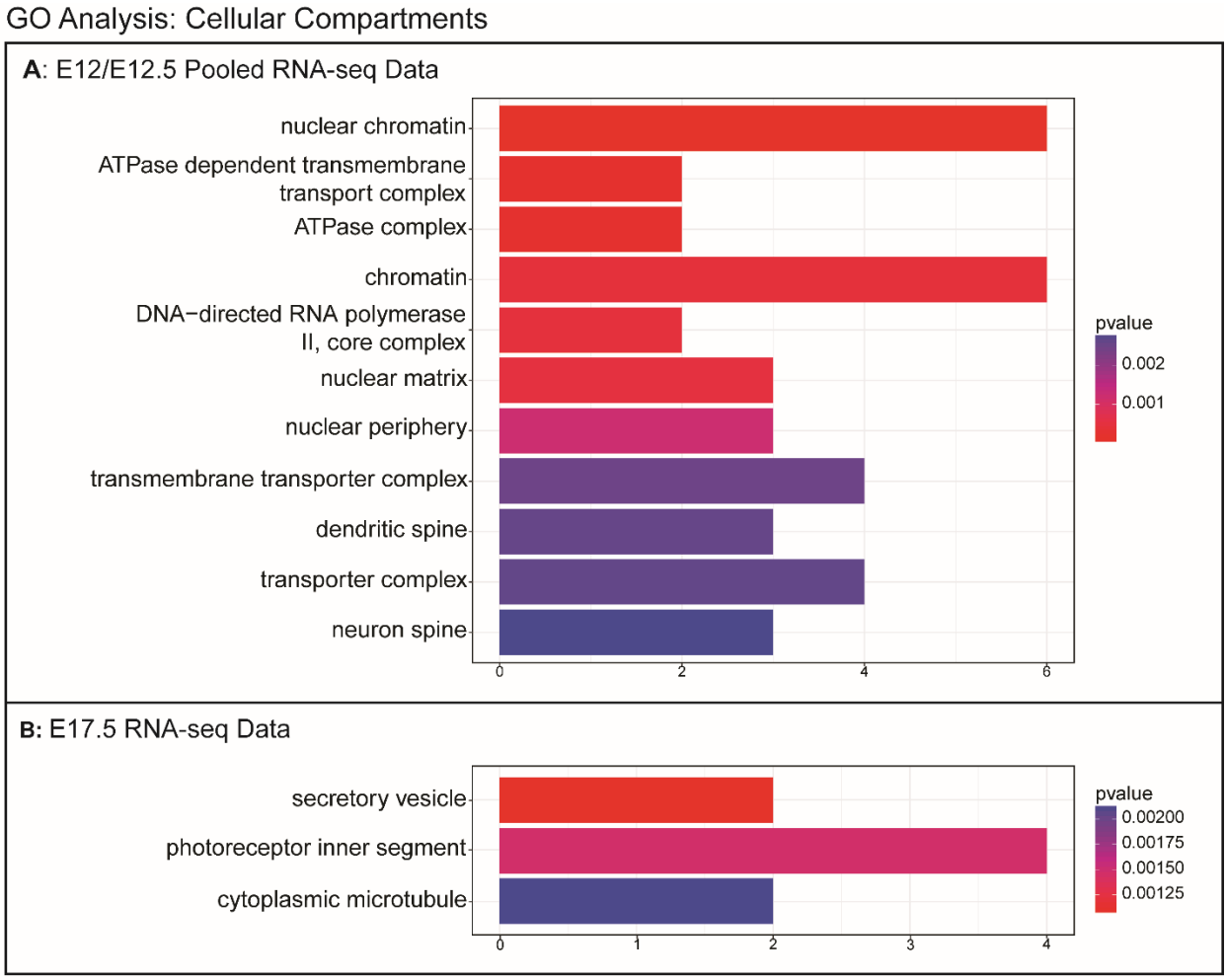

GO Analysis: Cellular Compartment.

Figure 2-9: GO Analysis: Cellular Compartment. A, B: Gene ontology analysis of cellular compartment localization performed on the significantly differentially expressed genes from RNA-Seq analysis of E12.0/E12.5 (A) and E17.5 (B) wild-type and *Foxd1*$^{-/-}$ data.

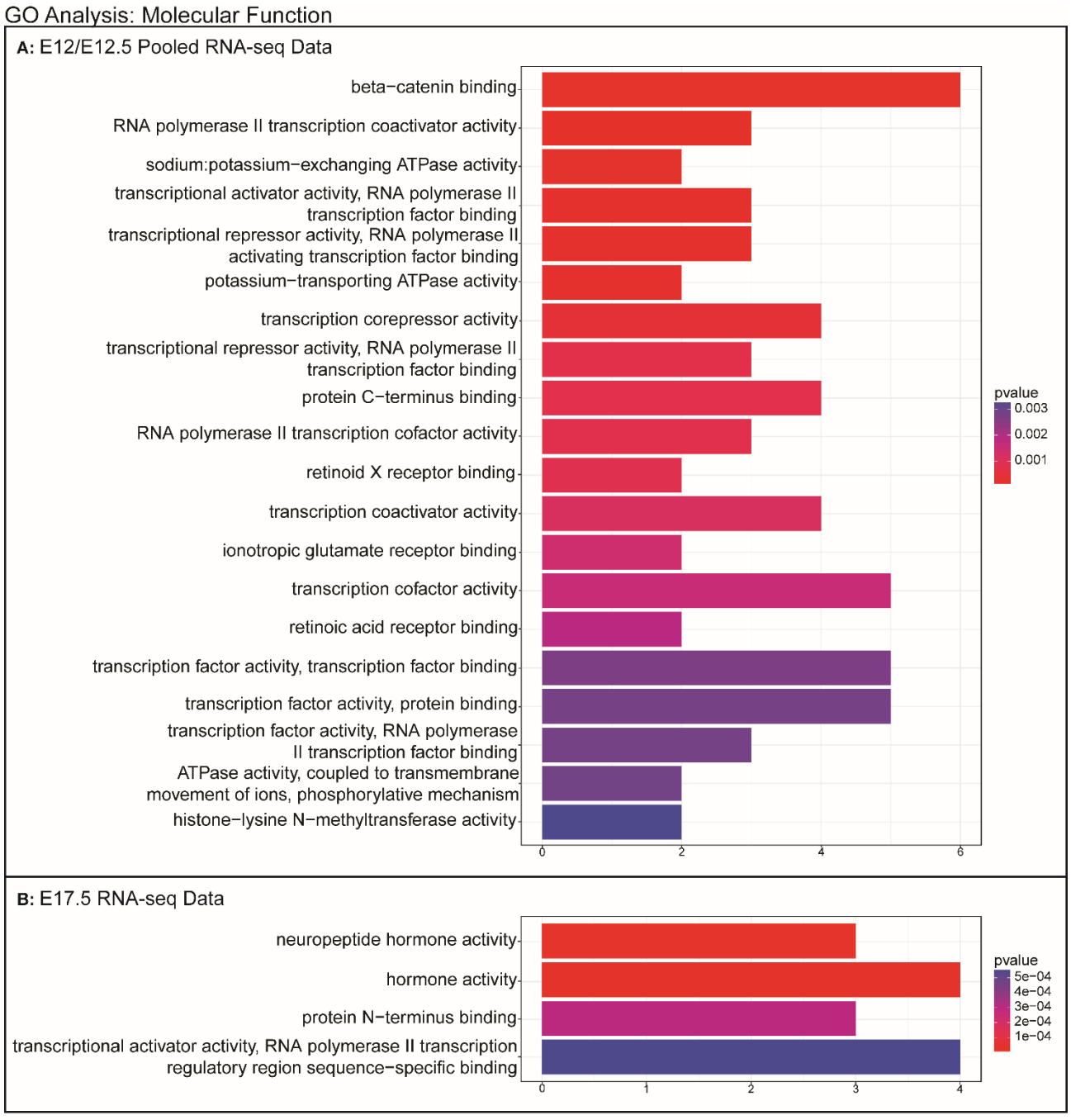

GO Analysis: Molecular Function.

Figure 2-10: GO Analysis: Molecular Function. A, B: Gene ontology analysis of molecular functions performed on the significantly differentially expressed genes from RNA-Seq analysis of E12.0/E12.5 (A) and E17.5 (B) wild-type and *Foxd1*$^{-/-}$ data.

Gene	Fold Change (log2)	p Value	q Value
Zbtb18	0.66	0.00005	0.040
Dynlt1c	1.62	0.00005	0.040
Dcn	0.71	0.00005	0.040
Cdh23	-1.04	0.00005	0.040
Foxg1	1.06	0.00005	0.040
Foxd1	-3.22	0.00005	0.040
Tbr1	0.77	0.00005	0.040
Dynlt1b	0.79	0.00005	0.040
Vax1	-1.21	0.00005	0.040
Neurod6	1.11	0.00005	0.040
Avp	-3.38	0.00005	0.040
Slc6a3	-1.65	0.00005	0.040
Eomes	1.06	0.00005	0.040
Irx1	-0.95	0.00005	0.040
Neurod2	1.18	0.00005	0.040
Oxt	-2.49	0.00005	0.040
Pou4f1	-1.83	0.00005	0.040
Kdm5d	1.17	0.00005	0.040
Ddx3y	0.98	0.00005	0.040
Eif2s3y	1.09	0.00005	0.040
Ttr	0.88	0.00005	0.040
Moxd1	1.12	0.00005	0.040
Bhlhe22	0.92	0.00005	0.040
Satb2	0.89	0.00005	0.040
4930555G01Rik	-1.49	0.00005	0.040
Crh	-1.29	0.00005	0.040

E17.5 RNA-Seq.

Table 2-1: E17.5 RNA-Seq. RNA-Seq analysis comparing RNA expression in wild-type and *Foxd1*$^{-/-}$ E17.5 hypothalami. Differentially expressed genes were determined by q-value <0.05.

Gene	Fold Change (log2)	p Value	q value
Foxd1	-3.32	5.0E-05	0.015
Setd1b	-2.58	5.0E-05	0.015
Atn1	-2.38	5.0E-05	0.015
Nova2	-2.16	5.0E-05	0.015
Rnf165	-2.14	5.0E-05	0.015
Kdm6b	-2.10	5.0E-05	0.015
Shank1	-2.10	5.0E-05	0.015
Prr36	-1.99	5.0E-05	0.015
Mirg,Mir410,Mir412,Mir369	-1.91	5.0E-05	0.015
Mir6236	-5.10	5.0E-05	0.015
Brd4	-1.87	5.0E-05	0.015
Gltscr1	-1.86	5.0E-05	0.015
Zfhx2	-1.82	5.0E-05	0.015
Scrt2	-1.78	5.0E-05	0.015
Fus	-1.74	5.0E-05	0.015
Six3	-1.72	5.0E-05	0.015
Ncor2	-1.66	5.0E-05	0.015
Zmiz1	-1.60	5.0E-05	0.015
Proser1	-1.58	5.0E-05	0.015
Eif4ebp2	-1.58	5.0E-05	0.015
Cdk5r2	-1.54	5.0E-05	0.015
Bcl9	-1.50	5.0E-05	0.015
Prr12	-1.49	5.0E-05	0.015
St8sia2	-1.48	5.0E-05	0.015
Clip3	-1.47	5.0E-05	0.015
Bcl9l	-1.45	5.0E-05	0.015
Polr2a	-1.45	5.0E-05	0.015
Vamp2	-1.41	5.0E-05	0.015
Hipk2	-1.41	5.0E-05	0.015
Dvl3	-1.36	5.0E-05	0.015
Hist1h2bf	-1.32	5.0E-05	0.015
Kmt2d	-1.31	5.0E-05	0.015
Rere	-1.29	5.0E-05	0.015
Sox9	-1.27	5.0E-05	0.015
Zfhx3	-1.25	5.0E-05	0.015
Tubb4a	-1.25	5.0E-05	0.015
Fam98b	-1.23	5.0E-05	0.015
Arhgap33	-1.21	5.0E-05	0.015
Fign	-1.18	5.0E-05	0.015
Atp1a3	-1.11	5.0E-05	0.015
Hist1h2an	1.36	5.0E-05	0.015
Oc90	inf	5.0E-05	0.015
Atp1b2	-1.87	0.0001	0.029
Tcf7l1	-1.86	0.00015	0.039
Tox2	-1.61	0.00015	0.039
Xist	-1.16	0.00015	0.039
Trim67	-1.13	0.00015	0.039
Soga1	-1.08	0.00015	0.039
Slc25a23	-1.21	0.0002	0.049
Wiz	-1.15	0.0002	0.049
Nav1	-1.05	0.0002	0.049

E12.0/E12.5 RNA-Seq.

Table 2-2: E12.0/E12.5 RNA-Seq. RNA-Seq analysis comparing pooled RNA expression in wild-type and *Foxd1*$^{-/-}$ E12.0 and E12.5 hypothalami. Differentially expressed genes were determined by q-value <0.05.

Go Analysis: E12/E12.5 Pooled RNAseq Data		
Molecular Functions	**Genes**	**P Value**
beta-catenin binding	Kdm6b,Bcl9,Bcl9l,Dvl3,Sox9,Tcf7l1	2.0E-08
RNA polymerase II transcription coactivator activity	Atn1,Hipk2,Rere	7.1E-05
sodium:potassium-exchanging ATPase activity	Atp1a3,Atp1b2	0.00018
transcriptional activator activity, RNA polymerase II transcription factor binding	Atn1,Hipk2,Rere	0.00021
transcriptional repressor activity, RNA polymerase II activating transcription factor binding	Atn1,Hipk2,Rere	0.00021
potassium-transporting ATPase activity	Atp1a3,Atp1b2	0.00023
transcription corepressor activity	Atn1,Ncor2,Hipk2,Rere	0.00039
transcriptional repressor activity, RNA polymerase II transcription factor binding	Atn1,Hipk2,Rere	0.00077
protein C-terminus binding	Shank1,Brd4,Vamp2,Fign	0.00079
RNA polymerase II transcription cofactor activity	Atn1,Hipk2,Rere	0.00079
retinoid X receptor binding	Fus,Ncor2	0.00085
transcription coactivator activity	Atn1,Six3,Hipk2,Rere	0.0011
ionotropic glutamate receptor binding	Shank1,Fus	0.0014
transcription cofactor activity	Atn1,Six3,Ncor2,Hipk2,Rere	0.0016
retinoic acid receptor binding	Fus,Ncor2	0.0019
transcription factor activity, transcription factor binding	Atn1,Six3,Ncor2,Hipk2,Rere	0.0027
transcription factor activity, protein binding	Atn1,Six3,Ncor2,Hipk2,Rere	0.0028
transcription factor activity, RNA polymerase II transcription factor binding	Atn1,Hipk2,Rere	0.0029
ATPase activity, coupled to transmembrane movement of ions, phosphorylative mechanism	Atp1a3,Atp1b2	0.0029
histone-lysine N-methyltransferase activity	Setd1b,Kmt2d	0.0034
glutamate receptor binding	Shank1,Fus	0.0042
core promoter binding	Polr2a,Sox9,Zfhx3	0.0055
histone methyltransferase activity	Setd1b,Kmt2d	0.0057
Cellular Compartments		
nuclear chromatin	Brd4,Ncor2,Polr2a,Dvl3,Hist1h2bf,Hist1h2an	5.4E-05
ATPase dependent transmembrane transport complex	Atp1a3,Atp1b2	0.00022
ATPase complex	Atp1a3,Atp1b2	0.00026
chromatin	Brd4,Ncor2,Polr2a,Dvl3,Hist1h2bf,Hist1h2an	0.00045
DNA-directed RNA polymerase II, core complex	Brd4,Polr2a	0.00047
nuclear matrix	Atn1,Ncor2,Fign	0.00051
nuclear periphery	Atn1,Ncor2,Fign	0.0012
transmembrane transporter complex	Shank1,Vamp2,Atp1a3,Atp1b2	0.0025
dendritic spine	Shank1,Fus,Atp1a3	0.0026
transporter complex	Shank1,Vamp2,Atp1a3,Atp1b2	0.0026
neuron spine	Shank1,Fus,Atp1a3	0.0028
Biological Processes		
somatic stem cell population maintenance	Bcl9,Bcl9l,Sox9,Tcf7l1	5.5E-06
cell surface receptor signaling pathway involved in cell-cell signaling	Shank1,Six3,Bcl9,Bcl9l,Dvl3,Sox9,Tcf7l1	4.2E-05
developmental induction	Six3,Hipk2,Sox9	7.0E-05
canonical Wnt signaling pathway	Bcl9,Bcl9l,Dvl3,Sox9,Tcf7l1	0.00012
Wnt signaling pathway	Six3,Bcl9,Bcl9l,Dvl3,Sox9,Tcf7l1	0.00014
cell-cell signaling by wnt	Six3,Bcl9,Bcl9l,Dvl3,Sox9,Tcf7l1	0.00015
neural retina development	Six3,Hipk2,Sox9	0.00021
sodium ion export from cell	Atp1a3,Atp1b2	0.00024
cellular potassium ion homeostasis	Atp1a3,Atp1b2	0.00028
sodium ion export	Atp1a3,Atp1b2	0.00028
stem cell population maintenance	Bcl9,Bcl9l,Sox9,Tcf7l1	0.00033
maintenance of cell number	Bcl9,Bcl9l,Sox9,Tcf7l1	0.00037
adult behavior	Shank1,Zfhx2,Hipk2,Atp1a3	0.00045
response to transforming growth factor beta	Bcl9l,Hipk2,Sox9,Zfhx3	0.00049
potassium ion homeostasis	Atp1a3,Atp1b2	0.00065

E12.0/E12.5 GO analysis summary.

Table 2-3: E12.0/E12.5 GO analysis summary. A summary of the GO analyses and the genes which have been included for each category within biological processes, cellular compartments, and molecular function, and the associated p-value, for the E12.0/E12.5 RNA-Seq data set.

GO Analysis: E17.5 RNAseq Data		
Cellular Compartment	**Genes**	**P Value**
photoreceptor inner segment	Cdh23,Dynlt1b	0.0011
secretory vesicle	Dynlt1c,Dynlt1b,Avp,Oxt	0.0015
cytoplasmic microtubule	Dynlt1c,Dynlt1b	0.0021
Molecular Function		
neuropeptide hormone activity	Avp/Oxt/Crh	4.7E-06
hormone activity	Avp/Oxt/Ttr/Crh	1.1E-05
protein N-terminus binding	Dcn/Cdh23/Slc6a3	0.00030
transcriptional activator activity, RNA polymerase II transcription regulatory region sequence-specific binding	Foxd1/Neurod6/Neurod2/I	0.00055

Table 2-4: E17.5 GO analysis summary for cellular compartments and molecular function. A summary of the GO analyses and the genes which have been included for each category within cellular compartments and molecular function, and the associated p-value, for the E17.5 RNA-Seq data set.

Biological Processes	Genes	P Value
forebrain development	Zbtb18,Foxg1,Tbr1,Neurod6,Slc6a3,Eomes,Pou4f1,Bhlhe22,Satb2	8.9E-11
central nervous system neuron differentiation	Foxg1,Tbr1,Eomes,Pou4f1,Bhlhe22,Satb2	8.2E-08
pallium development	Zbtb18,Foxg1,Neurod6,Eomes,Bhlhe22	4.5E-07
pattern specification process	Foxg1,Foxd1,Tbr1,Eomes,Irx1,Bhlhe22,Satb2	6.2E-07
neuron fate commitment	Foxg1,Tbr1,Pou4f1,Satb2	1.7E-06
regionalization	Foxg1,Foxd1,Tbr1,Eomes,Irx1,Bhlhe22	2.2E-06
telencephalon development	Zbtb18,Foxg1,Neurod6,Eomes,Bhlhe22	4.0E-06
cerebral cortex development	Zbtb18,Foxg1,Eomes,Bhlhe22	4.8E-06
cell fate commitment	Foxg1,Tbr1,Eomes,Pou4f1,Satb2	9.1E-06
single-organism behavior	Cdh23,Tbr1,Avp,Neurod2,Oxt,Crh	1.1E-05
hindbrain development	Zbtb18,Tbr1,Neurod2,Pou4f1	2.1E-05
catecholamine transport	Slc6a3,Oxt,Crh	4.9E-05
multi-organism behavior	Avp,Oxt,Pou4f1	5.2E-05
regulation of female receptivity	Avp,Oxt	6.6E-05
axon guidance	Foxg1,Foxd1,Tbr1,Vax1	6.6E-05
neuron projection guidance	Foxg1,Foxd1,Tbr1,Vax1	6.7E-05
forebrain neuron differentiation	Foxg1,Tbr1,Satb2	6.7E-05
luteinizing hormone secretion	Foxd1,Crh	7.9E-05
axonogenesis	Foxg1,Foxd1,Tbr1,Vax1,Bhlhe22	8.2E-05
forebrain generation of neurons	Foxg1,Tbr1,Satb2	9.6E-05
monoamine transport	Slc6a3,Oxt,Crh	0.00010
forebrain neuron fate commitment	Tbr1,Satb2	0.00011
female mating behavior	Avp,Oxt	0.00011
axon development	Foxg1,Foxd1,Tbr1,Vax1,Bhlhe22	0.00011
limbic system development	Zbtb18,Tbr1,Neurod6	0.00012
penile erection	Avp,Oxt	0.00013
locomotory behavior	Cdh23,Avp,Slc6a3,Crh	0.00014
telencephalon regionalization	Eomes,Bhlhe22	0.00014
associative learning	Tbr1,Neurod2,Crh	0.00015
regulation of norepinephrine secretion	Oxt,Crh	0.00016
gonadotropin secretion	Foxd1,Crh	0.00016
norepinephrine secretion	Oxt,Crh	0.00016
positive regulation of digestive system process	Oxt,Crh	0.00016
maternal behavior	Avp,Oxt	0.00018
parental behavior	Avp,Oxt	0.00020
grooming behavior	Avp,Oxt	0.00023
norepinephrine transport	Oxt,Crh	0.00023
renal sodium excretion	Avp,Oxt	0.00027
regulation of renal sodium excretion	Avp,Oxt	0.00027
neuromuscular process	Cdh23,Slc6a3,Pou4f1	0.00032
negative regulation of nervous system development	Foxg1,Dynlt1b,Vax1,Neurod2	0.00034
feeding behavior	Tbr1,Oxt,Pou4f1	0.00036
copulation	Avp,Oxt	0.00038
forebrain regionalization	Eomes,Bhlhe22	0.00045
regulation of excretion	Avp,Oxt	0.00045
synaptic transmission, dopaminergic	Slc6a3,Crh	0.00058
mating behavior	Avp,Oxt	0.00062
response to cocaine	Slc6a3,Crh	0.00062
learning	Tbr1,Neurod2,Crh	0.00066
neuron migration	Foxg1,Vax1,Satb2	0.00069
regulation of neuroblast proliferation	Foxg1,Vax1	0.00070
muscle organ development	Zbtb18,Vax1,Eomes,Pou4f1	0.00075
regulation of renal system process	Avp,Oxt	0.00078
metanephric nephron development	Foxd1,Irx1	0.00082
striated muscle tissue development	Zbtb18,Vax1,Eomes,Pou4f1	0.00091
regulation of blood pressure	Avp,Oxt,Crh	0.0010
regulation of digestive system process	Oxt,Crh	0.0010
skeletal muscle tissue development	Zbtb18,Vax1,Eomes	0.0010
positive regulation of anion transport	Avp,Oxt	0.0011

Biological Processes cont.	Genes	P Value
muscle tissue development	Zbtb18,Vax1,Eomes,Pou4f1	0.0011
social behavior	Avp,Oxt	0.0011
intraspecies interaction between organisms	Avp,Oxt	0.0011
organic hydroxy compound transport	Slc6a3,Oxt,Crh	0.0011
skeletal muscle organ development	Zbtb18,Vax1,Eomes	0.0012
regulation of ion homeostasis	Dcn,Avp,Oxt	0.0012
behavioral fear response	Neurod2,Crh	0.0012
behavioral defense response	Neurod2,Crh	0.0013
regulation of catecholamine secretion	Oxt,Crh	0.0013
sodium ion homeostasis	Avp,Oxt	0.0013
reproductive behavior	Avp,Oxt	0.0013
fear response	Neurod2,Crh	0.0014
positive regulation of blood pressure	Avp,Oxt	0.0014
catecholamine secretion	Oxt,Crh	0.0014
excretion	Avp,Oxt	0.0015
mating	Avp,Oxt	0.0015
regulation of homeostatic process	Dcn,Avp,Oxt,Crh	0.0016
embryonic organ development	Cdh23,Foxg1,Eomes,Satb2	0.0017
positive regulation of homeostatic process	Avp,Oxt,Crh	0.0017
negative regulation of blood pressure	Oxt,Crh	0.0018
positive regulation of lipid transport	Oxt,Crh	0.0018
endocrine hormone secretion	Foxd1,Crh	0.0019
hippocampus development	Zbtb18,Neurod6	0.0021
neuroblast proliferation	Foxg1,Vax1	0.0022
positive regulation of ion transport	Avp,Oxt,Crh	0.0023
neuromuscular process controlling balance	Cdh23,Pou4f1	0.0024
regulation of amine transport	Oxt,Crh	0.0025
learning or memory	Tbr1,Neurod2,Crh	0.0026
positive regulation of cAMP biosynthetic process	Avp,Crh	0.0027
diencephalon development	Slc6a3,Pou4f1	0.0028
amine transport	Oxt,Crh	0.0028
positive regulation of cAMP metabolic process	Avp,Crh	0.0031
nephron tubule morphogenesis	Foxd1,Irx1	0.0033
nephron epithelium morphogenesis	Foxd1,Irx1	0.0034
cognition	Tbr1,Neurod2,Crh	0.0035
nephron morphogenesis	Foxd1,Irx1	0.0035
regulation of stem cell proliferation	Foxg1,Vax1	0.0037
negative regulation of neurogenesis	Foxg1,Dynlt1b,Vax1	0.0038
central nervous system neuron development	Foxg1,Bhlhe22	0.0038
positive regulation of cyclic nucleotide biosynthetic process	Avp,Crh	0.0038
renal tubule morphogenesis	Foxd1,Irx1	0.0038
sensory organ morphogenesis	Cdh23,Foxg1,Bhlhe22	0.0038
regulation of anion transport	Avp,Oxt	0.0039
regulation of neurological system process	Avp,Oxt	0.0040
skeletal muscle cell differentiation	Vax1,Eomes	0.0040
metanephros development	Foxd1,Irx1	0.0041
regulation of cytosolic calcium ion concentration	Cdh23,Avp,Oxt	0.0042
cell fate specification	Eomes,Pou4f1	0.0042
positive regulation of nucleotide biosynthetic process	Avp,Crh	0.0043
positive regulation of purine nucleotide biosynthetic process	Avp,Crh	0.0043
positive regulation of cyclic nucleotide metabolic process	Avp,Crh	0.0044
multicellular organismal response to stress	Neurod2,Crh	0.0045
palate development	Vax1,Satb2	0.0045
cerebellum development	Zbtb18,Neurod2	0.0046
embryonic organ morphogenesis	Cdh23,Foxg1,Satb2	0.0047
renal system process	Avp,Oxt	0.0047
response to alkaloid	Slc6a3,Crh	0.0049
kidney morphogenesis	Foxd1,Irx1	0.0049
nephron tubule development	Foxd1,Irx1	0.0049

Biological Processes cont.	Genes	P Value
digestive system process	Oxt,Crh	0.0050
regulation of body fluid levels	Avp,Slc6a3,Oxt	0.0051
regulation of lipid transport	Oxt,Crh	0.0051
negative regulation of cell development	Foxg1,Dynlt1b,Vax1	0.0052
regulation of neural precursor cell proliferation	Foxg1,Vax1	0.0052
modulation of synaptic transmission	Neurod2,Oxt,Crh	0.0053
endocrine process	Foxd1,Crh	0.0055
regulation of cAMP biosynthetic process	Avp,Crh	0.0056
renal tubule development	Foxd1,Irx1	0.0056
translational initiation	Ddx3y,Eif2s3y	0.0059
metencephalon development	Zbtb18,Neurod2	0.0059
nephron epithelium development	Foxd1,Irx1	0.0061
hormone transport	Foxd1,Ttr,Crh	0.0061
inner ear morphogenesis	Cdh23,Foxg1	0.0062
cAMP biosynthetic process	Avp,Crh	0.0065
mesoderm development	Eomes,Pou4f1	0.0067
regulation of cAMP metabolic process	Avp,Crh	0.0070
positive regulation of nucleotide metabolic process	Avp,Crh	0.0073
positive regulation of purine nucleotide metabolic process	Avp,Crh	0.0073
regulation of cyclic nucleotide biosynthetic process	Avp,Crh	0.0074
positive regulation of neuron differentiation	Foxg1,Dynlt1b,Neurod2	0.0081
regulation of purine nucleotide biosynthetic process	Avp,Crh	0.0083
regulation of nucleotide biosynthetic process	Avp,Crh	0.0084
regulation of synapse organization	Neurod2,Oxt	0.0084

Table 2-5: E17.5 GO analysis summary for biological processes. A summary of the GO analyses and the genes which have been included for each category within biological processes, and the associated p-value, for the E17.5 RNA-Seq data set.

2.2 DISCUSSION

Nothing is known about the role of the transcription factor *Foxd1* in the development of the hypothalamus and prethalamus. *Foxd1* is a member of the forkhead family of transcription factors, which have a highly conserved binding domain sequence, RTAAAYA. *Foxd1* most closely resembles its family member, *Foxd4*; they are nearly identical in their forkhead domain but differ greatly in the amino acid sequence bordering the forkhead domain and both are capable of bending DNA at least 80-90^{0} upon binding (Pierrou et al., 1994). Previous research has shown through *in situ* hybridization and fate-mapping experiments that Foxd1 is expressed early in the anterior hypothalamus and prethalamus, and is expressed at some point in development in every cell of the prethalamus and hypothalamus (Shimogori et al., 2010; Salvatierra et al., 2014). We have confirmed this, and also shown that *Foxd1* expression is turned on early, at least as early as E8.5, and is broadly expressed in the presumptive hypothalamus and prethalamus at this time. By E12.5, its expression is restricted to the ventricular zone of the prethalamus and anterior hypothalamus. Despite its early broad expression, loss of *Foxd1* appears to have a very selective effect on the development of the anterior hypothalamus. However, this is consistent with its prolonged expression in this area.

The transcriptional network governing development of the dorsal anterior hypothalamus (the PVN and PeVN) has already been somewhat well established. Work in zebrafish has shown that *Fezf2* and *Olig2* are necessary for expression of the dorsal anterior hypothalamic markers *Otp* and *Sim1* (Blechman et al., 2007; Borodovsky et al., 2009), and are expressed in mouse hypothalamus by E11.5 (Bedont et al., 2015; Shimogori et al., 2010; http://www.brain-map.org). *Otp*, *Sim1* and the Sim1 binding partner *Arnt2* are known to be responsible for terminal factor and neuropeptide expression in these areas (Bedont et al., 2015, Borodovsky et al., 2009; Acampora et al., 1999; Goshu et al., 2004; Hosoya et al., 2001; Michaud et al., 1998; Ryu et al., 2007; Wang and Lufkin, 2000). *Brn2* and *Sim2* act downstream of *Otp* and *Sim1*; *Brn2* is necessary for the expression for *Avp* and *Oxt* in the PVN and the SON, and *Crh* in the PVN, while *Sim2* is necessary for expression of *Trh* in the PVN and PeVN and Sst in the PeVN (Goshu et al., 2004; Nakai et al., 1995; Schonemann et al., 1995). Interestingly, every one of these genes was downregulated in *Foxd1*$^{-/-}$ mice at P0, with the exception of *Trh* in the PVN and PeVN. Avp was down in the PVN at P0, as determined by *in situ* hybridization, and it was one of the significantly downregulated genes in the RNA-Seq analysis performed at E17.5. *Sst* was lost from both the PVN and the PeVN, as determined by *in situ* hybridization at P0. Both *Oxt* and *Crh* were also significantly downregulated according to the RNA-Seq results from E17.5. These results suggest that *Foxd1* acts upstream of *Fezf2*/*Olig2*/*Otp*/*Sim1* to specify anterior hypothalamic fate, although there must

some sort of compensatory mechanism that is able to drive *Trh* expression in the PVN in the absence of *Foxd1*. *Sim1* expression was unaltered in *Foxd1*$^{-/-}$ mice at E12.5, but it may show altered expression at later time points. Further work will be needed to determine if expression of *Fezf2*, *Olig2*, *Otp*, *Sim1*, *Brn2*, and *Sim2* are disrupted in the dorsal anterior hypothalamus of *Foxd1*$^{-/-}$ mice at other time points, as we hypothesize.

Much less is known about the molecular determinants of SCN development (Abrahamson and Moore, 2001). Four transcription factors have been shown to be essential for SCN formation in the hypothalamus: *Six3*, *Six6*, *Lhx2*, and *Rax* (Clark et al., 2013; Roy et al., 2013; VanDunk et al., 2011; Orquera et al., 2016). In the studies of *Lhx2* and *Rax*, the latest time point examined was E12.5, so in neither case was the development of the mature markers of the SCN truly examined. Rather, both saw a loss of ventral anterior hypothalamic markers after deletion of either *Lhx2* or *Rax*. In *Lhx2* KO mice, there was a reduction of *Lhx1* in the ID and a complete loss of *Lhx1* in the most ventral portion of its expression domain, from which the SCN develops. In addition, *Arx* and *Vax1* were both significantly down in *Lhx2*$^{-/-}$ embryos (Roy et al., 2013). In contrast, in *Foxd1*$^{-/-}$ mice, only *Vax1* was down at E12.5, and not as significantly as in *Lhx2*$^{-/-}$ mice.

Rax expression is detected in the presumptive hypothalamus as early as E7.5. When it is deleted at around E8.0 to E8.5, there is a reduction in markers of mature postmitotic neurons in the anterior hypothalamus including *Th*, *Sst*, *Otp* and *Lhx1* at

E12.5 (Orquera et al., 2016). Although *Foxd1* and *Rax* are both expressed in early hypothalamic progenitors, and appear to be required for anterior hypothalamic specification, they are not redundant factors; *Rax* is required for early expression of anterior hypothalamic markers, while *Foxd1* appears to be required for their maintenance, since there was only a mild phenotype at E12.5 in the Foxd1 null mutants. *Rax* and *Foxd1* null mutants are also not identical at P0; Rax deletion reduces *Th* expression in the anterior hypothalamus, while Foxd1 deletion does not, despite the fact that *Th* does have a Foxd1 binding domain in its promoter, at least in humans (Zhang et al., 2010).

Six3 is expressed as early as E10.5 in the ventral hypothalamus, and overlaps Rax expression (VanDunk et al., 2011; Oliver et al., 1995). By E11.5, *Six6* is expressed in an overlapping domain in the anteroventral hypothalamus with *Six3*. Conditional knock-out of *Six3* from the hypothalamus resulted in a complete loss of *Rora* and *Avp* from the ventral anterior hypothalamus at E18.5 (VanDunk et al., 2011). In addition, there was no cell clustering in the SCN or other histological evidence for nucleogenesis, which is also the case in *Foxd1*$^{-/-}$ mice. It also appeared as though *Avp* was partially reduced in the PVN as well in these mutants, although the authors of the original paper claim that defects were restricted to the SCN. At E15.5, *Six3* deletion also resulted in a loss of *Lhx1* and *Rora* from the SCN.

Lhx1 is the first marker expressed in mature, postmitotic SCN neurons, but loss of *Lhx1* results in a milder phenotype than loss of *Foxd1* (Bedont et al., 2015;

Bedont et al., 2014). *Lhx1* appears to be responsible for terminal differentiation of the SCN, and expression of its neuropeptides, but conditional *Lhx1* mutants still have a SCN, as shown by expression of markers like *Vipr2* and *Gad67*, as well as DAPI staining showing cell aggregation and nucleogenesis (Bedont et al., 2014). This suggests that *Foxd1* is acting upstream of *Lhx1*, as *Foxd1*$^{-/-}$ mice show a much more severe SCN defect.

When considered in the context of our current understanding of SCN and anterior hypothalamic development, our results from the analysis of *Foxd1*$^{-/-}$ mice suggest a model in which *Foxd1* is necessary to maintain expression of *Six3* and *Vax1*, and the loss of anterior hypothalamic markers is then primarily a result of reduced *Six3* and *Vax1* expression. Both *Six3* and *Vax1* expression were reduced at E12.5. Both of these genes were also pulled out of the RNA-Seq analysis as significantly downregulated genes in the *Foxd1*$^{-/-}$ mice hypothalamus; *Six3* was significantly down at E12.5 and *Vax1* was significantly down at E17.5. *Six3*$^{-/-}$ mice show similar developmental deficits as *Foxd1*$^{-/-}$ mice at E18.5/P0, including a loss of any discernible anatomical SCN, as well as a complete absence of any *Lhx1* expression. While *Rora* and *Avp* were completely absent in the *Six3*$^{-/-}$ mutant, these markers were significantly down but not gone in *Foxd1*$^{-/-}$ mice. This is likely a reflection of the fact that *Six3* expression was not completely lost in *Foxd1*$^{-/-}$ mice at E12.5.

It is not known what effect loss of *Six3* has on more dorsal anterior hypothalamic structures. There may have been an effect on *Avp* expression in the PVN in the *Six3*$^{-/-}$ mice, but there was no examination of PeVN markers or other PVN markers (VanDunk et al., 2011). A closer examination of *Six3*$^{-/-}$ mice would determine if *Six3* is also necessary for dorsal anterior hypothalamic structures, perhaps upstream of *Otp*/*Sim1*.

Although *Six3* and *Vax1* expression were both reduced at E12.5, there was no defect observed in postmitotic markers of the anterior hypothalamus until E16.5. It is unclear if this is due to a delayed need for *Six3* and *Vax1* in maintaining expression of these genes, or if expression of *Six3* and *Vax1* was lost completely at later stages of development in *Foxd1*$^{-/-}$ mice. To test this, *Six3* and *Vax1* expression must be examined at later time points in the *Foxd1*$^{-/-}$ mutants, however the RNA-Seq results suggest that *Vax1* expression stayed down until P0.

While *Rax* is necessary for expression of *Lhx1* and *Sst* at E12.5, *Foxd1* is not; this suggests that that although *Rax* and *Foxd1* are expressed around the same time, *Rax* is necessary to drive their expression early in development, while Foxd1 is necessary to maintain their expression through regulation of *Six3* and *Vax1*. *Foxd1* and Lhx2 may show partial redundancy in the regulation of *Vax1*, and potentially *Six3* as well (since the role of *Lhx2* in control of *Six3* expression is unknown). Both *Foxd1* and *Lhx2* null mutants show reduced *Vax1* expression, but *Vax1* was

preserved in the more dorsal part of its domain in the Lhx2 null mutant, and in the more ventral portion in *Foxd1*$^{-/-}$ mice.

Foxd1 does not appear to be essential for survival of cells in the anterior hypothalamus, nor does it regulate proliferation. In contrast, *Lhx1* conditional knock-out mice have increased cell death in the SCN by P0, which accounts for the reduced size of the SCN (Bedont et al., 2014). There was no increase in cell death in *Foxd1*$^{-/-}$ mice, despite the lack of *Lhx1* at P0, which is likely due to the fact that *Lhx1* is expressed at normal levels at E12.5, and does not show reduced expression until E16.5. Thus, the lack of a discernible SCN at P0 is most likely due to a failure of cellular aggregation in this area.

It is unclear why loss of Foxd1 has no effect on the development of the prethalamus. *Foxd1* expression persists longest in progenitors in this brain region, and *Six3* expression is reduced in the prethalamus at E12.5 in *Foxd1*$^{-/-}$ mice. . However, we only examined a limited number of prethalamic markers and it is possible that loss of *Foxd1* has a subtle effect on prethalamic development which we have yet to discover. Alternatively, *Six3* may not be necessary for prethalamic development, due to compensation by other transcription factors in this area.

Further work must be done to better understand the role of Foxd1 in anterior hypothalamic development. Targeted overexpression of *Six3* or *Vax1* using *in utero e*lectroporation in *Foxd1*$^{-/-}$ embryos could determine if Foxd1 is acting solely

through regulation of these transcription factors, or if it is mediating anterior hypothalamic development through other means. There still remains the question of why the loss of *Foxd1* has a selective effect on the development of the anterior hypothalamus, despite being expressed throughout the hypothalamus and prethalamus. Other forkhead transcription factors may be able to partially compensate for the loss of *Foxd1*, such as *Foxm1*, which is broadly expressed throughout the hypothalamus at E11.5 and E13.5 (http://www.brain-map.org). Further research will be needed to address this question.

A: Transcriptional pathways governing the dorsal anterior hypothalamus

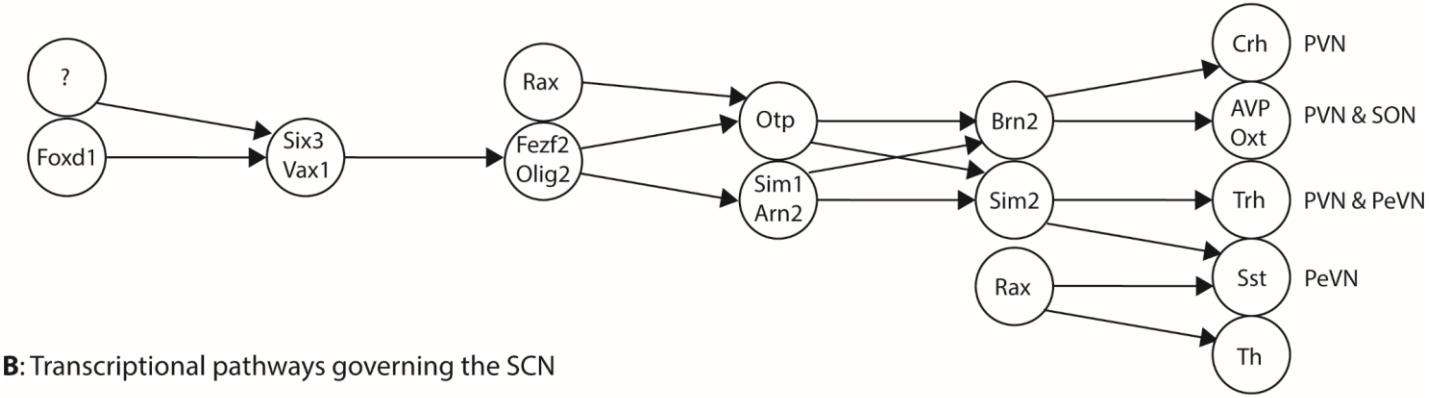

B: Transcriptional pathways governing the SCN

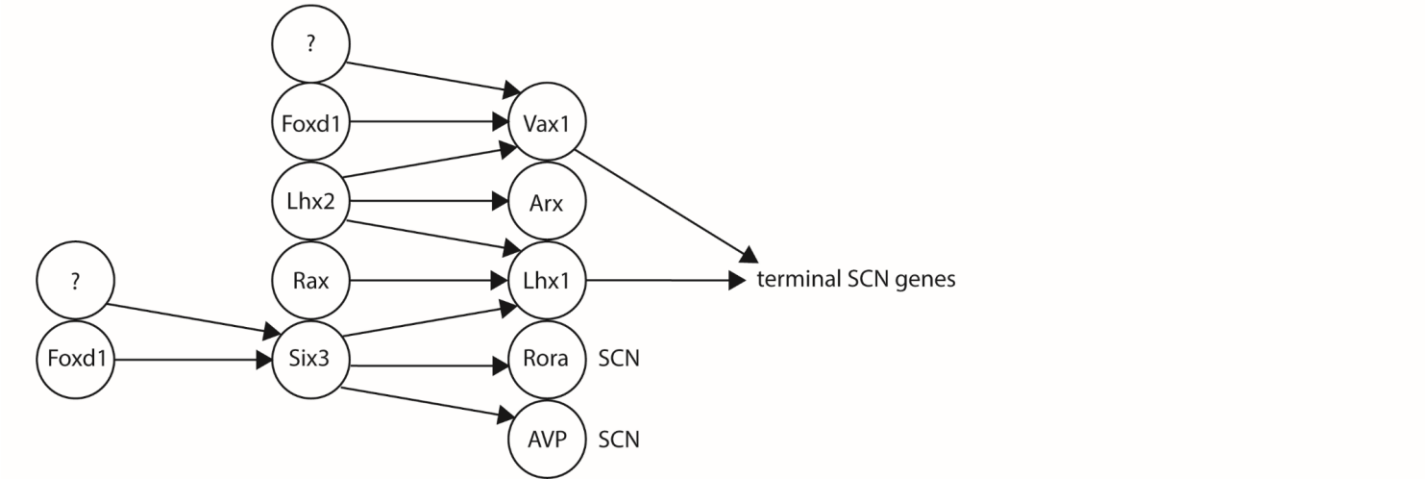

Figure 2-11: Schematic demonstrating our model of the role of *Foxd1* in anterior hypothalamic development. A: The known transcriptional regulatory pathways governing development of the dorsal anterior hypothalamus. We hypothesize that *Foxd1* regulates *Six3* and *Vax1*, which in turn may regulate *Fezf2* and *Olig2*. B: The transcription factors known to be involved in development of the SCN. We hypothesize that *Foxd1* is controlling SCN development through regulation of *Six3* and *Vax1*. In both the dorsal anterior hypothalamus and the SCN, we hypothesize that *Foxd1* is working in conjunction with other, unknown transcription factors, due to the incomplete loss of *Six3* and *Vax1* in the *Foxd1*-null animals.

2.3 METHODS AND MATERIALS

2.3.1 Embryo Collection

Matings were set up in the evenings and the presence of a plug the next morning indicated embryonic day 0.5 (E0.5). Embryos were harvested at embryonic day 12.5 (E12.5), E16.5, E17.5, E18.5 and P0. *Foxd1-Cre*$^{+/-}$ animals (Humphreys et al., 2008) were mated to each other to generated *Foxd1-Cre*$^{+/+}$ (*Foxd1*$^{-/-}$) embryos/pups.

2.3.2 High-Quality Chromogenic *In situ* Hybridization

Pregnant dams were sacrificed via cervical dislocation and the embryos were harvested into ice-cold 1xPBS (phosphate buffered saline) treated with DEPC. Embryos were dissected (tail samples were kept for genotyping) and their whole heads fixed in 4% PFA (paraformaldehyde) in 1xPBS-DEPC while rotating at 4^{0}C. Following fixation, embryos were washed 2x5 min in 1x-PBS-DEPC then sucrose sunk in 30% sucrose in 1xPBS-DEPC at 4^{0}C for a minimum of one day. Embryos were then embedded in gelatin (10% gelatin with 30% sucrose in 1xPBS-DEPC). Following hardening of the gelatin, the blocks were cut and stored in 4% PFA; 30% sucrose in 1xPBS-DEPC for a minimum of one week at 4^{0}C to allow the blocks to sufficiently fix before sectioning.

All steps after this point were done under RNAse-free conditions. The gelatin blocks were sectioned on a freezing microtome at 40μm thickness. Sections were collected in 1xPBS-DEPC and stored at 4^0C until mounting (stored for a maximum of 4 hours). Sections were mounted in 0.5x PB-DEPC (phosphate buffer) onto Superfrost Plus slides (Fisher Scientific) and allowed to dry vertically for a minimum of overnight to a maximum of two days. Following drying, sections were immediately put through the first day of the high-quality *in situ* hybridization protocol. All washes were performed in 5-slide mailers that had been treated with 0.3M NaOH. Briefly, slides were fixed in 4% PFA in 1xPBS-DEPC for 15 minutes followed by 3x5 minute washes in 1xPBS-DEPC (all done at room temperature). Slides were then digested in a proteinase K solution (1μg/ml in 100mM Tris-HCl pH 8.0 and 50mM EDTA pH 8.0) at 37^0C for 30 minutes, followed by another fixation with 4% PFA in 1xPBS-DEPC for 15 minutes at room temperature. Slides were then washed in 1xPBS-DEPC (3x5 min). At this point, slides were either placed in hybridization buffer and stored at -20^0C or immediately placed in hybridization buffer with probe and hybridized. For each new probe, 70μl probe was added to 1mL of hybridization buffer and heated at 80^0C in order to denature them, then immediately placed on ice before adding to the mailer for a total volume of 14mL hybridization buffer (including probe). Mailers with fewer than 5 slides were given RNAse-free blank slides. Used probe/hybridization solution was stored at -20^0C and used multiple times, refreshing with 15μl probe when needed. Slides were hybridized at 70^0C overnight in a hybridization oven. After hybridization,

RNAse-free conditions were no longer necessary. Slides were incubated in Solution X (50% formamide in 2x SSC and 1% SDS) 3x45 min at 70^{0}C. Slides were then washed 3x15 min in 1xTBST (25.0 mM Tris-HCl pH7.5, .136 M NaCl, 2.68 mM KCl, 1% Tween-20) at room temperature then blocked in 10% lamb serum in 1xTBST at room temperature for 1 hr. Slides were then incubated in preabsorbed primary antibody (1:5000 anti-DIG a.p. fab fragments; protocol below) in 1% lamb serum and 1xTBST, overnight at 4^{0}C. Following antibody incubation, the slides were washed in 1xTBST 3x15 min, then 1x10 min in NTMT (100 mM NaCl, 100 mM Tris-HCl pH 9.5, 50 mM $MgCl_2$, 1% Tween-20, 2mM levamisole). The slides were then developed in the color reaction step in NTMT containing the chromogens 5-bromo, 4-chloro, 3-indolylphosphate (BCIP) and nitroblue tetrazolium (NBT), at either room temperature or 4^{0}C. The color reaction was stopped in TE stop buffer (10 mM Tris-HCl pH 7.5, 50 mM EDTA pH 8.0) for a minimum of 1 hr, followed by DAPI staining for 5 min (1:5000 in 1xPBS) then a 1xPBS wash for 5 min. Slides were coverslipped with gelvatol and allowed to dry overnight before imaging.

2.3.3 Preabsorbed Antibody

Age appropriate embryo powder was rehydrated in 1xTBST at 70^{0}C for 30 min, rotating. It was cooled on ice for 10 minutes, then the primary antibody was added as

well as 1% lamb serum. It was then incubated at 4^0C for one hour, rotating. After allowing the solution and embryo powder to settle, the supernatant containing the antibody was taken and added to a solution of 1xTBST and 1% lamb serum.

2.3.4 Fresh-Frozen Chromogenic *In situ* Hybridization

Embryos were harvested fresh frozen and immediately embedded in OCT (Tissue-tek) and frozen on dry ice. Blocks were sectioned on the cryostat at 20μm thickness and immediately dry mounted onto Superfrost Plus slides. Slides were allowed to dry and then were stored at -80^0C. When ready to be used, the slides were allowed to thaw at room temperature a minimum of 30 min before beginning the protocol. The first day of the *in situ* hybridization was done under RNAse-free conditions, and all slide boxes and slide holders were soaked in 0.3M NaOH before use. All incubations were done at room temperature unless otherwise noted. Slides were fixed in 4% PFA in 1xPBS-DEPC for 10 min, then washed 3x 5 min in 1xPBS-DEPC. Slides were then incubated in acetic anhydride (.0027% in .1M TEA pH 8.0) for 10 min followed by another wash in 1xPBS-DEPC, 3x 5 min. Slides were then incubated in hybridization buffer for 2 hours prior to adding probe in hybridization buffer and coverslipping with siliconized coverslips. Slides were hybridized at 68^0C overnight. Probes were denatured at 80^0C for 5 minutes prior to hybridization. Hybridized slides were washed

in 5x SSC at 65^{0}C for approximately 45 min until the coverslips could be removed easily. Then the slides were washed in 0.2x SSC, 2x 45 min at 65^{0}C, followed by 1x 5 min at room temperature. Slides were then washed 1x 5 min in B1 buffer (.2M Tris-HCl pH 7.5, .3M NaCl) then blocked in 5% heat-inactivated sheep serum in B1 for 1 hour. Slides were incubated in primary antibody (1:5000 anti-DIG a.p. in 5% heat-inactivated in B1) overnight at 4^{0}C. Prior to developing, the slides were washed in B1 3x 5 min then 1x 5 min in B3 solution (.1 M Tris-HCl pH 9.5, .05 M $MgCl_2$, .1 M NaCl). The color reaction proceeded in B3 with BCIP and NBT with .24mg/mL levamisole) under dark conditions at either room temperature or 4^{0}C. The color reaction was extinguished in TE stop buffer (10 mM Tris-HCl pH 7.5, 50 mM EDTA pH 8.0). Slides were DAPI stained in 1:5000 DAPI in 1xPBS for 5 min, followed by a 1xPBS wash for 5 min before coverslipping with gelvatol. Slides were allowed to dry overnight before imaging.

2.3.5 Probes

Probes were generated using the following sequences as templates:

Probes	*GenBank accession #*
Arx	BE945936
Bsx	BC104386
Emx2	CB057818
Fgf15	BE952015
Foxa1	BC096524
Foxb1	BC111908
Foxg1	AW121918
Gsh2	AW491858
Irx5	AW492717
Isl1	AW125075
Lef1	BC038305
Lhx1	AI846049
Lhx5	BE943600
Lhx6	BC065077
Lhx9	AI854185
Nkx2.1	BC057607
Nr5a1	CD348290
Ntng2	AI850147
Otp	CA318525
Pitx2	BC075660
Pomc	AI849227
Rax	BC058757
Shh	BC063087
Sim1	Gift of C.M. Fan
Wnt8b	BC119544

2.3.6 EdU Staining and Cell Counting

Pregnant dams were injected with 50 mg/kg Edu (20 mg/mL in saline) on embryonic day E12.5 and then sacrificed via cervical dislocation 2 hours later. The embryos were harvested in ice cold 1xPBS and the whole heads fixed in 4% PFA in 1xPBS at 4^0C

overnight, rotating. The embryos were then washed 2x5 min in 1xPBS at 4^0C then sucrose sunk in 30% sucrose in 1xPBS and stored at 4^0C for a minimum of one day. Following cryoprotection, the embryos were embedded in OCT blocks on dry ice, then sectioned on a cryostat at 25μm thickness. Sections were immediately dry mounted onto Superfrost Plus slides and allowed to dry before storing at -20^0C. EdU staining was performed using the Click-iT EdU imaging kit from Invitrogen, then the slides were coverslipped using Vectashield. Stained slides were imaged at 40x on a Keyence microscope. Between 5 and 6 sections per animal were counted using ImageJ. All counting was done manually and blinded. The number of EdU-positive cells was taken as a fraction of the total area of the hypothalamus measured in μm^2. The values of the sections were averaged for each individual, and then compared using a 2-tailed t-test. Two animals per genotype were used.

2.3.7 TUNEL Staining

E12.5 embryos were harvested and post-fixed in 4% paraformaldehyde for a minimum of overnight at 4^0C. Slides were sucrose sunk in 30% sucrose in 1xPBS after 3x5 min 1xPBS washes. Following sucrose sinking, the embryos were embedded in OCT blocks on dry ice, and sectioned on a cryostat at 25μm thickness. Sections were immediately dry mounted onto Superfrost Plus slides and allowed to dry before

storing at -20^{0}C. Slides were allowed to thaw to room temperature until beginning the protocol. TUNEL staining was performed according to the protocol for cryopreserved tissue in the *In Situ* Cell Death Detection Kit-TMR red (Roche). A positive control was used (3000 U/mL DNAse I). Slides were DAPI stained then coverslipped using Vectashield, then imaged at 20x and 40x in the red channel on a Keyence microscope.

2.3.8 RNA-Seq

Hypothalami were dissected at E12.5 and stored at -80^{0}C. After genotyping, the RNA was extracted using the RNeasy kit from Qiagen. The RNA from each genotype were pooled and then sent for quality control analysis to determine concentration and purity via Nanodrop and electrophoresis. The E12.5 RNA had significant gDNA contamination, so DNAse digestion using the Qiagen kit was performed and then the RNA was resent for quality control before RNA-sequencing. A cDNA library was generated and barcoded for each pooled RNA sample, than sequenced to a paired-end read depth of 100 cycles using Illumina HiSeq 2500. The raw RNA-Seq results were mapped onto mm9 genome (NCBI37) using the default parameters in Tophat and Cufflinks (Trapnell et al, 2012) to generate gene expression FPKM (fragments per kilobase of exon per million). Cuffdiff was used to determine differentially expressed

genes between the control and mutant samples. Differentially expressed genes with a q-value of <0.05 were considered significant.

2.3.9 Immunohistochemistry

Embryos were harvested and post-fixed in 4% paraformaldehyde for a minimum of overnight at 4^0C. Slides were sucrose sunk in 30% sucrose in 1xPBS after 3x5 min 1xPBS washes. Following sucrose sinking, the embryos were embedded in OCT blocks on dry ice, and sectioned on a cryostat at 25μm thickness. Sections were immediately dry mounted onto Superfrost Plus slides and allowed to dry before storing at -20^0C. Before beginning immunohistochemistry, the slides were allowed to dry at room temperature, and then marked with a pap pen to isolate the sections. Slides were incubated in blocking buffer (10% HIHS in 0.1% TX-100 in 1xPBS) for at least two hours at room temperature, before incubating in primary antibody overnight at 4^0C. Antibodies used were as follows: rabbit anti-GFP 1:1000 (Life Technologies A6455 polyclonal) and rat anti-dsRed 1:1000 (Chromotek 5F8 monoclonal). Slides were washed 3x5 min in 1xPBS-T then incubated in secondary antibody in blocking buffer for two hours at room temperature. Secondary antibodies used were goat anti-rabbit-488 and donkey anti-rat-555. The slides were then washed 5 min in 1xPBS-T before DAPI staining in 1:5000 DAPII in 1xPBS-T for 5 min. Slides were then rinsed

3x5 min in 1x-PBS-T before coverslipping in Vectashield. Stained slides were imaged at 10x on a Keyence microscope.

3. WNT

3.1 RESULTS

3.1.1 Introduction

One of the many unanswered questions concerning hypothalamic development is the mechanism of patterning: how is the hypothalamus patterned such that anatomically and functionally diverse nuclei are specified in the correct location and relation to each other (Blackshaw et al., 2010)? The hypothalamus is unique in the brain for the complexity of its anatomy, which has complicated research into its development. One

way to better understand hypothalamic development has been to arrange it within a conceptual anatomical framework within the larger context of the forebrain, called the prosomere model. The prosomere model of forebrain development was originally proposed by John Rubenstein and Puelles in 1993, and held that the embryonic forebrain is composed of segmented domain structures known as "prosomeres," analogous to the rhombomeres of the hindbrain. Originally the theory held that there were 6 prosomeres (p1-p6), which were divided into the diencephalon (p1-p3), including the thalamus and prethalamus, and the secondary prosencephalon (p4-p6) including the hypothalamus and telencephalon (Rubenstein et al., 1994). In 2003, Rubenstein and Puelles updated the model due to new gene expression data (Puelles et al., 2000; Bulfone et al., 1995), Rohr et al., 2001). The p4-p6 prosomeres were condensed into the secondary prosencephalon which they divided into the telencephalon and the rostral diencephalon (hypothalamus) (Puelles and Rubenstein, 2003). The model maintained that these separate domains (p1-p3 and the secondary prosencephalon) and their corresponding unique gene expression patterns, are indicative of separate patterning mechanisms. Most importantly, it suggested that the hypothalamus and the prethalamus (located in p3) are patterned independently of each other[2].

[2] Since beginning this research, the prosomere model has been updated yet again, this time dividing the secondary prosencephalon into two hypothalamo-telencephalic prosomeres (hp1 and hp2) (Ferran et al., 2015). They argue that one would "expect[s] some differential molecular pattern across adjacent neuromeres that share other determinants…In that case, the crucial expected observation is that various partial zonal or microzonal patterns restricted to each of the units show

Gene expression data from a large screen (Shimogori et al., 2010), suggests that the prosomere model is inaccurate as regards the separation of the hypothalamus and prethalamus. Several genes (*Foxd1*, *Isl1*, *Emx2*, *Zfp312*, *Pitx2* and *Gdf10*) have expression patterns composed of stripes which transverse both the hypothalamus and prethalamus. Such contiguous gene expression patterns should not exist according to the prosomere model, and may have been missed due to the late timepoint (E15.5) used when developing the prosomere model. These stripes comprise parallel domains across the AP axis. These data suggest that the prethalamus and hypothalamus are more linked developmentally than suggested by the prosomere model and may be patterned together.

Little is known about how the hypothalamus and prethalamus develop and so to determine if they are patterned together, it was necessary to uncover a common patterning mechanism. Elsewhere in the nervous system, development is governed by a combination of intrinsic factors (such as transcription (Virolainen et al., 2012) and competency factors) and extrinsic factors (such as morphogens (Alvarez-Bolado et al., 2012)). Cells must then integrate this information in a probabilistic, rather than

a common transverse boundary that agrees with the postulated interneuromeric border." In other words, stripe gene expression patterns, such as those shown in Shimogori et al., 2010, can be ignored as long as smaller domains within the postulated prosomeric boundaries conform to their preconceived determination of their boundaries, i.e. their model is based on gene expression patterns until it is not. However by ignoring gene expression domains that run counter to the basic tenets of the prosomere model, one runs the risk of missing the clues such expression patterns suggest about potential patterning mechanisms which may exist that violate their model, such as the one discussed in this thesis.

deterministic, fashion, within the context of a larger overall selective process to maintain the correct population size of a particular cell type (Descalzo and Arias, 2012).

Morphogens are especially important in areas of high neuronal subtype diversity. They are often secreted from a single source (often an organizer) which establishes a concentration gradient so that progenitors at increasing distance from the source receive proportionally less morphogen signal. For example, in the spinal cord, Wnt and Shh are secreted in an opposing concentration gradient from the roof plate and floor plate, respectively (Yu et al., 2008; Alvarez-Medina et al., 2008). These two molecules together pattern the spinal cord and specify different neuronal subtypes found along the dorso-ventral axis, although Bmp plays a much more important role than Wnt in dorsal patterning.

There is evidence to suggest that Wnts may be similarly involved in hypothalamic and prethalamic development. There are two primary classes of Wnt signaling pathways: β-catenin dependent (canonical) and β-catenin-independent (non-canonical) signaling (Valenta et al., 2012). In the canonical signaling pathways, under basal conditions, cytosolic β-catenin (i.e. not actively involved in adherens junctions) is targeted for degradation by a destruction complex (Hagemann et al., 2015). Upon Wnt binding to its Frizzled receptor, it triggers the inhibition of the destruction complex, thereby allowing cytosolic β-catenin to accumulate in the cell and enter the nucleus where it activates (or in some cases, represses) target genes through its

interactions with the Tcf/Lef family of transcription factors (Freese et al., 2010, Logan and Nusse, 2004, Hagemann et al., 2015). Canonical Wnt signaling has been implicated in Wnt-mediated patterning elsewhere in the central nervous system, where it often serves as a posteriorizing factor (Gulacsi and Anderson, 2008; Bluske et al., 2012; Kapsimali et al., 2004), and we suspected its involvement in the hypothalamus and prethalamus as well. Our goal, therefore, was two-fold: to demonstrate the role of canonical Wnt signaling in patterning of the hypothalamus and prethalamus, and by so doing, determine whether these two structures are patterned together as a single developmental unit.

3.1.2 Loss of Canonical Wnt Signaling Results in an Anteriorized Hypothalamus and Displaced Pituitary

There are two main sources of Wnt within the developing hypothalamus, as well as a third source of Wnt within the zona limitans intrathalamica (ZLI) (an organizer adjacent to the developing prethalamus): Wnt8b in the mammillary, which forms a contiguous stripe with Wnt3/3a in the prethalamus, and Wnt7a/b in the prethalamus and anterodorsal hypothalamus (Clements et al., 2009) (Figure 1 A, B). They are expressed at different times and most likely serve different developmental functions. Wnt 3/3a and Wnt8b are first expressed at embryonic day 8.5 (E8.5), well before hypothalamic neurogenesis begins (Byerly and Blackshaw, 2009) (Figure 1A),

suggesting that it may regulate spatial identity within the developing hypothalamus. This is supported by studies in zebrafish showing that Wnt8b and Lef1 are important for neurogenesis (Wang et al., 2009; Lee et al., 2006) and differentiation in the posterior hypothalamus (Wang et al., 2012). We therefore hypothesized that a Wnt8b concentration gradient established from the posterior mammillary region patterns the murine hypothalamus through β-catenin-dependent signaling. In addition to this posterior-restricted expression of Wnt8b prior to neurogenesis, we observed Wnt7a/b expression in hypothalamic and prethalamic interneuron progenitors, coincident with the onset of neurogenesis (~E10.5, Figure 1B). The role of Wnt7a/b in interneuronal development is unclear. Given the many developmental functions of Wnts, it may have a role in progenitor proliferation or neuronal subtype specification and differentiation.

To address the role of canonical Wnt signaling in patterning of the hypothalamus alone, we utilized a Cre line driven by the *Nkx2.1* gene promoter. *Nkx2.1* is one of the earliest markers of the presumptive hypothalamus and is turned on early in development, approximately E9.0-9.5. It is expressed along the ventral surface of the anterior-posterior (AP) axis but is excluded from more dorsal structures. Crucially, it is not expressed in the prethalamus (Figure 1C). By crossing *Nkx2.1-Cre*$^{+/-}$*; β-catenin*$^{f/+}$ mice to floxed *β-catenin*-expressing mice, we were able to selectively delete *β-catenin* from early hypothalamic progenitors.

If canonical Wnt signaling was functioning to posteriorize the hypothalamus, then by removing *β-catenin* we would expect to see an anteriorization phenotype; an expansion of anterior structures at the expense of posterior structures, and concomitant loss of markers of posterior structures. This is indeed what we saw. Markers of the supramammillary nucleus, including *Foxa1* (Figure 2 A, B) and *Irx5* (Figure 2 C, D) were significantly reduced. The mammillary was similarly affected, with *Foxb1* (Figure 2 E, F), *Sim1* (black arrowheads, Figure 2 G, H; Figure 4 A-J) and *Zfp312* (data not shown) all significantly down. The gene *Lef1*, in addition to being a marker of the premammillary nucleus (PMN), is also one of the early effector genes of canonical Wnt signaling and so was an effective readout of the level of reduction achieved in our loss-of-function (LOF) mutants. It was significantly reduced in the premammillary (Figure 2 I, J), although not eliminated, suggesting that we did not achieve a complete ablation of canonical Wnt signaling, but further confirming the posterior phenotype. *Sim1* expression in the paraventricular nucleus (PVN) was unaffected (open arrowheads, Figure 2 G, H; Figure 4 A-J), however, likely because *Nkx2.1* is not expressed in this area and thus the Nkx2.1-Cre is not active here. Conversely, anterior structures appeared to have expanded posteriorly, filling the void left by the loss of the posterior structures. Both *Pomc* (a marker of the arcuate nucleus; Figure 2 Q, R; Figure 3 I-R) and *Nr5a1* (a marker of the ventromedial hypothalamus (VMH); Figure 2 S, T; Figure 3 S-B') were expanded into the posterior hypothalamus.

Canonical Wnt signaling plays an important role in proliferation in the hypothalamus, so it was unsurprising that there appeared to be a significant thinning of the ventral surface of the hypothalamus in the LOF mutants. This can be seen most dramatically with *Arx* (Figure 2 O and P), which is normally expressed as a stripe through the more dorsal part of the hypothalamus, but in the LOF mutants was directly abutting the ventral surface. A similar phenotype can be seen with *Isl1* (Figure 2 M and N), which is normally expressed in a stripe from the prethalamus through the hypothalamus, excluding the posterior hypothalamus, but which occupies the ventral portion of the posterior hypothalamus in the LOF mutant. Another affected marker was *Lhx6*, which is normally expressed in the tuberomammillary terminal (TT) and the intrahypothalamic diagonal (ID). In the LOF mutants, the long TT was significantly reduced (open arrowheads, Figure 2 K, L; Figure 3 A-H) and the ID, which is normally a more dorsal structure, is positioned close to the ventral surface of the hypothalamus (black arrowheads, Figure 2 K, L; Figure 3 A-H). *Nkx2.1* itself was also affected; although its expression pattern was not grossly altered, there was a clear reduction in the thickness of its expression area, corresponding to the thinned ventral portion of the hypothalamus (Figure 4 K-U).

An unexpected phenotype we observed was a misplacement of the pituitary gland. Normally, the pituitary gland is formed from two structures: Rathke's pouch, which forms the anterior pituitary, originates off of the roof of the oral ectoderm and migrates to meet the posterior pituitary, and the posterior pituitary which forms from

a bud off of the ventral hypothalamus itself. The intermediate lobe then forms from the posterior portion of the anterior pituitary (Davis and Camper, 2007; Gaston-Massuet et al., 2016). The ventral hypothalamus secretes factors such as Fgf8 which are crucial for this process to occur. In the LOF mutants, the pituitary was displaced and invading the hypothalamus proper, forming a wedge within it that can be seen most clearly in the sections stained for *Nr5a1* (open arrowheads, Figure 3 S-B') and *Nkx2.1* (open arrowheads, Figure 4 K-U). This phenotype was likely a byproduct of the disruption of the hypothalamus and altered levels of signaling molecules to the pituitary.

The use of the *Nkx2.1-Cre*, while informative for investigating the role of canonical Wnt signaling within the hypothalamus proper, did not allow us to address the possibility of coupled patterning between the prethalamus and hypothalamus. We therefore utilized a different Cre-line driven by a gene which is expressed throughout the whole of the prethalamus and hypothalamus during development, Foxd1 (Figure 1D), and again crossed it to a floxed *β-catenin* line to generate *Foxd1-Cre;Ctnnb1*$^{lox/lox}$ mice, in which *β-catenin* is selectively deleted from neural progenitors within the hypothalamus and prethalamus starting at approximately E8.5.

The phenotype observed for the LOF mutants using the *Foxd1-Cre* was in most respects similar to that achieved with the *Nkx2.1-Cre*; notably, a reduction in posterior structures, and an expansion of anterior ones (these results are summarized in Figure 15). *Lef1* in the premammillary was reduced but not absent (and less so than in the

Nkx2.1-Cre driven LOF), indicating again that *β-catenin* was not completely excised in *Foxd1-Cre;Ctnnb1*$^{lox/lox}$ mutants. However, the consistent anteriorization phenotype seen suggests that even a modest reduction in canonical Wnt signaling can affect hypothalamic patterning. *Pitx2* (open arrowheads, Figure 5 M, N), *Shh* (open arrowheads, Figure 5 S, T) and *Otp* (open arrowheads, Figure 5 K, L) in the supramammillary and mammillary were significantly reduced in the LOF mutant, as was *Sim1* in the mammillary (red arrowheads, Figure 5 Q, R). Surprisingly, we saw no phenotype in more dorsal structures such as the PVN, even though *Foxd1-Cre* is expressed there (unlike the *Nkx2.1-Cre*) and although there is a small, local source of Wnt8b (open arrowhead, Figure 10 S) and corresponding *Lef1* expression in the anterior hypothalamus (yellow arrowhead, Figure 9 I). This can be seen with *Otp* (black arrowheads, Figure 5 K, L) and *Sim1* (black arrowheads, Figure 5 Q, R). There was also no phenotype within the prethalamus, which is shown by *Arx* (black arrowheads, Figure 5 A, B), and *Isl1* (black arrowheads, Figure 5 C, D), despite strong expression of the *Cre* there and its close proximity to the source of Wnt8b in the mammillary area of the hypothalamus.

We observed in this mutant model a similar thinning of the ventral surface of the hypothalamus as was seen in *Nkx2.1-Cre;Ctnnb1*$^{lox/lox}$ mice. This can be most clearly appreciated with *Arx* (Figure 5 A, B; Figure 6 A-F)) and *Isl1* (Figure 5 C, D; Figure 6 G-L)) in which the hypothalamic expression domains were significantly thinned and closer to the ventral surface of the hypothalamus than in the control condition. A

similar defect was seen with *Lhx6*, which is expressed in the ID and TT (Figure 5 G, H). As in *Nkx2.1-Cre; Ctnnb1*$^{lox/lox}$ mice, in these mutants, the TT was completely absent (black arrowhead, Figure 5 G, H) and the ID (open arrowhead, Figure 5 G, H) was positioned more ventrally than in controls. Similarly, *Lhx9*, which is normally expressed in a dorsal stripe parallel to the AP axis of the ventral surface of the hypothalamus, was instead positioned perpendicular to, and in near contact with, the ventral surface (black arrowheads, Figure 5 I, J, Figure 6 M-R).

Given the well-documented role of canonical Wnt signaling in proliferation during development, we hypothesized that the thinned hypothalamic neuroepithelium was a result of reduced proliferation. To test this, we injected pregnant dams with EdU on day E12.5, and sacrificed them two hours later. We stained for EdU and counted all EdU positive cells relative to total area within the hypothalamus and prethalamus. However, we saw no significant difference in EdU-positive cells between control and LOF animals (Figure 7). We also performed TUNEL staining on E12.5 tissue and saw no increase in apoptosis at this time in the LOF mutants (data not shown), although there was very little cell death observed in the control tissue (approximately 1-2 TUNEL-positive cells per section). It is possible that we may have captured a difference had we looked at proliferation and cell death earlier in development (neurogenesis begins at approximately E10.5 in mouse hypothalamus).

3.1.3 Constitutively Active Canonical Wnt Signaling Results in Disrupted Patterning of the Hypothalamus Pituitary and Prethalamus

If loss (or knockdown) of canonical Wnt signaling leads to a reduction in posterior structures and a corresponding expansion of anterior structures, then we would expect that enhanced canonical Wnt signaling should have the opposite effect on hypothalamic development. To test this, we generated a constitutively active form of β-catenin by deleting the inhibitory domain of the gene. We achieved this using a line in which the third exon (containing the phosphorylation site which targets it for degradation) was floxed, and then crossed it to our *Foxd1-Cre* line to generate *Foxd1-Cre ;Ctnnb1*$^{ex3lox/\ ex3lox}$, a specific gain-of-function (GOF) mutation within the prethalamus and hypothalamus. We hypothesized that we would see a posteriorization of the hypothalamus, with an expansion of posterior markers and a corresponding reduction in anterior markers. The result, however, was much more complex, and less straightforward, than we anticipated (these results are summarized in Figure 15).

We observed an overall hyperproliferation phenotype (via EdU staining, Figure 7C) resulting in a gross morphological defect consisting of a bend in the ventral surface of the hypothalamus, forming two bulges on either side. This defect can be seen most clearly via MRI (Figure 8). The MRI demonstrated that the 3rd ventricle was distended and misshapen in the GOF mutants. This had the effect of disrupting the normal organization of the radial glia which form the ventricular zone. In addition,

the neuroepithelium of the hypothalamus was significantly thicker, resulting from the hyperproliferation defect. However, despite these morphological changes, there was no alteration in the position of the diencephalic-telencephalic junction (DTJ), delineated by *Foxg1* expression in the telencephalon (Figure 10 E, F).

The canonical Wnt-signaling effector gene, *Lef1*, is normally expressed in the premammillary (green arrowhead, Figure 9I), ID (open arrowhead, Figure 9I), anterior hypothalamus (yellow arrowhead, Figure 9I), and prethalamus bordering the ZLI (red arrowhead and black arrowhead, respectively, Figure 9I). In *Foxd1-Cre;Ctnnb1*$^{ex3/\ ex3}$ mice, Lef1 staining was expanded, filling the entirety of the hypothalamus and prethalamus (Figure 9J). However, there was a clear mosaicism to the signal, suggesting that the Cre was not fully efficient.

There were two posterior markers which were expanded, as we expected: *Pitx2* in the supramammillary and mammillary (open arrowheads, Figure 9 K, L; open arrowheads, Figure 12 S-X) and *Lhx5* in the mammillary (open arrowheads, Figure 9 O, P), which both showed expansion into the anterior domain. However, all other markers of the posterior hypothalamus were either unaffected, or reduced. The nuclear domain of *Foxb1* expression in the mammillary was significantly reduced (black arrowheads, Figure 9 G, H), but the migratory *Foxb1*-positive neuronal population that originates in the mammillary was expanded throughout the hypothalamus in the mutants (open arrowheads, Figure 9 G, H). *Sim1* staining in the mammillary was completely absent (red arrowhead, Figure 10 Q, R), while *Emx2* expression was

relatively unaffected (Figure 9 E, F). *Wnt8b* itself was reduced in the mammillary, suggesting a negative feed-back loop (black arrowheads, Figure 9 S, T), while *Lhx1* was reduced but still present in the mammillary (black arrowheads, Figure 9 M, N).

Another marker which was expanded was *Lhx9*, a marker of orexinergic cells (Shimogori et al., 2010). *Lhx9* is normally expressed in a thin stripe domain in the dorsal hypothalamus, just ventral to the *Lhx6* stripe of the ID and the hypothalamic domain of *Arx* expression (Shimogori et al. 2010). In *Foxd1-Cre;Ctnnb1*$^{ex3/\ ex3}$ mice, Lhx9-positive cells were expanded posteriorly, and showed significant disruption of the normal condensed stripe pattern (black arrowheads, Figure 9 S, T and Figure 12 G-L).

More medial and dorsal structures such as the ID (*Lhx1*: red-outlined arrowhead, Figure 9 M, N; and *Lhx6*: open arrowhead, Figure 9 Q, R; Figure 12A) and the TT (Lhx6: black arrowhead, Figure 9 Q, R; Figure 12 B, C) were completely absent. The PVN appeared to be relatively unaffected. *Sim1* expression was distorted by the bending of the hypothalamus, but the overall level was fairly similar (open arrowheads, Figure 10 Q, R). *Rax* expression in the PVN was potentially expanded (open arrowheads, Figure 10 I, J).

Lhx1 staining in the ventral anterior hypothalamus (and presumptive suprachiasmatic nucleus) was lost (open arrowhead, Figure 9 M, N), however *Fgf15* in the more dorsal portion of the ventral anterior hypothalamus was preserved, albeit

more diffuse (open arrowheads, Figure 10 A, B). In the arcuate, *Pomc* expression was diffuse, mosaic, and severely disorganized, including displaced *Pomc*-positive cells in the dorsal hypothalamus (Figure 10 C, D and Figure 13 A-F).

We found two main phenotypes when examining stripe markers. The most ventral stripe markers, *Rax* and *Nkx2.1*, were both lost from their anterior expression domains, with only limited, extremely mosaic [3] expression in the posterior hypothalamus remaining (Figure 10 G, H and Figure 13 G-L; black arrowheads, Figure 10 I, J, respectively). The more dorsal stripe markers *Arx* and *Isl1*, which are both expressed in stripes from the prethalamus down through the basal plate of the hypothalamus to the anterior hypothalamus, were both significantly down, although there was some variability among embryos in the extent of the defect, probably a reflection of variability in Cre activity. In the case of *Arx*, most *Foxd1-Cre;Ctnnb1*$^{ex3/ex3}$ embryos lost all expression in the hypothalamus (open arrowheads, Figure 11 A-F), although one embryo tested had some diffuse *Arx* staining in its large hypothalamic mass (data not shown). *Isl1* expression was completely absent from one *Foxd1-Cre ;Ctnnb1*$^{ex3/ex3}$ mouse (data not shown). In another, there was diffuse staining in the

[3] The mosaicism observed with many of the markers tested as well as Lef1 itself is likely a function of the Cre and its incomplete excision activity. We suspect that much of the mosaicism may reflect cells which have failed to excise the autoinhibitory domain of the β-catenin gene. The only way to test this would be to perform two-color *in situ* hybridization to determine if there is any co-localization between Lef1 and the mosaic expressed genes (Pomc, Fgf15, Rax, and Nkx2.1); we would expect not to see any colocalization.

hypothalamic mass, much like the staining seen with *Arx* (open arrowheads, Figure 11 M-R). There was one mutant in which *Isl1* expression was reduced, but present in the correct location in the hypothalamus, and its expression in the anterior hypothalamus was preserved as well (open and red arrowheads, respectively, Figure 10 M, N). The morphogen *Shh*, which is also expressed in a stripe extending through the ZLI and basal plate of the hypothalamus, was completely unaffected in the hypothalamus (open arrowheads, Figure 10 K, L).

Since *Foxd1*, and thus the *Foxd1-Cre*, is expressed in the prethalamus and adjacent to the ZLI (an organizer regulating development of the thalamus), and since *Lef1* is also expressed in the prethalamus with a strong zone of expression along the ZLI, we expected to observe a patterning defect in these areas. However, the ZLI was completely unaffected, as indicated by expression of *Shh* (black arrowheads, Figure 10 K, L), *Pitx2* (black arrowheads, Figure 9 K, L; Figure 12 S, V), *Lhx1* (green arrowheads, Figure 9 M, N; black arrowheads, Figure 11 S-X), *Lhx5* (expressed in a zone adjacent to the ZLI; black arrowheads, Figure 9 O, P), and *Sim1* (black arrowheads, Figure 10 Q, R). Development of the prethalamus was disrupted, but it was not a patterning defect *per se*. The prethalamus was moderately reduced in size, but still expressed the markers *Fgf15* (black arrowheads, Figure 10 A, B) and *Gsh2* (Figure 9 C, D). *Arx* (black arrowheads, Figure 9 A, B and Figure 11 A-F) and Isl1 (black arrowheads, Figure 10 M, N and Figure 11 M-R) were both reduced to a small portion immediately adjacent to the ZLI. *Lhx1* was completely absent from the prethalamus (red

arrowhead, Figure 9 M, N). In contrast, the thalamic eminence, which sits directly adjacent and anterior to the prethalamus, was completely preserved in the GOF mutants as indicated by *Lhx1* (yellow arrowheads, Figure 9 M, N), *Lhx5* (yellow arrowheads, Figure 9 O, P), *Lhx9* (yellow arrowheads, Figure 9 S, T) and *Wnt8b* (red arrowheads, Figure 10 S, T).

In collaboration with Richard Dorsky, we tested two markers which had been pulled out of a RNA-Seq screen his lab performed on *Lef1*-knockout zebrafish: *Bsx* and *Ntng2*. Both of these genes are expressed in a dorsal stripe in the premammillary, although Bsx also has an arcuate domain and *Ntng2* is expressed in a stripe through the ZLI. Given that they were significantly reduced in the *Lef1*$^{-/-}$ zebrafish, we expected to see an expansion in these markers in our GOF mutants. *Bsx* was preserved (but not expanded) in the premammillary (black arrowheads, Figure 11 G-L) but was completely absent from the arcuate domain (open arrowheads, Figure 11 G-L). In contrast, *Ntng2* in the premammillary was significantly expanded, as we expected (open arrowheads, Figure 10 O, P and Figure 12 M-R) although the ZLI expression domain was normal (black arrowheads, Figure 10 O, P and Figure 12 M-R).

Intriguingly, while the *Nkx2.1-Cre;Ctnnb1*$^{lox/lox}$ LOF mutants had a displaced pituitary invading the hypothalamus proper, in our *Foxd1-Cre ;Ctnnb1*$^{ex3/ ex3}$ GOF mutants we observed the exact opposite phenotype, although there was considerable variability in the severity of the phenotype. Instead of migrating from the oral

ectoderm to the ventral hypothalamus, the anterior pituitary remained stuck to the room of the mouth (red arrowhead, Figure 14 A-B). In addition, there was a fate change within the pituitary. Normally, only the intermediate lobe expresses *Pitx2* and *Pomc* but in the GOF mutants, the entire pituitary expressed *Pomc* (black arrowheads, Figure 14 A, B) and the *Pitx2* expression domain was significantly expanded (black arrowheads, Figure 14 C, D).

3.1.4 Constitutively Active Shh Signaling Does Not Disrupt Hypothalamic Patterning

Our study of canonical Wnt regulation of hypothalamic and prethalamic patterning via knockdown and over-activation of its effector protein is a classic approach at teasing out the functions of known signaling molecules. This method, although very fruitful in some ways, does not take into account the developmental milieu in which Wnt is operating. In the hypothalamus, Wnt is expressed concurrently and in a partially overlapping expression domain with another important morphogen, Shh, although Shh's expression begins earlier and changes dynamically over the course of development. We hypothesized that the complex phenotype observed in *Foxd1-Cre;Ctnnb1*$^{ex3/+}$ mice might be a result of concurrent changes in Shh signaling, which would explain why we do not see a simple posteriorization phenotype as expected.

Previous research has looked at the effects of loss-of-function of Shh signaling on development of the hypothalamus (Shimogori et al., 2010). They used *Nkx2.1-Cre* to delete *Shh* from the hypothalamic neuroepithelium starting at approximately E9.5. In contrast to the anteriorization we observed using the same *Cre* to knockdown canonical Wnt signaling in the hypothalamus, they observed the opposite phenotype: a loss of anterior hypothalamic markers and a preservation of posterior markers resulting in an overall posteriorization of the hypothalamus. Combining these two data sets starts to paint a picture of how hypothalamic patterning might occur under the dueling forces of the posteriorizing Wnt and the anteriorizing Shh, however, a study performed in zebrafish complicates this simple narrative and may help explain our complex GOF phenotype. In their study, Wnt was found to inhibit *Foxb1* expression in the mammillary, a posterior structure, while Shh was necessary to drive its expression. This may explain why Foxb1 was lost in the mammillary in both the *Nkx2.1-Cre;Shh*$^{lox/lox}$ LOF *and* the *Foxd1-Cre ;Ctnnb1*$^{ex3/+}$ Wnt GOF mutants.

To better understand how these two morphogens might work in concert to pattern the hypothalamus, we used a similar approach to our Wnt GOF mice to generate a Shh GOF mouse using the *Foxd1-Cre* driver. We utilized a mouse line which has a constitutively active point mutation (W539L) of its *smoothened* (*Smo*) gene, however expression of this gene is prevented by a floxed STOP fragment placed in-between the promoter and the gene sequence so that the gene is only expressed after recombination by Cre. In the Shh pathway, Smo is a transmembrane protein which is

inhibited by the Shh receptor Patched in the absence of ligand; upon Shh binding to its receptor the repression is relieved and Smo is able to activate Gli transcription factors to affect transcription. In our case, using *Foxd1-Cre*, the constitutively active Smo would be expressed in every cell of the hypothalamus and prethalamus (Figure 1 D), generating a Smo GOF mutant embryo.

We had a two-step approach: first we analyzed the *Foxd1-Cre;Smo*$^{CA/+}$ Shh GOF embryos at E12.5 to determine what patterning defects, if any, these mutants would have, then we created *Foxd1-Cre;Smo*$^{CA/+}$*;Ctnnb1*$^{ex3/+}$ double GOF mutants, to simultaneously activate both Wnt and Shh signaling, to determine if we could rescue the patterning defects observed in the *Foxd1-Cre ;Ctnnb1*$^{ex3/+}$ β-catenin GOF mutant. To our great surprise, the Smo GOF single mutants had no discernible patterning defect in either the prethalamus or hypothalamus. The prethalamic domains of *Arx* (black arrowheads, Figure 16 A, B), *Isl1* (black arrowheads, Figure 16 E, F), *Lef1* (open arrowheads, Figure 16 G, H), and *Lhx1* (open arrowheads, Figure 16 I, J) were all normal in the Smo GOF mutant, as were the hypothalamic stripe domains of *Arx* (open arrowheads, Figure 16 A, B) and *Isl1* (open arrowheads, Figure 16 E, F). The anterior hypothalamus was patterned normally, as indicated by *Lef1* and *Lhx1* in the ventral AH (yellow arrowheads, Figure 16 G-J) and *Pomc* in the arcuate nucleus (black arrowheads, Figure 16 K, L). The posterior hypothalamus was also intact, as demonstrated by *Lef1* in the premammillary (red arrowheads, Figure 16 G, H), and *Lhx1* (green arrowheads, Figure 16 I, J) and *Foxb1* (black arrowheads, Figure 16 C, D)

in the mammillary. Normal *Lef1* expression also suggested that there was no effect on Wnt signaling. There was similarly no effect on the *Foxb1*-positive migratory cell population (open arrowheads, Figure 16 C, D) in the Smo GOF mutant. There was also no change in the ZLI (*Lef1* and *Lhx1*, black arrowheads, Figure 16 G-J) or thalamic eminence (*Lhx1*, red arrowheads, Figure 16 I, J).

There was a mild hyperproliferation defect as shown by a thickening of the hypothalamic neuroepithelium, although this was not confirmed via EdU cell counting. This can be most clearly seen with *Arx*, in which the *Arx*-negative portion of the hypothalamus was significantly expanded (red brackets, Figure 16 A, B), and with *Isl1*, in which the *Isl1*-positive hypothalamic expression domain was considerably widened (red brackets, Figure 16 E, F). However, this hyperproliferation defect was too mild to cause the gross morphological defects observed in the β-catenin GOF mutant (Figure 8 D-F).

We then generated *Foxd1-Cre;Smo*$^{CA/+}$*;Ctnnb1*$^{ex3/+}$ β-catenin/Smo double GOF mutants, which appeared to be phenotypically wild-type (Figure 16 M-X). In contrast to the severe patterning defects observed in the *Foxd1-Cre;Ctnnb1*$^{ex3/+}$ β-catenin GOF single mutant, and the hyperproliferation defects in both the β-catenin and Smo GOF single mutants, there was neither a patterning nor a hyperproliferation defect in the double GOF mutants, indicating that we had achieved a complete rescue. The stripe markers *Arx* and *Isl1* had normal expression in both the prethalamus (black arrowheads, Figure 16 M, N, Q, R) and the hypothalamus (open arrowheads, Figure

16 M, N, Q, R). *Foxb1*, which had a reduction in the mammillary domain and an expansion of the migratory domain in the β-catenin GOF mutant (see Figure 9 G, H) was completely normal in the double mutants in both the mammillary (black arrowheads, Figure 16 O, P) and migratory cell population (open arrowheads, Figure 16 O, P). In contrast, *Pitx2*, which was expanded in both the supramammillary and mammillary in the β-catenin GOF mutants (see Figure 9 K, L), was restricted to its normal domain in the double mutants (open arrowheads, Figure 16 U, V). The dramatic expansion of *Lef1* in the entire hypothalamus of the *Foxd1-Cre;Ctnnb1*$^{ex3/+}$ mutants was absent from the double mutants (Figure 16 S, T), and its expression domains in the premammillary (red arrowheads), ventral AH (yellow arrowheads), prethalamus (open arrowheads) and ZLI (black arrowheads) were once against separate and distinct (compare to Figure 9 I, J). The arcuate expression of *Pomc* was also normal in the double mutant (black arrowheads, Figure 16 W, X), in contrast to the mosaic and disrupted *Pomc* expression domain in the *Foxd1-Cre;Ctnnb1*$^{ex3/+}$ β-catenin GOF mutant (see Figure 10 C, D).

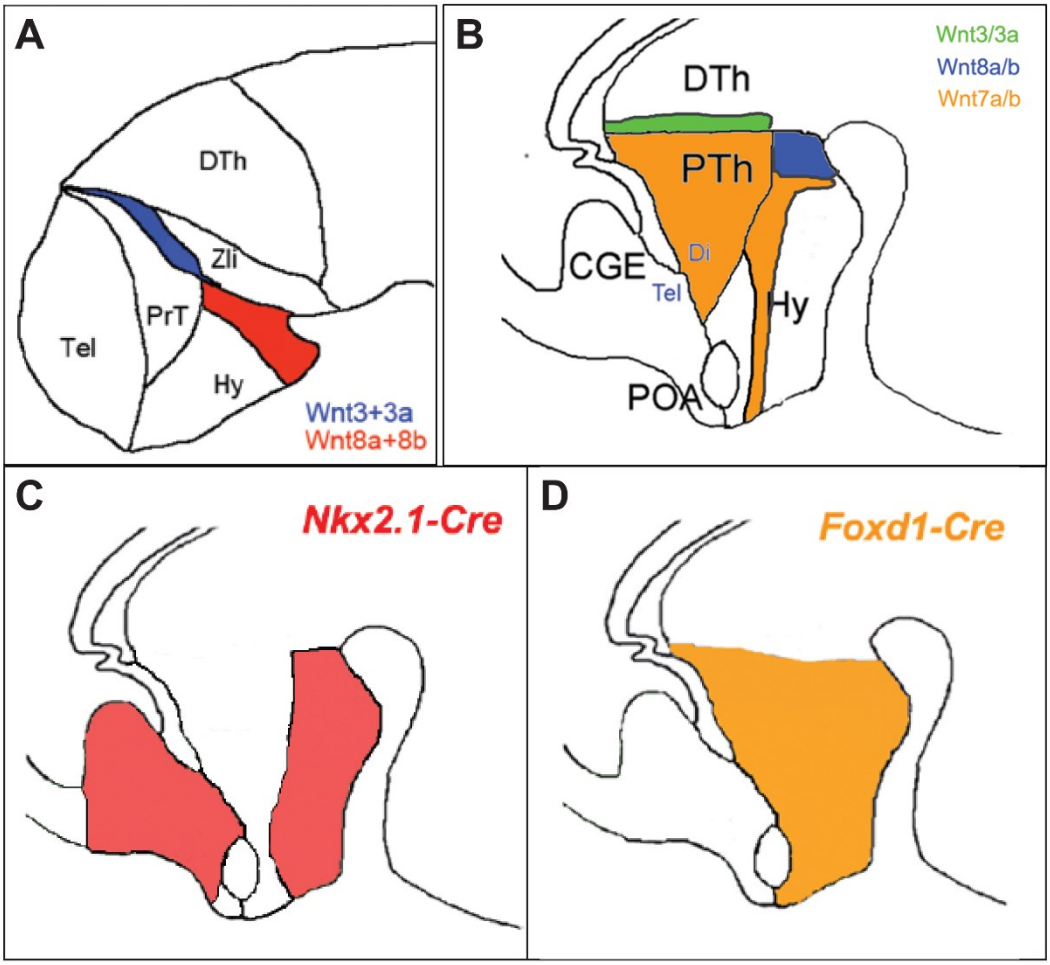

Figure 3-1: Wnt and Cre Expression in the Developing Hypothalamus. A. Wnt3/3a and Wnt8a/8b are expressed in a contiguous stripe across the developing prethalamus and hypothalamus at E9.5. B. At E12.5, Wnt3/3a are expressed in a stripe across the posterior prethalamus and Wnt8a/8b is restricted to the mammillary of the hypothalamus. At this time, Wnt7a/7b is expressed in interneuron progenitors across the hypothalamus. C-D. Schematics showing where

Nkx2.1-Cre (C) and *Foxd1-Cre* (D) are expressed at E12.5. *Nkx2.1-Cre* is restricted to a ventral stripe across the anterior-posterior axis and is excluded from the prethalamus. *Foxd1-Cre* is expressed throughout the whole of the hypothalamus and prethalamus.

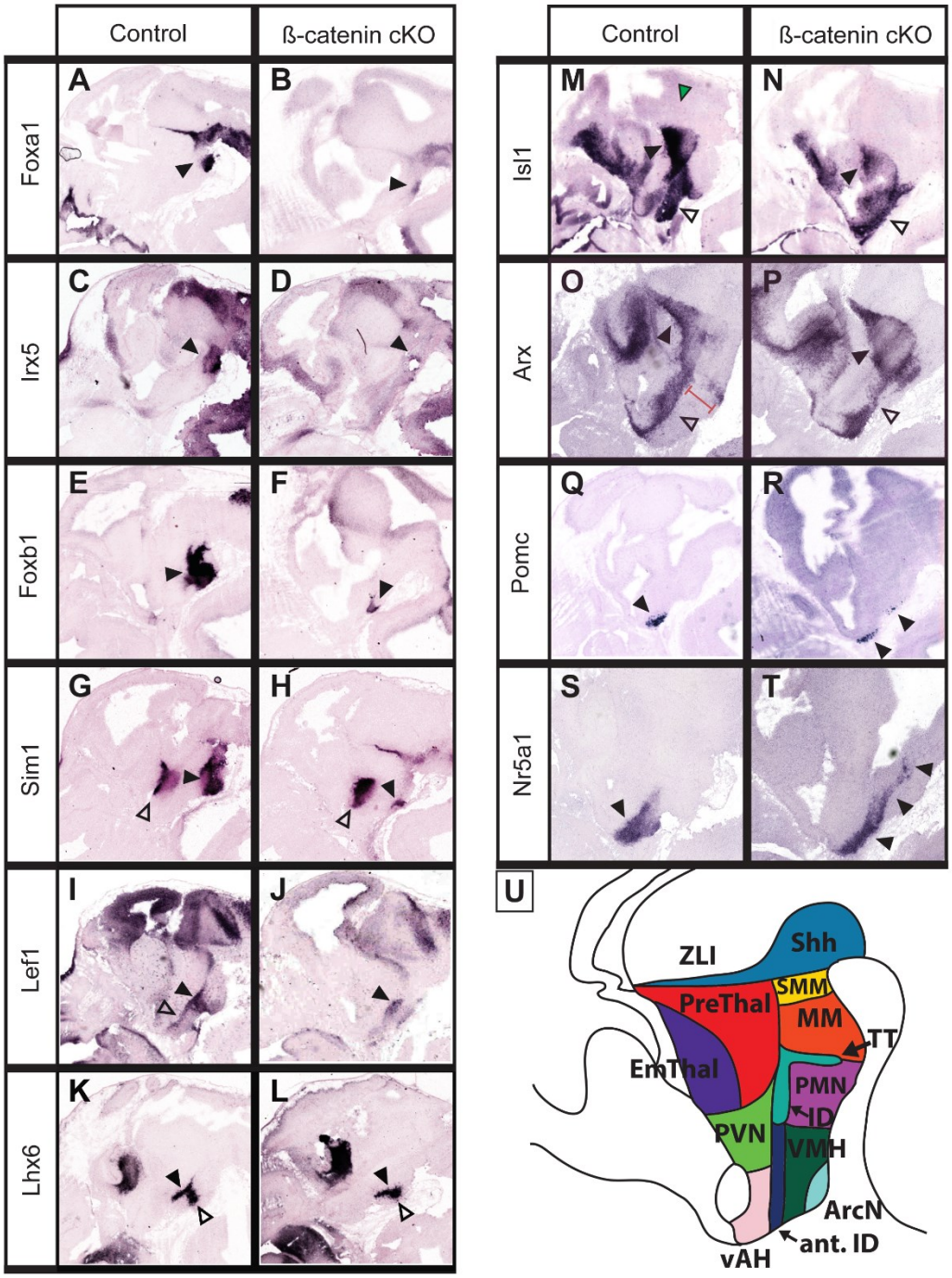
Control
ß-catenin cKO
Foxa1
A
B
Irx5
C
D
Foxb1
E
F
Sim1
G
H
Lef1
I
J
Lhx6
K
L
Control
ß-catenin cKO
Isl1
M
N
Arx
O
P
Pomc
Q
R
Nr5a1
S
T
U
ZLI
Shh
SMM
PreThal
MM
TT
EmThal
PMN
ID
PVN
VMH
ArcN
ant. ID
vAH

Figure 3-2: Loss of β-catenin results in an anteriorization of the hypothalamus: Part 1. A-T: *In situ* hybridization of hypothalamic markers on E12.5 control (*Cre*-negative, either *Ctnnb1*$^{lox/lox}$ or *Ctnnb1*$^{lox/+}$) and *Nkx2.1-Cre;Ctnnb1*$^{lox/lox}$ sagittal sections. A-J: Black arrowheads indicate the supramammillary (A-D), mammillary (E-H) and premammillary (I-J), all of which were reduced in the mutant. The PVN was unaffected (open arrowheads, G and H). The ID lost *Lef1* expression (open arrowheads, I and J) but not *Lhx6* expression (black arrowheads, K and L). The TT was reduced (open arrowheads, K and L). M-P: Black arrowheads indicate the prethalamus, which was intact in mutants. Open arrowheads indicate the hypothalamic stripe domain, which was ventralized in the mutants. Red bar in O represents the *Arx*-negative hypothalamic domain which was missing in the mutant. Q-T: Anterior structures were expanded into the posterior domain. Q-R: black arrowheads indicate the arcuate. S-T: black arrowheads indicate the VMH. U: A schematic showing wild-type anatomy of the hypothalamus and prethalamus.

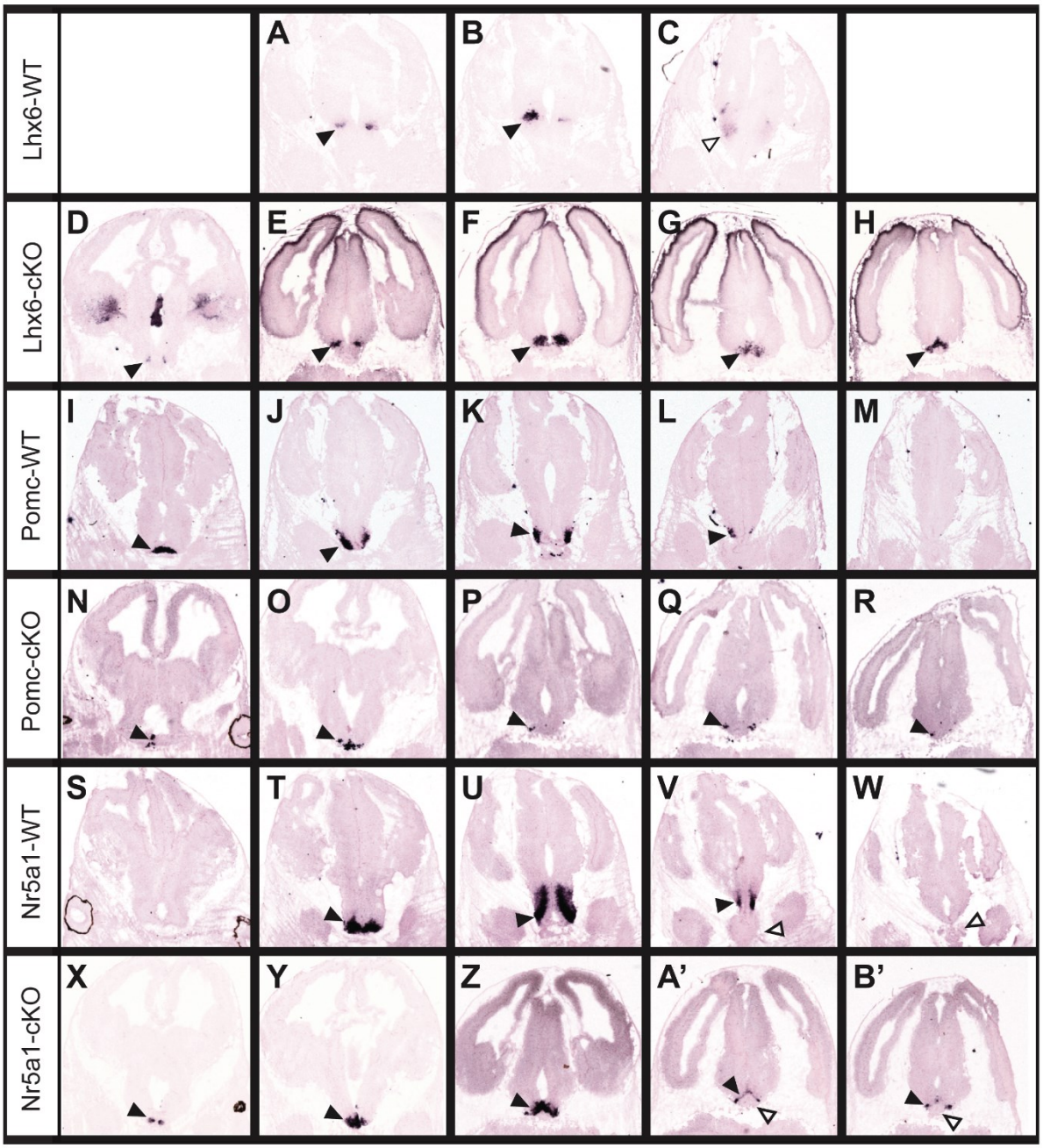
Lhx6-WT
Lhx6-cKO
Pomc-WT
Pomc-cKO
Nr5a1-WT
Nr5a1-cKO
A
B
C
D
E
F
G
H
I
J
K
L
M
N
O
P
Q
R
S
T
U
V
W
X
Y
Z
A'
B'

Figure 3-3: Loss of β-catenin results in an anteriorization of the hypothalamus: Part 2. A-B': *In situ* hybridization of hypothalamic markers on E12.5 control (*Cre*-negative, either *Ctnnb1*$^{lox/lox}$ or *Ctnnb1*$^{lox/+}$) and *Nkx2.1-Cre;Ctnnb1*$^{lox/lox}$ coronal sections. A-H: The TT (open arrowheads) was lost and ID (black arrowheads) ventralized in the mutant. I-B': Anterior structures were expanded posteriorly in the mutants. I-R: black arrowheads indicate the arcuate. S-B': black arrowheads indicate the VMH and open arrowheads indicate the misplaced pituitary gland.

Sim1-WT
Sim1-cKO
Nkx2.1-WT
Nkx2.1-cKO
A
B
C
D
E
F
G
H
I
J
K
L
M
N
O
P
Q
R
T
U

Figure 3-4: Loss of β-catenin results in an anteriorization of the hypothalamus: Part 3. A-U: In situ hybridization of hypothalamic markers on E12.5 control (*Cre*-negative, either *Ctnnb1*$^{lox/lox}$ or *Ctnnb1*$^{lox/+}$) and *Nkx2.1-Cre;Ctnnb1*$^{lox/lox}$ coronal sections. A-J: The mammillary was reduced (black arrowheads) but the PVN was unaffected (open arrowheads). K-U: The hypothalamic neuroepithelium was thinned in the mutant (black arrowheads), while the pituitary was misplaced (open arrowheads).

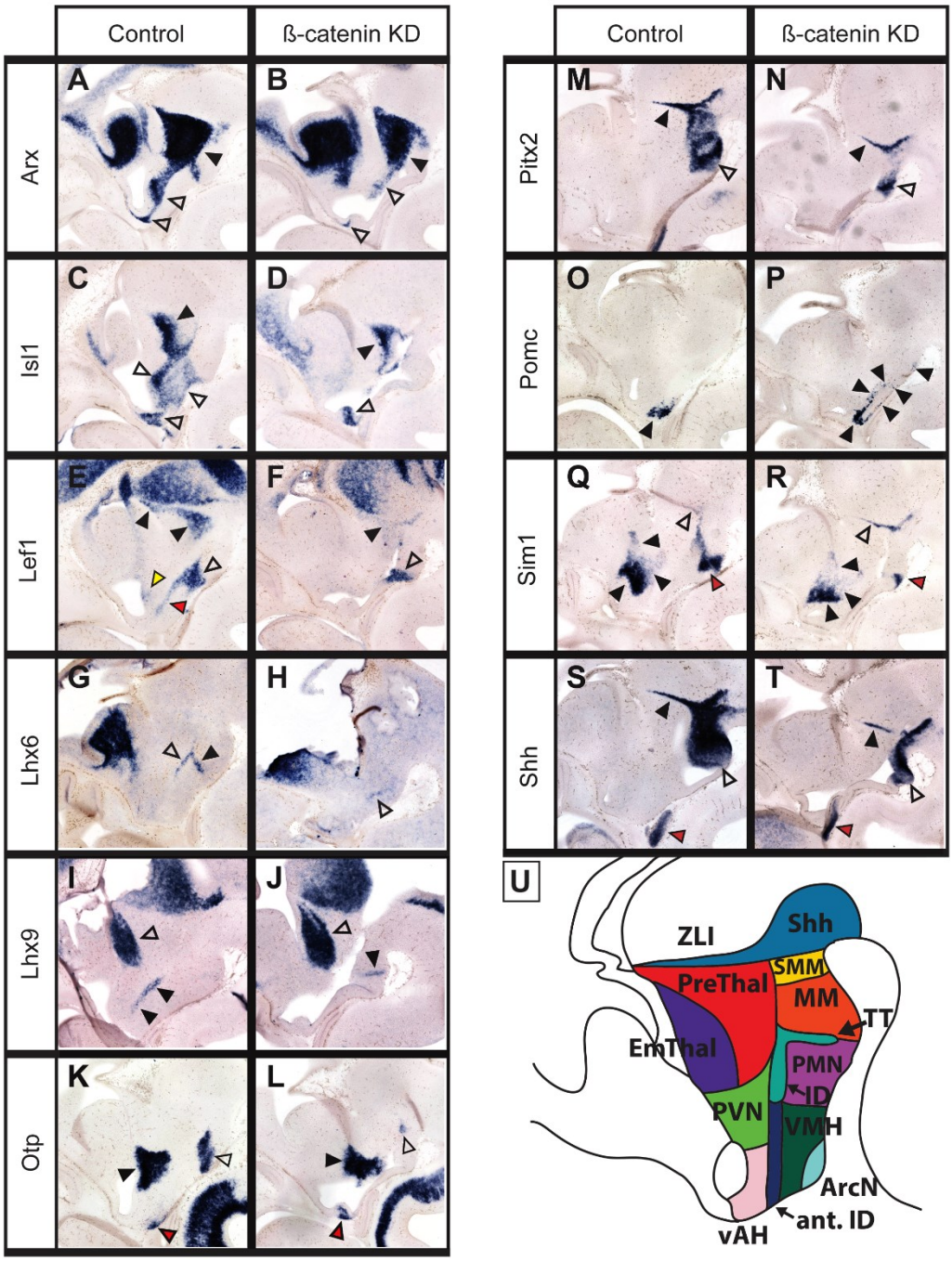
Control
ß-catenin KD
Arx
Isl1
Lef1
Lhx6
Lhx9
Otp
Pitx2
Pomc
Sim1
Shh
A
B
C
D
E
F
G
H
I
J
K
L
M
N
O
P
Q
R
S
T
U
ZLI
Shh
SMM
PreThal
MM
TT
EmThal
PMN
ID
PVN
VMH
ArcN
ant. ID
vAH

Figure 3-5: Knock-down of β-catenin results in a thinning and anteriorization of the hypothalamus but has no effect on the prethalamus: Part 1. A-T: *In situ* hybridization on E12.5 control (*Cre*-negative, either *Ctnnb1*$^{lox/lox}$ or *Ctnnb1*$^{lox/+}$) and *Foxd1-Cre;Ctnnb1*$^{lox/lox}$ sagittal sections. A-D: Black arrowheads indicate the prethalamus, which was unaffected in the mutants. White arrowheads indicate the thinned hypothalamic domain. The *Lef1* domain of the ID was absent in the mutants (red arrowhead, E and F) but the *Lhx6* domain was unaffected (open arrowhead, G and H). The TT was gone (black arrowheads, G and H). E, F: The premammillary domain of *Lef1* was reduced (open arrowheads), as was the prethalamic domain (black arrowheads), and the anterior domain was absent in the mutants (yellow arrowhead). I, J: The thalamic eminence was unaffected (open arrowheads), as were the orexigenic neurons labelled by Lhx9, although this domain was ventralized (black arrowheads). K-N, S, T: Markers encompassing the supramammillary and mammillary were reduced in the mutants (open arrowheads). The PVN was unaffected in the mutant (black arrowheads, K, L, Q, and R). The *Otp* domain of the anterior hypothalamus was unaffected (red arrowheads, K and L) but *Pomc* in the arcuate was expanded into the posterior domain (black arrowheads, O and P). The ZLI was unaffected (black arrowheads, M, N, S and T; open arrowheads, Q, R). The pituitary was displaced into the hypothalamic neuroepithelium (red arrowheads, S and T). U: A schematic showing wild-type anatomy of the hypothalamus and prethalamus.

Arx Control
Arx β-cat LOF
Isl1 Control
Isl1 β-cat LOF
Lhx9 Control
Lhx9 β-cat LOF
Pomc Control
Pomc β-cat LOF
A
B
C
D
E
F
G
H
I
J
K
L
M
N
O
P
Q
R
S
T
U
V
W
X

Figure 3-6: Knock-down of β-catenin results in a thinning and anteriorization of the hypothalamus but has no effect on the prethalamus: Part 2. In situ hybridization on E12.5 control (*Cre*-negative, either *Ctnnb1*$^{lox/lox}$ or *Ctnnb1*$^{lox/+}$) and *Foxd1-Cre;Ctnnb1*$^{lox/lox}$ coronal sections. A-L: The hypothalamic domains were reduced (open arrowheads), but the prethalamic domains were unaffected (black arrowheads). M-R: Precursors of orexinergic hypocretin neurons (marked here by *Lhx9* expression) were normal, but ventralized due to the thinned hypothalamus (black arrowheads). S-X: The arcuate (black arrowheads) was displaced due to the invasion of the pituitary (dashed circle in X).

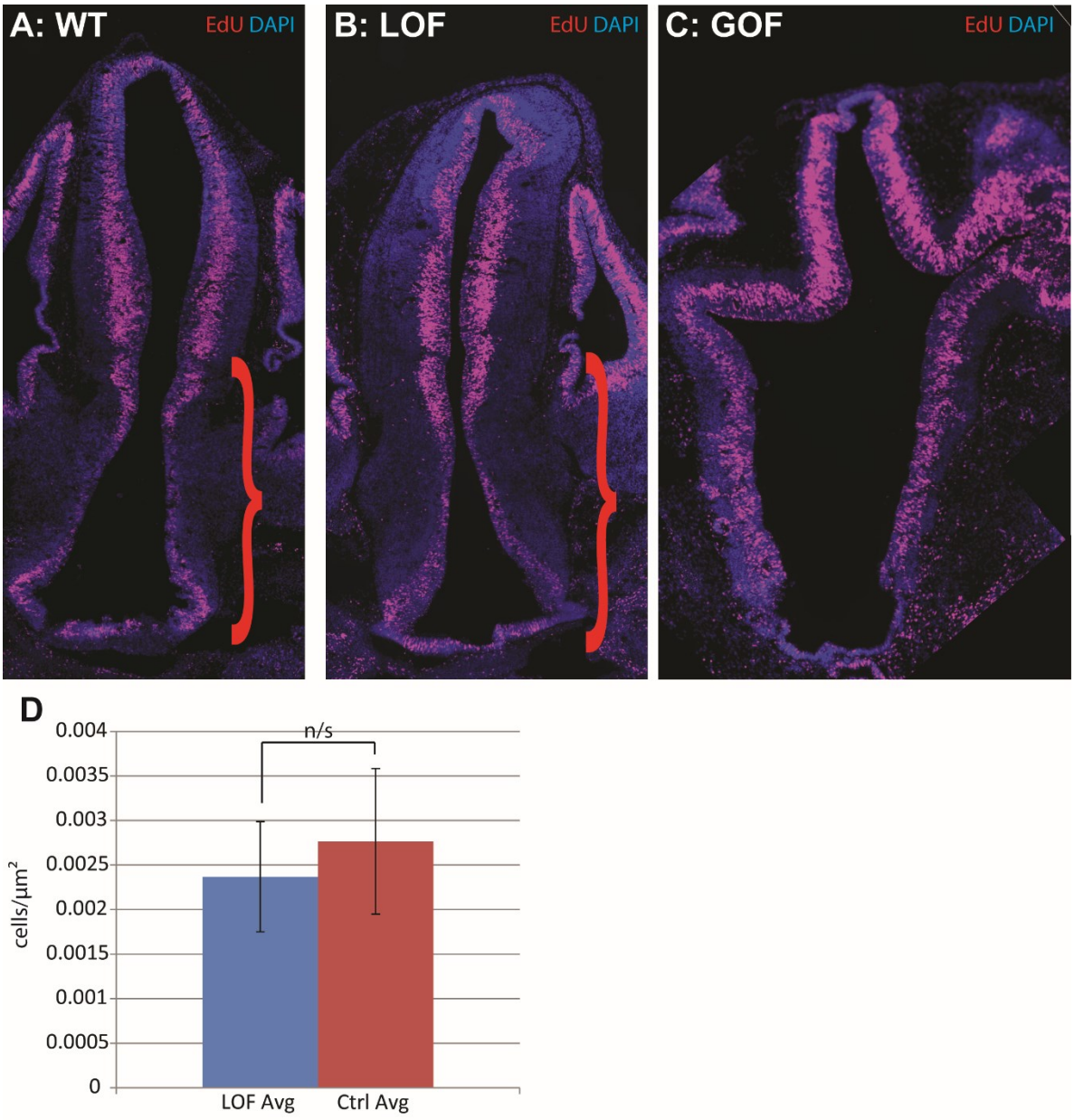

Figure 3-7: Knock-down of β-catenin had no effect on proliferation, but constitutively active β-catenin increased proliferation. A-C: EdU and DAPI

staining after a 2hr EdU pulse in coronal E12.5 sections from *Foxd1-Cre*-negative;*Ctnnb1*$^{lox/lox}$, *Foxd1-Cre;Ctnnb1*$^{lox/lox}$ and *Foxd1-Cre;Ctnnb1*$^{ex3/+}$embryos. Red scroll bars indicate the boundary of the prethalamus and hypothalamus. D: Quantification of EdU counts relative to area in control versus β-catenin LOF brains (n=3).

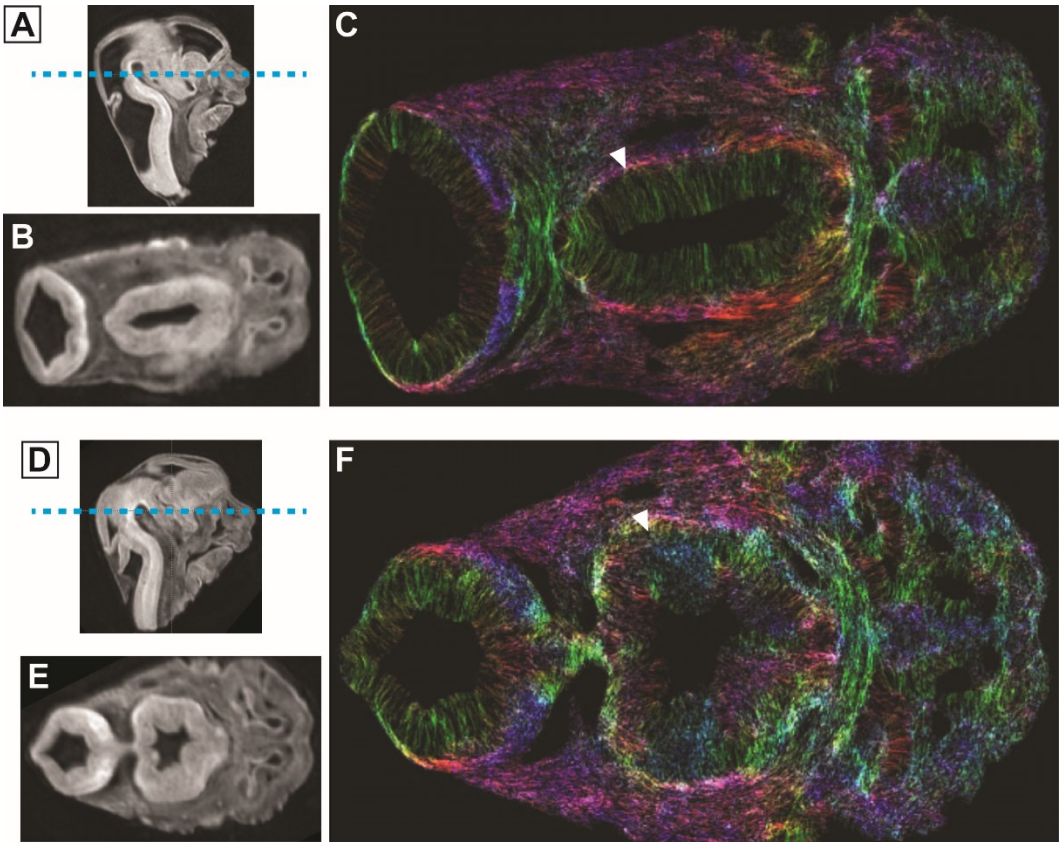

Figure 3-8: Disrupted ventricular organization in a constitutively active β-catenin embryo. A-F: MRI on *Foxd1-Cre*-negative;*Ctnnb1*$^{ex3/+}$ (A-C) and *Foxd1-Cre;Ctnnb1*$^{ex3/+}$ GOF (D-F) E12.5 embryos. A, D: dashed line indicates the level at which the horizontal sections in B, C, E and F were taken. C and F: Colored lines indicate the orientation of the fiber tracts, which can either represent axons or radial glia, but in this case most likely represents radial glia. The hypothalamic neuroepithelium was significantly disrupted in the GOF mutant.

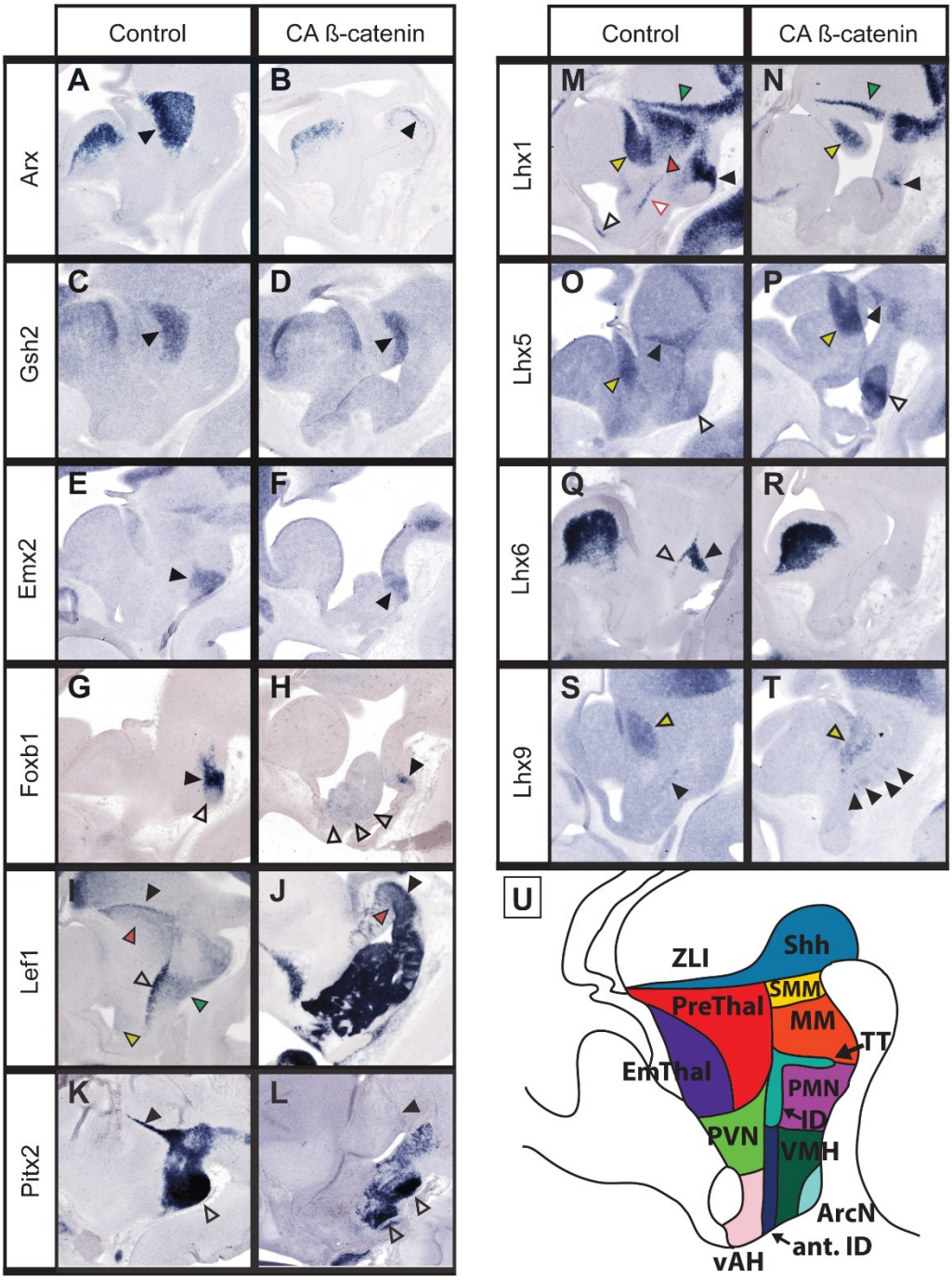
Control
CA ß-catenin
Arx
Gsh2
Emx2
Foxb1
Lef1
Pitx2
A
B
C
D
E
F
G
H
I
J
K
L
Control
CA ß-catenin
Lhx1
Lhx5
Lhx6
Lhx9
M
N
O
P
Q
R
S
T
U
ZLI
Shh
SMM
PreThal
MM
TT
EmThal
PMN
ID
PVN
VMH
ArcN
ant. ID
vAH

Figure 3-9: Constitutively active β-catenin results in disrupted patterning and development of the hypothalamus and prethalamus: Part 1. A-T: *In situ* hybridization on E12.5 control (*Foxd1-Cre*-negative;*Ctnnb1*$^{ex3/+}$) and *Foxd1-Cre;Ctnnb1*$^{ex3/+}$ sagittal sections. A-D: Black arrowheads indicate the prethalamus, which was absent except for a tiny sliver in B, and reduced but still present in D. E-H: The mammillary is reduced in the GOF mutants. Black arrowheads indicate the mammillary, open arrowheads indicate the migratory *Foxb1*-expressing cells which were expanded into the anterior domain in the GOF mutants. I-J: *Lef1* was expanded throughout the hypothalamus, indicating a successful upregulation in canonical Wnt signaling. Red arrowheads=prethalamus, black arrowheads=ZLI adjacent, green arrowhead=premammillary, open arrowhead=ID, yellow arrowhead=ventral AH. K-L: The supramammillary and mammillary (open arrowheads) were expanded in the GOF mutant and the ZLI expression was maintained (black arrowheads). M-T: Lim homeodomain transcription factors were differentially disrupted by constitutively active β-catenin. M-P, S, T: Yellow arrowheads designate the thalamic eminence, which was unaffected in the GOF mutants. M-N: The prethalamus was absent (red arrowhead), while the mammillary was reduced (black arrowheads). The ZLI was unaffected (green arrowheads). The anterior and ID domains were absent (open arrowhead and red-outlined arrowhead, respectively). O-P: *Lhx5* was expanded in the mammillary (open arrowheads) and unaffected in the ZLI-adjacent (black arrowheads). Q-R: *Lhx6* was completely absent from the ID (open arrowhead) and

TT (black arrowhead). S-T: Orexigenic neurons were expanded in the GOF mutant (black arrowheads). U: A schematic showing wild-type anatomy of the hypothalamus and prethalamus.

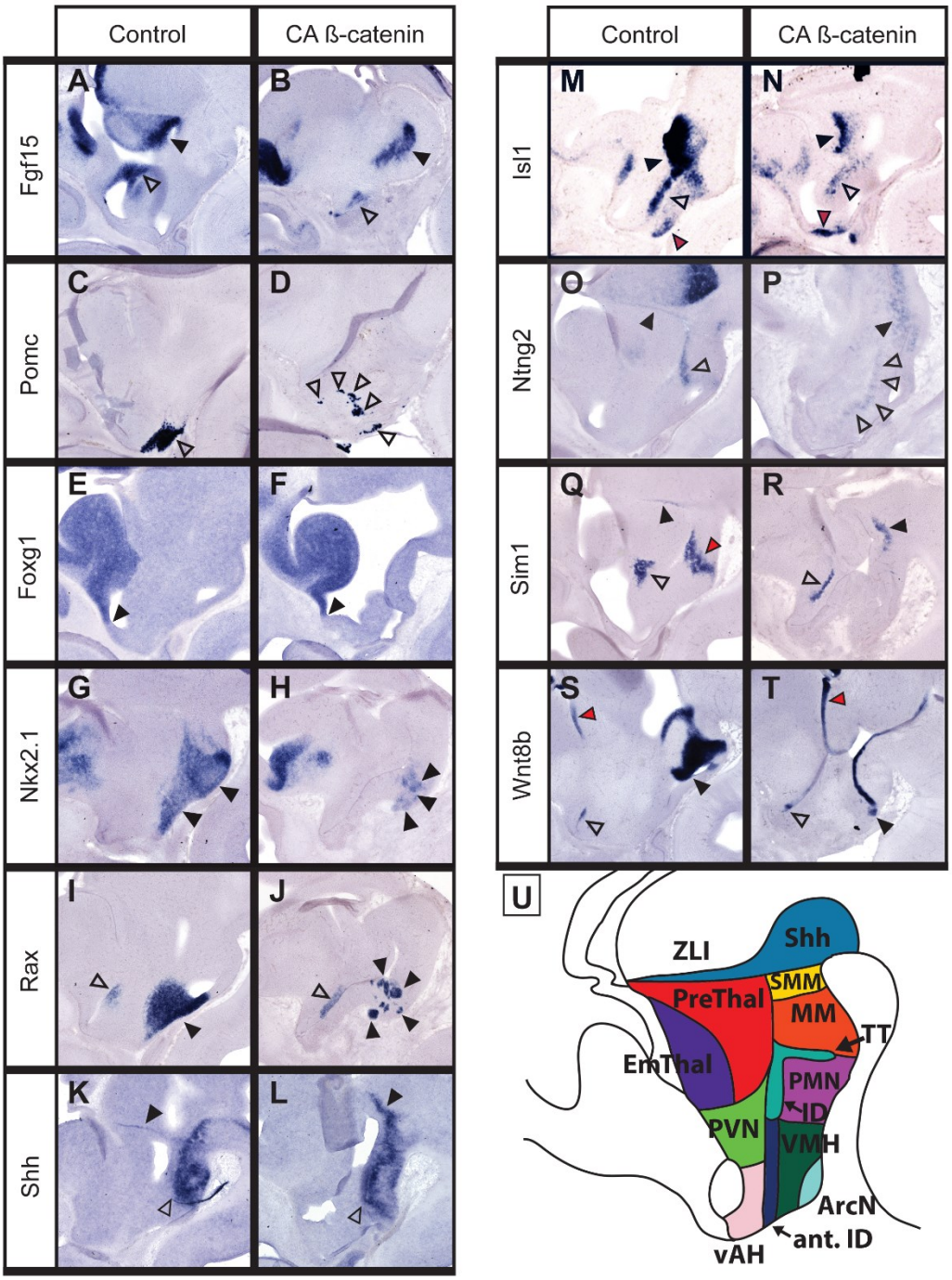
Control
CA ß-catenin
Fgf15
Pomc
Foxg1
Nkx2.1
Rax
Shh
A
B
C
D
E
F
G
H
I
J
K
L
Control
CA ß-catenin
Isl1
Ntng2
Sim1
Wnt8b
M
N
O
P
Q
R
S
T
U
ZLI
Shh
PreThal
SMM
MM
TT
EmThal
PMN
ID
PVN
VMH
ArcN
ant. ID
vAH

Figure 3-10: Constitutively active β-catenin results in disrupted patterning and development of the hypothalamus and prethalamus: Part 2. A-T: *In situ* hybridization on E12.5 control (*Foxd1-Cre*-negative;*Ctnnb1*$^{ex3/+}$) and *Foxd1-Cre;Ctnnb1*$^{ex3/+}$sagittal sections. A-B: *Fgf15* expression was preserved in the prethalamus (black arrowheads) and dorsal anterior hypothalamus (open arrowheads). C-D: The arcuate (open arrowheads) was severely disrupted in the GOF mutant. E-F: There was no shift in the location of the DTJ (black arrowheads). G-J: In the mutant, ventral stripe markers were reduced to their posterior domain and were extremely mosaic (black arrowheads). The PVN was unaffected (open arrowheads, I, J, Q, R). K-L: Expression of the morphogen *Shh* was unaffected in the supramammillary/mammillary (open arrowheads). The ZLI was unaffected (black arrowheads, K, L, O-R). M-N: Expression of the stripe marker *Isl1* was reduced in the prethalamus (black arrowheads), hypothalamus (open arrowheads), but not the ventral AH (red arrowheads). O-P: The dorsal premammillary was expanded (open arrowheads). Staining in the mammillary of the GOF mutants was either completely absent (red arrowhead, Q, R) or reduced (black arrowheads, S, T). The anterior domain of *Wnt8b* expression was unaffected (open arrowheads, S, T). U: A schematic showing wild-type anatomy of the hypothalamus and prethalamus.

A
B
C
Arx Control
D
E
F
Arx β-cat GOF
G
H
I
Bsx Control
J
K
L
Bsx β-cat GOF
M
N
O
Isl1 Control
P
Q
R
Isl1 β-cat GOF
S
T
U
Lhx1 Control
V
W
X
Lhx1 β-cat GOF

Figure 3-11: Constitutively active β-catenin results in disrupted patterning and development of the hypothalamus and prethalamus: Part 3. A-X: In situ hybridization on E12.5 control (*Foxd1-Cre*-negative;*Ctnnb1*$^{ex3/+}$) and *Foxd1-Cre;Ctnnb1*$^{ex3/+}$ coronal sections. A-F, M-R: The prethalamic (black arrowheads) and hypothalamic (open arrowheads) expression domains were reduced. G-L: The premammillary domain of *Bsx* was present (black arrowheads) but the arcuate expression was lost (open arrowheads) in the GOF mutant. There was ectopic expression in the developing habenula (red arrowhead). S-X: *Lhx1* expression in the ZLI (black arrowheads), prethalamus (open arrowheads), ID (red arrowheads), anterior hypothalamus (yellow arrowhead) and mammillary (green arrowheads) was lost everywhere except the ZLI and mammillary, which was albeit reduced.

Lhx6 Control
Lhx6 β-cat GOF
Lhx9 Control
Lhx9 β-cat GOF
Ntng2 Control
Ntng2 β-cat GOF
Pitx2 Control
Pitx2 β-cat GOF
A
B
C
D
E
F
G
H
I
J
K
L
M
N
O
P
Q
R
S
T
U
V
W
X

Figure 3-12: Constitutively active β-catenin results in disrupted patterning and development of the hypothalamus: Part 1. A-X: *In situ* hybridization on E12.5 control (*Foxd1-Cre*-negative*;Ctnnb1*$^{ex3/+}$) and *Foxd1-Cre;Ctnnb1*$^{ex3/+}$ coronal sections. *Lhx6* was lost in the ID (open arrowhead, A-F) and TT (black arrowheads, A-F), but *Lhx9* in the orexigenic neurons (black arrowheads, G-L), *Ntng2* in the premammillary (open arrowheads, M-R) and *Pitx2* in the supramammillary/mammillary region (open arrowheads, S-X) were all expanded. The ZLI was unaffected (black arrowheads, M-X).

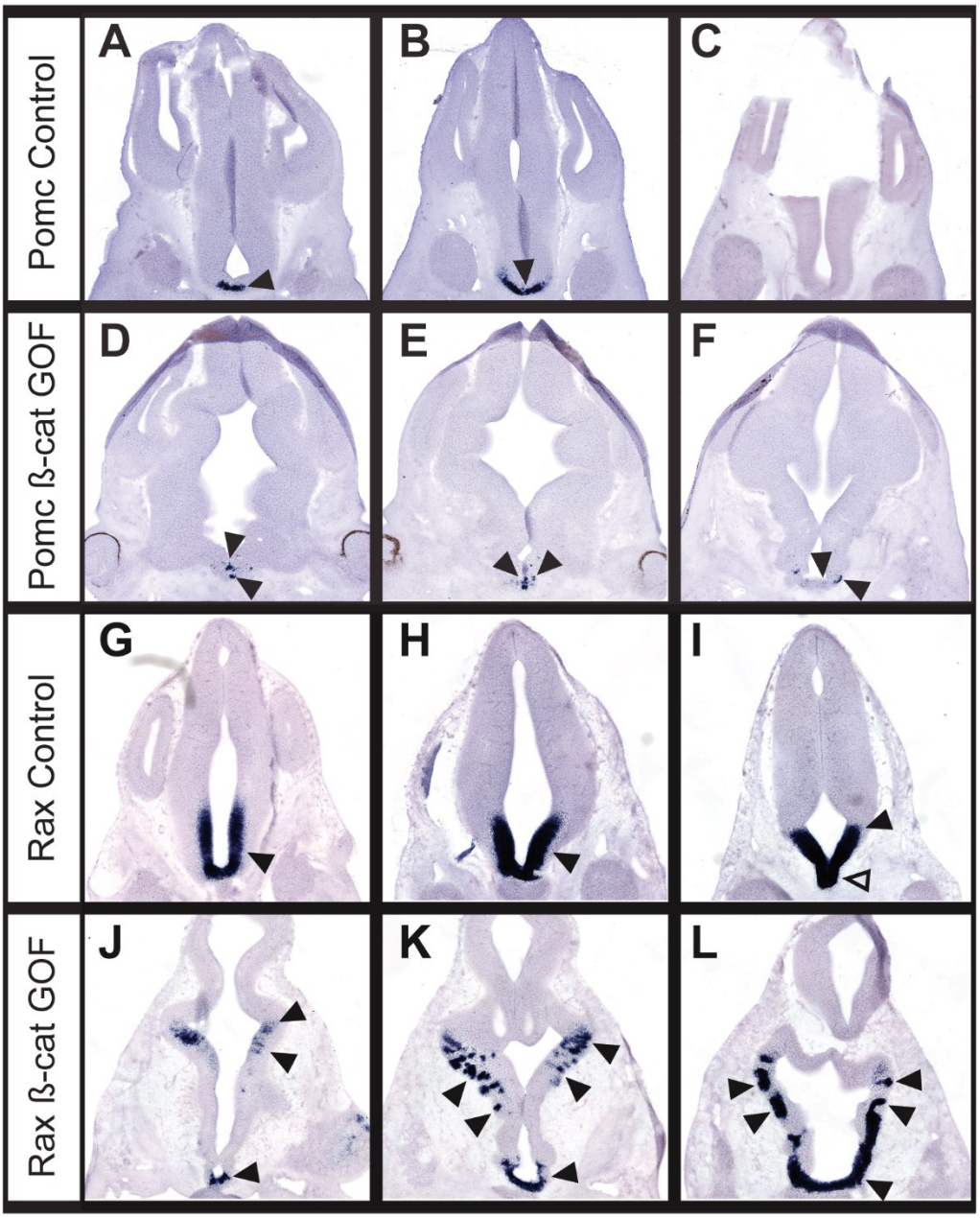

Figure 3-13: Constitutively active β-catenin results in disrupted patterning and development of the hypothalamus: Part 2. Constitutively active β-catenin results

in a disrupted and expanded arcuate (A-F) and ventral hypothalamus (G-L) and mosaic expression of *Pomc* (black arrowheads, A-F) and Rax (black arrowheads, G-L). I: Open arrowhead indicates the infundibulum.

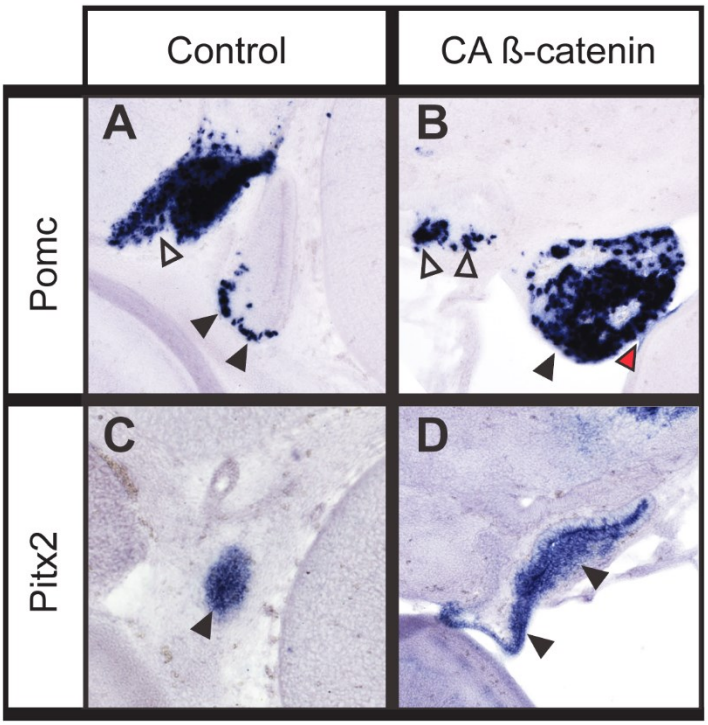

Figure 3-14: The specification and migration of the pituitary is disrupted by constitutively active β-catenin. A-D: *In situ* hybridization on E12.5 control (*Foxd1-Cre*-negative;*Ctnnb1*$^{ex3/+}$) and *Foxd1-Cre;Ctnnb1*$^{ex3/+}$sagittal sections. In constitutively active β-catenin mutant embryos, the pituitary was enlarged and had expanded expression of pituitary markers *Pomc* (black arrowheads, A, B) and *Pitx2* (black arrowheads, C, D). In at least one mutant, the pituitary remained stuck to the oral ectoderm (junction is indicated by red arrowhead in B). Open arrowheads in A, B indicate arcuate expression of *Pomc*.

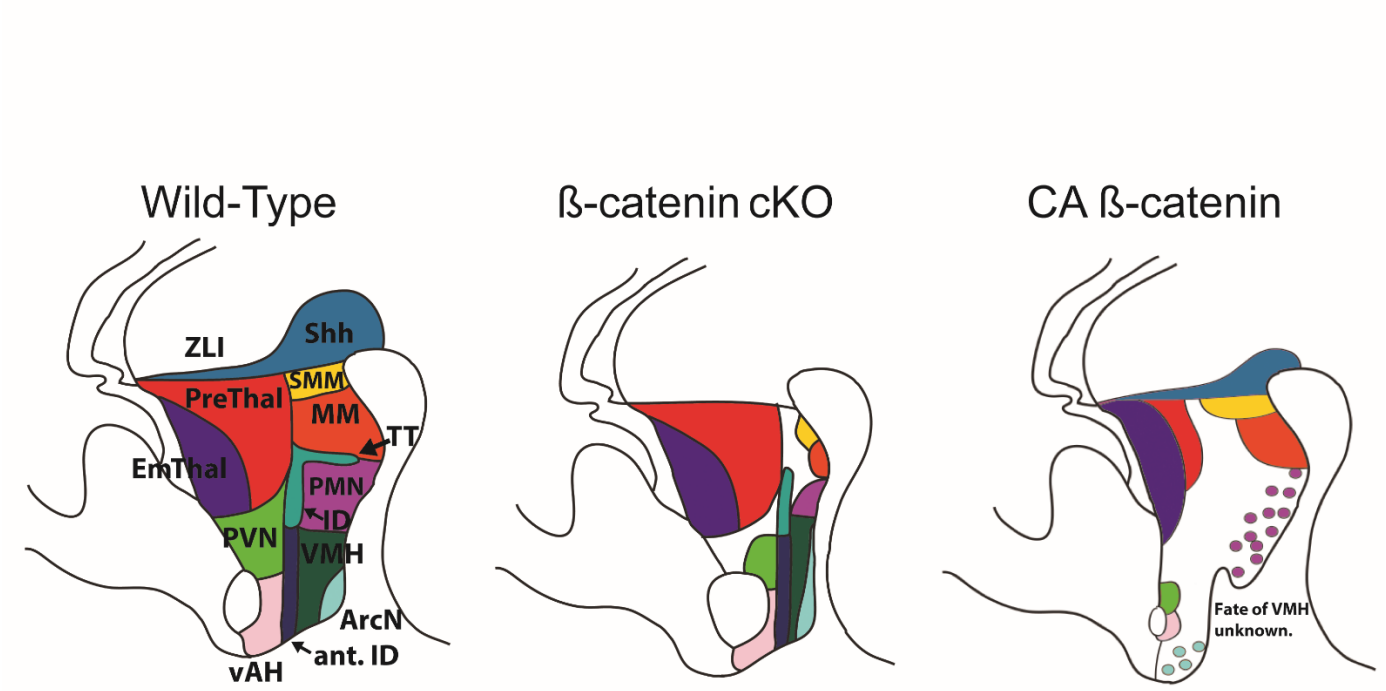
Wild-Type
ß-catenin cKO
CA ß-catenin
ZLI
Shh
SMM
PreThal
MM
TT
EmThal
PMN
ID
PVN
VMH
ArcN
ant. ID
vAH
Fate of VMH
unknown.

Figure 3-15: Schematic demonstrating the developmental changes observed in β-catenin LOF and GOF mutant embryos. In LOF mutants, the hypothalamus was anteriorized, and thinned resulting in more dorsal structures shifting ventrally. The prethalamus was unaffected. In GOF mutants, the phenotype was much more complex, with some posterior markers expanded but others lost. For the most part, anterior markers were preserved but reduced and often mosaic. The prethalamus was smaller in size and missing expression of some, but not all markers. The fate of the VMH is unknown in these mutants.

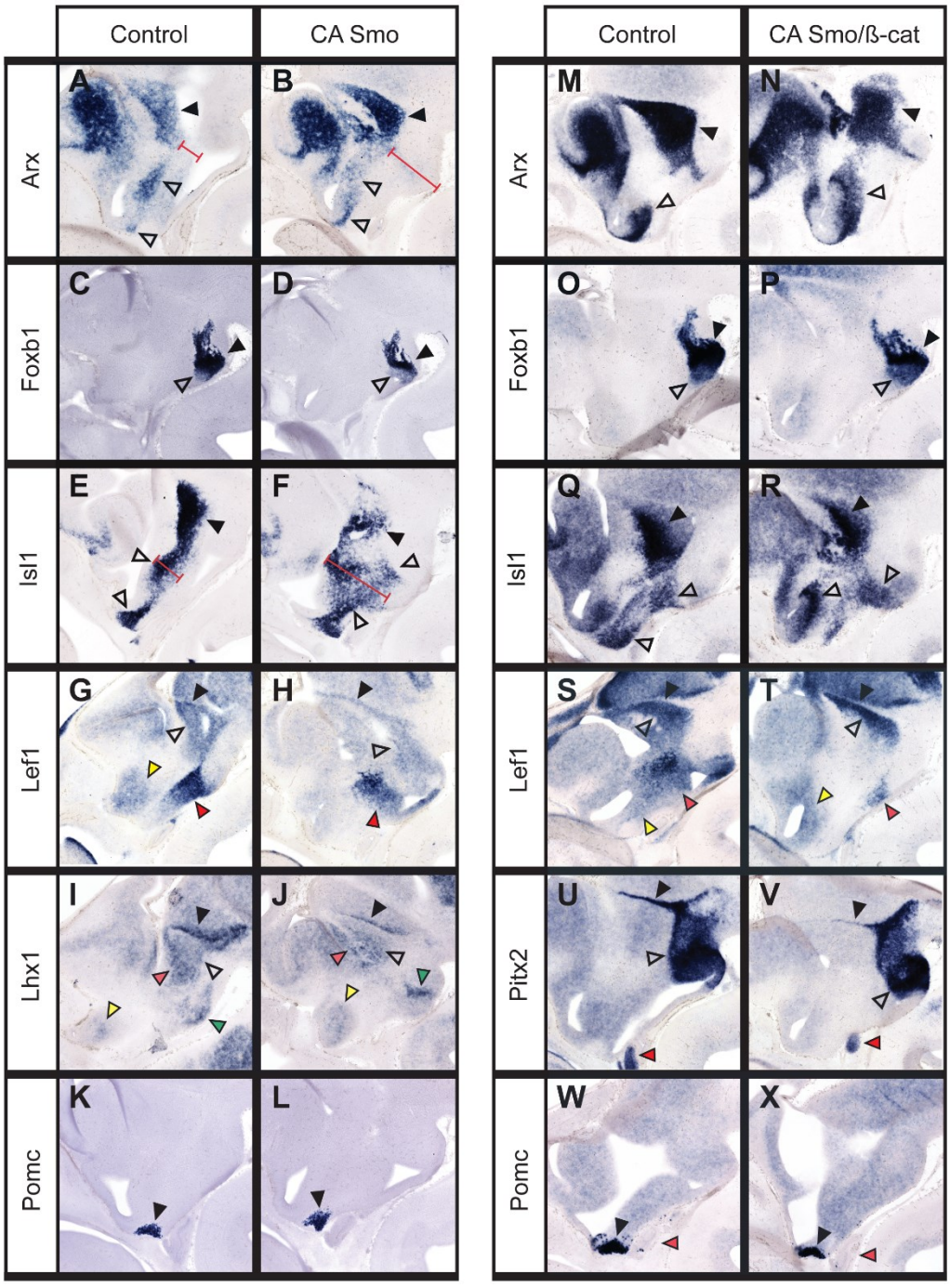
Control
CA Smo
Control
CA Smo/ß-cat
Arx
Foxb1
Isl1
Lef1
Lhx1
Pomc
Pitx2
A
B
C
D
E
F
G
H
I
J
K
L
M
N
O
P
Q
R
S
T
U
V
W
X

Figure 3-16: Constitutively active Smo had no effect on patterning. Constitutively active Smo had no effect on patterning of the hypothalamus or prethalamus, but does cause increased proliferation; constitutively active Smo/β-catenin double mutants rescue the defects seen in constitutively active β-catenin single mutants. In situ hybridization performed on E12.5 control (*Foxd1-Cre*-negative;*SmoCA*$^{/+}$) and *Foxd1-Cre*;*Smo*$^{CA/+}$ (A-L) and control (*Foxd1-Cre*-negative;*Ctnnb1*$^{ex3/+}$;*Smo*$^{CA/+}$) and *Foxd1-Cre* ;*Smo*$^{CA/+}$;*Ctnnb1*$^{ex3/+}$ (M-X) sagittal sections. Other than a deformed, hyperproliferative hypothalamus, there were no patterning defects observed with any markers tested. *Arx* and *Isl1* expression in the prethalamus (black arrowheads, A, B, E, F) and hypothalamus (open arrowheads, A, B, E, F) were normal, but the hypothalamic domain was expanded (red brackets). Both the *Foxb1* nuclear mammillary domain (black arrowheads, C, D) and the migratory population of *Foxb1* expressing cells (open arrowheads, C, D) were unaffected. G-J: *Lef1* and *Lhx1* in the prethalamus (open arrowheads), ZLI (black arrowheads) and anterior hypothalamus (yellow arrowheads) were normal, as was *Lef1* in the premammillary (red arrowheads, G, H), and *Lhx1* in the thalamic eminence (red arrowheads, I, J) and mammillary (green arrowheads, I, J). The arcuate nucleus was also normal in the Smo GOF mutants (black arrowheads, K, L). The GOF double mutants were identical to wild-type, in contrast to the severe patterning defects observed in the β-catenin GOF single mutants and the hyperproliferative defect seen in the Smo GOF single mutants (compare to Figures 9 and 10). *Arx* and *Isl1*

expression in the prethalamus (black arrowheads, M, N, Q, R) and hypothalamus (open arrowheads, M, N, Q, R) were unaffected. Both the *Foxb1* nuclear mammillary domain (black arrowheads, O, P) and the migratory population of *Foxb1* expressing cells (open arrowheads, O, P) were unaffected. The ZLI (black arrowheads, S-V) was intact. S, T: In contrast to the dramatic upregulation of *Lef1* expression in the β-catenin GOF mutants, in the double mutants, *Lef1* expression had returned to normal in the premammillary (red arrowheads), anterior hypothalamus (yellow arrowheads) and prethalamus (open arrowheads). U, V: *Pitx2* expression was no longer expanded in the supramammillary/mammmillary of the double mutants (open arrowheads). W, X: The arcuate was normal (black arrowheads. U-X: The pituitary was in the correct position and was not misexpressing any pituitary markers (red arrowheads, contrast this with Figure 14).

3.2 DISCUSSION

3.2.1 Introduction

We have demonstrated that canonical Wnt signaling plays an important role in the early patterning and specification of the hypothalamus and prethalamus. We have manipulated activity of the canonical Wnt signaling effector protein, β-catenin, using two different Cre lines, and used a wide panel of *in situ* hybridization probes to reveal altered expression of specific nuclei markers in each of the experimental conditions. We had two main goals in examining canonical Wnt signaling in the hypothalamus and prethalamus: first to demonstrate that it plays an important function in patterning these structures analogously to its role in other brain regions, and second, to reveal a common patterning mechanism governing the hypothalamus and prethalamus together as a single developmental unit, in opposition to the prosomere model of forebrain development. The results, however, were much less straightforward than anticipated.

3.2.2 The Role of Canonical Wnt Signaling in the Patterning and Specification of the Hypothalamus and Prethalamus

Both the *Nkx2.1-Cre;Ctnnb1*$^{lox/lox}$ and the *Foxd1-Cre;Ctnnb1*$^{lox/lox}$ LOF mutant lines showed an anteriorization of the hypothalamus, although to varying degrees of disruption due to the differing efficiencies of the Cre-lines used. This is consistent with the known function of canonical Wnt signaling as a posteriorizing factor during neural development, although what is considered posterior is relative and changes over the course of development. Earlier in development, for example, the forebrain is considered an anterior structure and is protected from Wnt signaling by the secretion of Wnt antagonists from the prechordal plate (Shinya et al., 2000; Dorsky et al., 2003). Within the diencephalon (of which the hypothalamus is the most rostral component), the anterior-posterior dichotomy shifts over the rostrocaudal axis. Wnt signaling is thought to pattern the thalamus as well, as it is necessary to prevent the thalamus from adopting a prethalamic fate; in this case the prethalamus is considered the anterior structure, although the prethalamus is posterior to the anterior hypothalamus (Hagemann and Scholpp, 2012).

We believe that mammillary–derived Wnt8b is likely mediating the patterning of the hypothalamus, which would be consistent with research in zebrafish (Kim et al., 2002; Lee et al., 2006). Surprisingly, *Wnt8b*$^{-/-}$ mice have no discernible defects in patterning in the diencephalon (Fotaki et al., 2010). It is likely that other Wnts are compensating for the loss of Wnt8b in these mutants, with the best candidate being Wnt8a, which is expressed in a very similar pattern to Wnt8b. However the authors of the paper only looked at three markers of the diencephalon, one of which was *Isl1*,

a gene which was ventralized in our β-catenin LOF mutants, but whose expression levels did not necessarily change.

Regardless of which Wnt is mediating the effects, the overall phenotypes in both β-catenin LOF mutants were consistent. All posterior markers tested were reduced, and all anterior markers tested were expanded into the posterior domain. We expected to see the complete opposite phenotype in the *Foxd1-Cre;Ctnnb1*$^{ex3/+}$ GOF mutant, i.e. a reduction in all anterior markers and an expansion of all posterior markers into the anterior domain, but this was not the case for the majority of markers tested. It appeared that in the case of the GOF mutant, the specification of individual genes within each nucleus had become uncoupled from one another and their broader nuclear fate. For example, while *Pitx2* and *Lhx5* were expanded in the mammillary, *Foxb1*, *Emx2*, and *Lhx1* were all reduced. Thus, each gene has differential requirements for, and interactions with, β-catenin and canonical Wnt signaling.

A good example of this is the Lim homeodomain family of transcription factors. *Lhx1* and *Lhx5* are known in zebrafish to inhibit Wnt signaling by inducing expression of the Wnt inhibitors sFRPs (Hagemann and Scholpp, 2012; Peng and Westerfield, 2006; Peukert et al., 2011). In *Lhx5* zebrafish morpholinos, the forebrain is significantly disrupted and Wnt8b is expanded into what remains of the forebrain (Peng and Westerfield, 2006). This is consistent with the loss or reduction of *Lhx1* in its various expression domains. However in *Lhx5*$^{-/-}$ mice, there are no gastrulation defects as observed in zebrafish, and in the case of our GOF mutants, *Lhx5* was

expanded in the mammillary, suggesting that the interactions between β-catenin and Lhx5 may differ across species. It may also be a reflection of the different developmental time points, as gastrulation occurs well before the patterning mechanisms described here. In the case of *Lhx9*, *Lef1* has been shown to be co-expressed with *Lhx9* in the mouse thalamus, and *Lhx9/Lhx2* double KO mice have a reduction in *Lef1* expression in the thalamus (Peukert et al., 2011). This is consistent with the expansion of Lhx9 observed in our GOF mutants. There appeared to be little effect on *Lhx9* in the *Foxd1-Cre;Ctnnb1*$^{lox/lox}$ LOF mutant, but this was not a complete knock-out of β-catenin, and it may not have been a significant enough reduction to affect *Lhx9* expression.

In the anterior hypothalamus, *Lhx1* was the only marker that was lost completely. Other markers were preserved, such as *Pomc* in the arcuate, *Fgf15* in the dorsal anterior hypothalamus, *Otp* in the ventral anterior hypothalamus, *Rax* in the PVN, *Wnt8b* in the anterior hypothalamus, and *Sim1* in the PVN. Markers of the PVN were not affected in either the LOF or GOF mutants, suggesting that this nucleus does not require canonical Wnt signaling for its development, and may not even be competent to respond to Wnt signaling, although this could be tested by using a reporter of Wnt-responsive cells. There is a small, local source of Wnt8b, and corresponding *Lef1* expression, in the anterior hypothalamus. This local source may have served to 'protect' the anterior markers in the GOF mutant, since they are capable of expression even under elevated basal levels of Wnt signaling. This would explain

why the only portion of *Isl1* expression remaining in the *Foxd1-Cre;Ctnnb1*$^{ex3/+}$ hypothalamus was in the anterior hypothalamus. However both *Pomc* and *Fgf15* showed disrupted, mosaic expression. This may simply be the result of mosaicism in *Foxd1-Cre* activity, as demonstrated by the patchy *Lef1* staining in the hypothalamus. If this were the case, then double staining between *Lef1* and *Pomc* or *Fgf15* should reveal no co-labeling. However, an alternative possibility is that the constitutively active β-catenin disrupted normal expression of adhesion molecules, preventing proper nuclear aggregation. Research in the thalamus has linked canonical Wnt signaling to control of *Pcdh10b* expression, and cells in the caudal and rostral thalamus intermingle when these areas express similar levels of *Pcdh10b* (Peukert et al., 2011).

A puzzling result in the *Foxd1-Cre;Ctnnb1*$^{lox/lox}$ LOF mutant was the clear thinning of the hypothalamic neuroepithelium, but without a concomitant decrease in proliferation or increase in apoptosis, as determined via EdU staining and TUNEL staining, respectively. It is possible that we simply did not look early enough; neurogenesis in the hypothalamus begins at approximately E10.5, and we may have observed an effect had we done an EdU pulse or TUNEL staining at that age. Another possible reason that we did not see a change in proliferation was that we counted cells within both the hypothalamus and prethalamus. The prethalamus was not affected in the LOF mutants, and by including it in the cell counts, we may have inadvertently masked a small but significant change in proliferation in the hypothalamus. Interestingly, early conditional *Rax* knock-out embryos also have a

significant thinning of the hypothalamus, but no concomitant decrease in proliferation or increase in TUNEL at E11.5, which the researchers were unable to explain (Orquera et al., 2016).

One of the main unanswered questions arising from our results is what becomes of the cells in the large *Lef1*-positive hypothalamic mass in the *Foxd1-Cre;Ctnnb1*$^{ex3/+}$ GOF mutant. Although there were several markers that were expanded (*Pitx2*, *Lhx5*, *Lhx9*, *Ntng2*), there were many parts of the hypothalamus that only expressed *Lef1* (which is a readout of constitutively active β-catenin, and not necessarily indicative of a premammillary fate change). Follow-up studies need to be performed to determine the fate of these cells, such as staining for *Sox2*, which is a marker of undifferentiated hypothalamic neurons, which would suggest that these cells are locked in an undifferentiated state. This would be consistent with other research which has shown that in some cases, cells which normally require canonical Wnt signaling for their specification must downregulate β-catenin before completing differentiation (Wrobel et al., 2007). For example in the midbrain, in the presence of constitutively active β-catenin, cells which have already been specified towards a dopaminergic fate are precluded from fully differentiating (Joksimovic et al., 2009). An alternative way to test this would be to look at expression of Wnt inhibitors as a potential negative feedback compensatory mechanism.

3.2.3 The Prethalamus and the Prosomere Model

We would have expected, were the prethalamus and hypothalamus patterned together as we hypothesized, that there would be a patterning defect within the prethalamus and potentially a fate switch between these two structures or within the prethalamus itself. This is not what we observed. The prethalamus was completely unaffected in both β-catenin LOF mutants, and was significantly disrupted in the β-catenin GOF mutant, but it was not a patterning defect per se. Rather, the prethalamus was reduced in size and maintained expression of some, but not all, region-specific markers.

The prethalamic markers which were lost -- *Isl1*, *Arx*, and *Lhx1* --, are all markers of GABAergic neurons, while the retained markers, *Fgf15* and *Gsh2*, are both neural progenitor markers. This suggests that in the presence of constitutively active β-catenin, the prethalamus was frozen in a partially undifferentiated state. This is in keeping with other research on prethalamic development, which has shown that the prethalamus must actively inhibit Wnt in order to be fully specified, in contrast to the thalamus, which requires Wnt signaling to prevent it from adopting a prethalamic fate (Bluske et al., 2012; Peng and Westerfield, 2006; Hagemann and Scholpp, 2012). This would also explain why the prethalamus fails to fully differentiate in the presence of constitutively active canonical Wnt signaling, and is not affected by the loss of β-catenin, even though it is in close apposition to a source of Wnt in the posterior hypothalamus.

The lack of a clear patterning phenotype in the prethalamus in any of the mutants we examined is inconsistent with our model of a single developmental unit comprising the hypothalamus and prethalamus. Such patterning changes in the prethalamus have been observed in other research, but only when signaling to the prethalamus was manipulated in the context of studies of thalamic development (Bluske et al., 2012). This would suggest that the prethalamus is being patterned in conjunction with the thalamus (in putative prosomere p2), which would also violate the prosomere model. However, in a study of brain diversity in cichlid fish, they observed coordinated changes in the relative sizes of the telencephalon and thalamus among three species according to their differing ecological needs, but the prethalamus and hypothalamus were identical in size across all species. The fish with a relatively larger thalamus showed elevated levels of posteriorizing Wnt1 signaling, while the fish with the larger telencephalon were more under the control of Six3 expressed in the anterior neuroectoderm (Sylvester et al., 2010). In this instance, the development of the thalamus and prethalamus have become uncoupled from one another, which would argue against a common developmental patterning mechanism for these two structures.

Although our results do not support our original theory of a common developmental unit comprising the prethalamus and hypothalamus, nor do they support the prosomere model. One of the stipulations of the prosomere model is that the telencephalon is located anterior to the hypothalamus in the so-called secondary

prosencephalon, so that the dorso-ventral axis of the prosomere model corresponds to the anterior-posterior axis in our model. The patterning changes that we observed in both of our β-catenin LOF mutants argues in favor of our rendering of the anterior-posterior axis. Wnt is expected to act as a posteriorizing factor, and the patterning shift we observed was entirely along the anterior-posterior axis, and there were no patterning shifts along the dorso-ventral axis. Our results do not fit into any one model of forebrain development, but they suggest a system of development that is much more complex than the prosomere model would suggest.

3.2.4 A Non-Cell Autonomous Effect on Pituitary Development

One of the more surprising results was the disruption of the pituitary in all three mutant lines examined. Normally, the anterior pituitary forms from the oral ectoderm and migrates to meet the posterior pituitary ventral to the hypothalamus. In both the *Nkx2.1-Cre;Ctnnb1*$^{lox/lox}$ and the *Foxd1-Cre;Ctnnb1*$^{lox/lox}$ LOF mutants the migrating pituitary appeared to have failed to receive any 'stop' signal and was invading the hypothalamus itself. In the *Foxd1-Cre;Ctnnb1*$^{ex3/+}$ GOF mutant, the opposite phenotype occurred. The pituitary failed to migrate at all, and remained stuck to the roof of the mouth. It also exhibited a fate change, as the *Pomc* and *Pitx2* expression domains were significantly expanded. The effects on pituitary development are non-cell autonomous as the *Foxd1-Cre* is not expressed in the pituitary. Rather, the effect

must have been mediated by changes in the hypothalamus, which secretes many important signaling molecules important for pituitary development, including Fgfs and Bmp7 (Potok et al., 2008). An apoptotic domain on the ventral side of Rathke's pouch is necessary for successful 'pinching off' from the oral ectoderm; this domain is most likely lacking in the GOF mutant, perhaps due to increased survival factors from the hypothalamus (Davis and Camper, 2007). Altered levels of noggin and Bmps may be mediating the expanded marker domains, as they are known to affect *Pomc* expression in the pituitary (Davis and Camper, 2007). More research needs to be done to determine the cause of the migratory defect in the LOF mutants and the precise cause of the fate shift in the GOF mutants.

3.2.5 Wnt and Shh May Cooperatively Pattern the Hypothalamus and Prethalamus

One danger in parsing out individual morphogens to look at their separate functions is that it risks missing important interactions between signaling pathways. Individual progenitor cells exist within a vast developmental milieu in which they are being influenced by cell-autonomous factors, patterning morphogens, as well as the developmental fates of their cellular neighbors, and each individual influencer can only affect an individual cell's fate decision in a probabilistic, rather than deterministic fashion (Muñoz Descalzo and Arias, 2012). Wnt may seek to drive an individual cell

toward a mammillary fate, for example, but its immediate neighbor may receive the same precise level of signal and adopt a premammillary fate instead. The formation of nuclear borders is just as important as the formation of the nuclear body itself, and becomes more important as networks begin to be established later in development. In this model, rather than Wnt driving expression of all posterior markers, and Shh driving expression of all anterior markers, Shh and Wnt actually work together to both specify and then refine development of hypothalamic nuclei. The hypothalamus is unique in the extreme complexity of its anatomy, and so this area may have coopted these morphogen systems to ensure not only that these areas are specified correctly, but that they are localized within the correct boundaries. Such a model is suggested by their expression patterns themselves, as Shh and Wnt are coexpressed in many of the same cells, particularly in the posterior hypothalamus, in contrast to the more typical arrangement seen in areas like the spinal cord, where they are expressed in opposition to each other on either side of the dorso-ventral axis of the neural tube (Yu et al., 2008; Alvarez-Medina et al., 2008).

A major complication in parsing out the potential interactions between Wnt and Shh signaling in the hypothalamus is that there is no developmental 'rule' governing such interactions: they seem to behave differently in different brain areas and at different times during development. For example, Wnt8b in the posterior hypothalamus has been shown to be required for the initiation of Shh signaling in the formation of the ZLI, by creating a permissive environment for Shh by inhibiting *Gli3*

expression (the main repressor of the Shh pathway) (Martinez-Ferre et al., 2013). In contrast, in the neural tube, dorsal Wnt acting via canonical signaling inhibits Shh through activation of *Gli3*, thereby restricting ventral fates to their proper domain and ensuring the correct patterning of the spinal cord (Alvarez-Medina et al., 2008). And in the midbrain, Wnt antagonism of Shh signaling is necessary for floor plate neurogenesis (Joksimovic et al., 2009; Joksimovic and Awatramani, 2014). Thus, depending on the timing and context, canonical Wnt signaling can function as a repressor or activator of Shh signaling. This may also reflect the varying competences of different neural tissue to respond to Wnt. β-catenin has no DNA binding domain, so its ability to affect transcription and chromatin conformation is entirely dependent on the transcriptional state of the cell (Valenta et al., 2012).

One clue as to the potential mode of interaction between Shh and Wnt was suggested by the surprising loss of *Foxb1* expression in the mammillary in the constitutively active β-catenin mouse (black arrowheads, Figure 9 G, H). Previous research had shown that in mouse, Shh is necessary for maintenance of Foxb1 expression in the mammillary, while Wnt signaling, potentially via Wnt8b, can inhibit its expression (Szabo et al., 2009). This runs counter to the model that Wnt is a strictly posteriorizing factor, but is consistent with our results, and explains them. It also helps to elucidate a puzzling find from another paper, in which loss of Shh signaling in the hypothalamus had a posteriorizing effect with the notable exception of the loss of *Foxb1* in the mammillary (Shimogori et al., 2010). Consistent with all of these

findings, there was a complete rescue of the *Foxb1* phenotype in our double *Foxd1-Cre;Ctnnb1*$^{ex3/+}$*;Smo*$^{CA/+}$ GOF mouse (Figure 16 O, P). However, there was no effect on *Foxb1* expression in the single Smo GOF mouse (Figure 16 C, D). This may be because in the case of *Foxb1* expression, Shh and Wnt are not inhibiting each other through direct pathway modulation, but rather Shh and Wnt have opposing effects on *Foxb1* transcriptional regulation. In other words, if Shh is not inhibiting the Wnt pathway directly, then excess Shh signaling cannot drive *Foxb1* expression beyond a certain point because of the continued presence of the inhibitory Wnt[4]. We suspect that any interactions between Shh and Wnt must be indirect, downstream interactions, since *Shh* expression was not affected in the β-catenin GOF mutant, and *Lef1* expression was not affected in the Smo GOF mutant.

An important caveat is that in both our single Smo GOF mouse and our double β-catenin/Smo GOF mouse, we were not able to directly confirm that the Shh pathway was indeed constitutively activated. This would be shown either through upregulation of the Shh co-receptor *Ptch*, or through its effector genes, *Gli1* or *Gli3*, which are analogous to *Lef1* in the canonical Wnt signaling pathway. However, in both mutants, there was a loss of retinal pigmented epithelium in the temporal half of the eye (where *Foxd1* is expressed) indicating that there was successful recombination in at least one brain area, although this does not guarantee successful recombination in

[4] There was also a loss of *Foxb1* expression in both β-catenin LOF mutants tested, but this is likely secondary to the overall reduced size of the posterior hypothalamus in these animals.

the hypothalamus. Further work needs to be done to confirm that we have achieved a true double Smo/β-catenin GOF mutant. However, if it is confirmed, it would represent a much more complete rescue than has been achieved previously in the diencephalon. In the thalamus, constitutively active β-catenin has a similarly disrupted patterning phenotype as reduced Shh signaling; both result in a fate switch in the rostral thalamus towards a more caudal thalamic fate. However double β-catenin/Shh LOF mutants have a similar phenotype as β-catenin single LOF embryos, with the exception of a single gene whose expression level and localization was restored to normal in the double mutant (Bluske et al., 2012).

3.2.6 Conclusion

Our research is a step towards better understanding of the patterning processes underlying the development of the hypothalamus. We have shown that canonical Wnt signaling is most likely acting as a general posteriorizing factor, however it is working within the environment of other signaling pathways, and is most likely coordinating its activity with theirs. Specifically, the Shh and canonical Wnt pathways are thought to be working downstream of each other in order to both pattern the hypothalamus and refine nuclear borders. Our results do not support a model in which the hypothalamus and prethalamus are being patterned together, nor do they support the prosomeric model of forebrain development. More research needs to be done both on the specific

mechanisms of Wnt regulation of hypothalamic patterning, and its potential interactions with other signaling pathways.

3.3 METHODS AND MATERIALS

3.3.1 Embryo Collection

Matings were set up in the evenings and the presence of a plug the next morning indicated embryonic day 0.5 (E0.5). Embryos were harvested at embryonic day 12.5 (E12.5). The lines used were as follows:

Nkx2.1-Cre (Brault et al., 2001)

Nkx2.1-cre$^{+/-}$*;Ctnnb1*$^{lox/+}$

Foxd1-Cre (Humphreys, et al. 2008)

Foxd1-Cre$^{+/-}$*;Ctnnb1*$^{lox/+}$

Ctnnb1$^{lox/lox}$ (Brault et al., 2001)

β-catenin-Ex3$^{f/f}$ (hereafter designated as *Ctnnb1*$^{ex3/\ ex3}$) (Harada *et al*, 1999)

Smo-W539L$^{f/f}$ (hereafter designated as *Smo*$^{CA/CA}$) (Jeong et al., 2004)

Ctnnb1$^{ex3/\ +}$;*Smo*$^{CA/+}$

The crosses set up were as follows:

Foxd1-Cre$^{+/-}$;*Ctnnb1*$^{lox/+}$x *Ctnnb1*$^{lox/lox}$

Foxd1-Cre$^{+/-}$ x *Ctnnb1*$^{ex3/ ex3}$

Foxd1-Cre$^{+/-}$ x *Smo*$^{CA/CA}$

Foxd1-Cre$^{+/-}$ x *Ctnnb1*$^{ex3/ +}$;*Smo*$^{CA/+}$

3.3.2 High-Quality Chromogenic *In situ* Hybridization

Pregnant dams were sacrificed via cervical dislocation and the embryos were harvested into ice-cold 1xPBS (phosphate buffered saline) treated with DEPC. Embryos were dissected (tail samples were kept for genotyping) and their whole heads fixed in 4% PFA (paraformaldehyde) in 1xPBS-DEPC while rotating at 4^0C. Following fixation, embryos were washed 2x5 min in 1x-PBS-DEPC then sucrose sunk in 30% sucrose in 1xPBS-DEPC at 4^0C for a minimum of one day. Embryos were then embedded in gelatin (10% gelatin with 30% sucrose in 1xPBS-DEPC). Following hardening of the gelatin, the blocks were cut and stored in 4% PFA; 30% sucrose in 1xPBS-DEPC for a minimum of one week at 4^0C to allow the blocks to sufficiently fix before sectioning. All steps after this point were done under RNAse-free conditions. The gelatin blocks were sectioned on a freezing microtome at 40μm thickness. Sections were collected

in 1xPBS-DEPC and stored at 4^{0}C until mounting (stored for a maximum of 4 hours). Sections were mounted in 0.5x PB-DEPC (phosphate buffer) onto Superfrost Plus slides (Fisher Scientific) and allowed to dry vertically for a minimum of overnight to a maximum of two days. Following drying, sections were immediately put through the first day of the high-quality *in situ* hybridization protocol. All washes were performed in 5-slide mailers that had been treated with 0.3M NaOH. Briefly, slides were fixed in 4% PFA in 1xPBS-DEPC for 15 minutes followed by 3x5 minute washes in 1xPBS-DEPC (all done at room temperature). Slides were then digested in a proteinase K solution (1μg/ml in 100mM Tris-HCl pH 8.0 and 50mM EDTA pH 8.0) at 37^{0}C for 30 minutes, followed by another fixation with 4% PFA in 1xPBS-DEPC for 15 minutes at room temperature. Slides were then washed in 1xPBS-DEPC (3x5 min). At this point, slides were either placed in hybridization buffer and stored at -20^{0}C or immediately placed in hybridization buffer with probe and hybridized. For each new probe, 70μl probe was added to 1mL of hybridization buffer and heated at 80^{0}C in order to denature them, then immediately placed on ice before adding to the mailer for a total volume of 14mL hybridization buffer (including probe). Mailers with fewer than 5 slides were given RNAse-free blank slides. Used probe/hybridization solution was stored at -20^{0}C and used multiple times, refreshing with 15μl probe when needed. Slides were hybridized at 70^{0}C overnight in a hybridization oven. After hybridization, RNAse-free conditions were no longer necessary. Slides were incubated in Solution X (50% formamide in 2x SSC and 1% SDS) 3x45 min at 70^{0}C. Slides were then

washed 3x15 min in 1xTBST (25.0 mM Tris-HCl pH7.5, .136 M NaCl, 2.68 mM KCl, 1% Tween-20) at room temperature then blocked in 10% lamb serum in 1xTBST at room temperature for 1 hr. Slides were then incubated in preabsorbed primary antibody (1:5000 anti-DIG a.p. fab fragments; protocol below) in 1% lamb serum and 1xTBST, overnight at 4^0C. Following antibody incubation, the slides were washed in 1xTBST 3x15 min, then 1x10 min in NTMT (100 mM NaCl, 100 mM Tris-HCl pH 9.5, 50 mM $MgCl_2$, 1% Tween-20, 2mM levamisole). The slides were then developed in the color reaction step in NTMT containing the chromogens 5-bromo, 4-chloro, 3-indolylphosphate (BCIP) and nitroblue tetrazolium (NBT), at either room temperature or 4^0C. The color reaction was stopped in TE stop buffer (10 mM Tris-HCl pH 7.5, 50 mM EDTA pH 8.0) for a minimum of 1 hr, followed by DAPI staining for 5 min (1:5000 in 1xPBS) then a 1xPBS wash for 5 min. Slides were coverslipped with gelvatol and allowed to dry overnight before imaging.

3.3.3 Preabsorbed Antibody

Age appropriate embryo powder (in this case E12.5 embryo powder made from wild-type embryo heads) was rehydrated in 1xTBST at 70^0C for 30 min, rotating. It was cooled on ice for 10 minutes, then the primary antibody was added as well as 1% lamb serum. It was then incubated at 4^0C for one hour, rotating. After allowing the solution

and embryo powder to settle, the supernatant containing the antibody was taken and added to a solution of 1xTBST and 1% lamb serum.

3.3.4 Low-Quality Chromogenic *In situ* Hybridization

Embryos were harvested fresh frozen and immediately embedded in OCT (Tissue-tek) and frozen on dry ice. Blocks were sectioned on the cryostat at 20μm thickness and immediately dry mounted onto Superfrost Plus slides. Slides were allowed to dry and then were stored at -80^{0}C. When ready to be used, the slides were allowed to thaw at room temperature a minimum of 30 min before beginning the protocol. The first day of the *in situ* hybridization was done under RNAse-free conditions, and all slide boxes and slide holders were soaked in 0.3M NaOH before use. All incubations were done at room temperature unless otherwise noted. Slides were fixed in 4% PFA in 1xPBS-DEPC for 10 min, then washed 3x 5 min in 1xPBS-DEPC. Slides were then incubated in acetic anhydride (.0027% in .1M TEA pH 8.0) for 10 min followed by another wash in 1xPBS-DEPC, 3x 5 min. Slides were then incubated in hybridization buffer for 2 hours prior to adding probe in hybridization buffer and coverslipping with siliconized coverslips. Slides were hybridized at 68^{0}C overnight. Probes were denatured at 80^{0}C for 5 minutes prior to hybridization. Hybridized slides were washed in 5x SSC at 65^{0}C for approximately 45 min until the coverslips could be removed

easily. Then the slides were washed in 0.2x SSC, 2x 45 min at 65^{0}C, followed by 1x 5 min at room temperature. Slides were then washed 1x 5 min in B1 buffer (.2M Tris-HCl pH 7.5, .3M NaCl) then blocked in 5% heat-inactivated sheep serum in B1 for 1 hour. Slides were incubated in primary antibody (1:5000 anti-DIG-AP. in 5% heat-inactivated in B1) overnight at 4^{0}C. Prior to developing, the slides were washed in B1 3x 5 min then 1x 5 min in B3 solution (.1 M Tris-HCl pH 9.5, .05 M $MgCl_2$, .1 M NaCl). The color reaction proceeded in B3 with BCIP and NBT with .24mg/mL levamisole) under dark conditions at either room temperature or 4^{0}C. The color reaction was extinguished in TE stop buffer (10 mM Tris-HCl pH 7.5, 50 mM EDTA pH 8.0). Slides were DAPI stained in 1:5000 DAPI in 1xPBS for 5 min, followed by a 1xPBS wash for 5 min before coverslipping with gelvatol. Slides were allowed to dry overnight before imaging.

3.3.5 Whole Mount *In Situ* Hybridization

All incubations were at room temperature unless otherwise noted, and performed in 24-well mesh plates. E9.0 and E10.0 wild-type embryos were harvested in cold 1xPBS-DEPC. E10 embryos were cut down the midline of the brain to allow for probe access. Embryos were fixed in 4% PFA in 1xPBS-DEPC for approximately one week. After fixation, the embryos were washed 2x15 min in PTw (1% Tween-20 in 1xPBS-

DEPC) then dehydrated with 25%, 50%, then 75% methanol in PTw for 15 min each then 100% methanol in PTw 3x15 min. Embryos were stored overnight at -20^{0}C, before they were rehydrated in reverse methanol washes, 75%, 50%, 25% methanol in PTw for 15 min each, followed by PTw 2x15 min. Embryos were then incubated in 6% hydrogen peroxide in PTw 60 min, followed by PTw wash 2x15 min. As these were young embryos (younger than E13.5) they then had 3x30 min incubations in detergent mix (1% Igepal CA-630, 1% SDS, 0.5% Na Deoxycholate, 50mM Tris-HCl pH 8.0, 1mM EDTA, 150 mM NaCl) followed by a 10 min PTw wash. Embryos were digested in 10µg/mL Proteinase K in PTw for 20 min, post-fixed in 0.2% glutaraldehyde, 4% PFA in PTw for 20 min, then washed in PTw 2x10 min. A prehybridization step followed, with room temperature hybridization buffer added to the embryos in sterile glass vials before incubating at 70^{0}C for one hour. Probe was added straight to the vials (25µl per 5 mL hybridization buffer) and embryos were hybridized overnight at 70^{0}C. Following hybridization, embryos were incubated in Solution X 4x45 min. At this point, the protocol is identical to the high-quality *in situ* hybridization protocol up to and including adding the antibody. Following antibody incubation, the embryos were washed in 1xTBST 3x10 min, 5x60 min, then overnight. Embryos were washed in NTMT 3x10 min then incubated in an NBT/BCIP color reaction solution at either room temperature or 4^{0}C. Embryos were washed in 1xTBST to remove the background signal, then the color reaction was stopped in TE buffer for a few hours. Embryos were immediately imaged on a dissecting scope.

3.3.6 Probes

Probes were generated using the following sequences as templates:

Probes	GenBank accession #
Arx	BE945936
Bsx	BC104386
Emx2	CB057818
Fgf15	BE952015
Foxa1	BC096524
Foxb1	BC111908
Foxg1	AW121918
Gsh2	AW491858
Irx5	AW492717
Isl1	AW125075
Lef1	BC038305
Lhx1	AI846049
Lhx5	BE943600
Lhx6	BC065077
Lhx9	AI854185
Nkx2.1	BC057607
Nr5a1	CD348290
Ntng2	AI850147
Otp	CA318525
Pitx2	BC075660
Pomc	AI849227
Rax	BC058757
Shh	BC063087
Sim1	Gift of C.M. Fan
Wnt8b	BC119544
Zfp312	AI852056

3.3.7 EdU Staining and Cell Counting

Pregnant dams were injected with 50 mg/kg Edu (20 mg/mL in saline) on embryonic day E12.5 and then sacrificed via cervical dislocation 2 hours later. The embryos were harvested in ice cold 1xPBS and the whole heads fixed in 4% PFA in 1xPBS at 4^0C overnight, rotating. The embryos were then washed 2x5 min in 1xPBS at 4^0C then sucrose sunk in 30% sucrose in 1xPBS and stored at 4^0C for a minimum of one day. Following cryoprotection, the embryos were embedded in OCT blocks on dry ice, then sectioned on a cryostat at 25μm thickness. Sections were immediately dry mounted onto Superfrost Plus slides and allowed to dry before storing at -20^0C. EdU staining was performed using the Click-iT EdU imaging kit from Invitrogen, then the slides were coverslipped using Vectashield. Stained slides were imaged at 40x on a Keyence microscope. Between 5 and 6 sections per animal were counted using ImageJ. All counting was done manually and blinded. The number of EdU-positive cells was taken as a fraction of the total area of the hypothalamus measured in μm^2. The values of the sections were averaged for each individual, and then compared using a 2-tailed t-test. Three animals per genotype were used.

3.3.8 TUNEL Staining

E12.5 embryos were harvested and post-fixed in 4% paraformaldehyde for a minimum of overnight at 4^0C. Slides were sucrose sunk in 30% sucrose in 1xPBS after 3x5 min 1xPBS washes. Following sucrose sinking, the embryos were embedded in OCT blocks on dry ice, and sectioned on a cryostat at 25μm thickness. Sections were immediately dry mounted onto Superfrost Plus slides and allowed to dry before storing at -20^0C. Slides were allowed to thaw to room temperature until beginning the protocol. TUNEL staining was performed according to the protocol for cryopreserved tissue in the *In Situ* Cell Death Detection Kit-TMR red (Roche). A positive control was used (3000 U/mL DNAse I). Slides were DAPI stained then coverslipped using Vectashield, then imaged at 20x and 40x in the red channel on a Keyence microscope.

3.3.9 MRI

MRI was performed on E12.5 wild-type and β-catenin GOF embryos. MRI data were acquired on a Bruker 11.7T spectrometer, using a 10mm volume transceiver coil. High angular resolution diffusion MRI data was acquired at the following parameters: field of view = 6x7x7.5mm, 35um isotropic resolution, 4 non-diffusion weighted, 30 diffusion directions, b-value of 1313 s/mm^2, and scan time of 34hrs.

4. REFERENCES

1. Abrahamson EE, Moore RY. Suprachiasmatic nucleus in the mouse: retinal innervation, intrinsic organization and efferent projections. *Brain Res* 2001, **916**: 172-191.
2. Acampora D, Postiglione MP, Avantaggiato V, Di Bonito M, Vaccarino FM, Michaud J, Simeone A. Progressive impairment of developing neuroendocrine cell lineages in the hypothalamus of mice lacking the Orthopedia gene. *Genes Dev* 1999, **13**: 2787-2800
3. Alvarez-Bolado G, Paul FA, Blaess S. Sonic hedgehog lineage in the mouse hypothalamus: from progenitor domains to hypothalamic regions. *Neural Dev* 2012, **7**:4.
4. Alvarez-Medina R, Cayuso J, Okubo T, Takada S, Martí E. Wnt canonical pathway restricts graded Shh/Gli patterning activity through the regulation of Gli3 expression. *Development* 2008, **135**: 237-247.
5. Aujla PK, Naratadam GT, Xu L, Raetzman LT. Notch/Rbpjκ signaling regulates progenitor maintenance and differentiation of hypothalamic arcuate neurons. *Development* 2013, **140**:3511–3521.

6. Beccari L, Marco-Ferreres R, Bovolenta P. The logic of gene regulatory networks in early vertebrate forebrain patterning. *Mech Dev* 2013, **130**:95–111.
7. Bedont J, Newman E, Blackshaw S. Patterning, specification, and differentiation in the developing hypothalamus. *Wiley Interdiscip Rev Dev Biol* 2015, **4**: 445-468
8. Bedont JL, LeGates TA, Slat EA, Byerly MS, Wang H, Hu J, Rupp AC, Qian J, Wong GW, Herzog ED, et al. Lhx1 controls terminal differentiation and circadian function of the suprachiasmatic nucleus. *Cell Rep* 2014, **7**:609–622.
9. Blackshaw S, Scholpp S, Placzek M, Ingraham H, Simerly R, Shimogori T. Molecular pathways controlling development of thalamus and hypothalamus: from neural specification to circuit formation. *J Neurosci* 2010, **30**:14925–14930.
10. Blechman J, Borodovsky N, Eisenberg M, Nabel-Rosen H, Grimm J, Levkowitz G. Specification of hypothalamic neurons by dual regulation of the homeodomain protein Orthopedia. *Development* 2007, **134**: 4417-4426.
11. Bluske KK, Vue TY, Kawakami Y, Taketo MM, Yoshikawa K, Johnson JE, Nakagawa Y. β-catenin signaling specifies progenitor cell identity in parallel with shh signaling in the developing mammalian thalamus. *Development* 2012, **139**: 2692-2702.
12. Borodovsky N, Ponomaryov T, Frenkel S, Levkowitz G. Neural protein Olig2 acts upstream of the transcriptional regulator Sim1 to specify diencephalic dopaminergic neurons. *Dev Dyn* 2009, **238**: 826-834.
13. Brault V, Moore R, Kutsch S, Ishibashi M, Rowitch DH, McMahon AP, Sommer L, Boussadia O, Kemler R. Inactivation of the beta-catenin gene by Wnt1-Cre mediated deletion results in dramatic brain malformation and failure of craniofacial development. *Development* 2001, **128**: 1253-1264.
14. Braun MM, Etheridge A, Bernard A, Robertson CP, Roelink H. Wnt signaling is required at distinct stages of development for the induction of the posterior forebrain. *Development* 2003, **130**:5579–5587.
15. Bulfone A, Smiga SM, Shimamura K, Peterson A, Puelles L, Rubenstein JL. T-brain-1: a homolog of Brachyura whose expression defines molecularly distinct domains within the cerebral cortex. *Neuron* 1995, **15**: 63-78.
16. Byerly MS, Blackshaw S. Vertebrate retina and hypothalamus development. *Wiley Interdiscip Rev Syst Biol Med* 2009, **1**: 380-389.

17. Byerly MS, Blackshaw S. Vertebrate retina and hypothalamus development. *WIREs Syst Biol Med* 2009, **1**:380–389.
18. Carreres MI, Escalante A, Murillo B, Chauvin G, Gaspar P, Vegar C, Herrera E. Transcription factor Foxd1 is required for the specification of the temporal retina in mammals. *J Neurosci* 2011, **31**: 5673-5681.
19. Chapman SC, Brown R, Lees L, Schoenwolf GC, Lumsden A. Expression analysis of chick Wnt and frizzled genes and selected inhibitors in early chick patterning. *Dev Dyn* 2004, **229**:668–676.
20. Chatterjee M, Li JY. Patterning and compartment formation in the diencephalon. *Front Neurosci* 2012, **6**:66.
21. Chiang C, Litingtung Y, Lee E, Young KE, Corden JL, Westphal H, Beachy PA. Cyclopia and defective axial patterning in mice lacking Sonic hedgehog gene function. *Nature* 1996, **383**:407–413.
22. Clark DD, Gorman MR, Hatori M, Meadows JD, Panda S, Mellon PL. Aberrant development of the suprachiasmatic nucleus and circadian rhythms in mice lacking the homeodomain protein Six6. *J Biol Rhythms* 2013, **28**: 15–25.
23. Clements W, Ong K, Traver D. Zebrafish wnt3 is expressed in developing neural tissue. *Dev Dyn* 2009, **238**: 1788-1795.
24. Dalal J, Roh JH, Maloney SE, Akuffo A, Shah S, Yuan H, Wamsley B, Jones WB, Strong C, Gray PA, et al. Translational profiling of hypocretin neurons identifies candidate molecules for sleep regulation. *Genes Dev*2013, **27**:565–578.
25. Dale JK, Vesque C, Lints TJ, Sampath TK, Furley A, Dodd J, Placzek M. Cooperation of BMP7 and SHH in the induction of forebrain ventral midline cells by prechordal mesoderm. *Cell* 1997, **90**:257–269.
26. Dale K, Sattar N, Heemskerk J, Clarke JDW, Placzek M, Dodd J. Differential patterning of ventral midline cells by axial mesoderm is regulated by BMP7 and chordin. *Development* 1999, **126**:397–408.
27. Davis SW, Camper SA. Noggin regulates Bmp4 activity during pituitary induction. *Dev Biol* 2007, **305**: 145-160.
28. Dorsky RI, Itoh M, Moon RT, Chitnis A. Two *tcf3* genes cooperate to pattern the zebrafish brain. *Development* 2003, **130**: 1937-1947.
29. Erter CE, Wilm TP, Basler N, Wright CV, Solnica-Krezel L. Wnt8 is required in lateral mesendodermal precursors for neural posteriorization in vivo. *Development* 2001, **128**:3571–3583.

30. Fan M, Tessier-Lavigne M. Patterning of mammalian somites by surface ectoderm and notochord: evidence for sclerotome induction by a hedgehog homolog. *Cell* 1994, **79**: 1175-1186.
31. Ferran JL, Puelles L, Rubenstein JL. Molecular codes defining rostrocaudal domains in the embryonic mouse hypothalamus. *Front Neuroanat* 2015, **9**: 46.
32. Fotaki V, Larralde O, Zeng S, McLaughlin D, Nichols J, Price DJ, Theil T, Mason JO. Loss of *Wnt8b* has no overt effect on hippocampus development but leads to altered *Wnt* gene expression levels in dorsomedial telencephalon. *Dev Dyn* 2010, **239**: 284-296
33. Freese JL, Pino D, Pleasure SJ. Wnt signaling in development and disease. *Neurobiol Dis* 2010, **38**: 148-153.
34. Garda AL, Puelles L, Rubenstein JL, Medina L. Expression patterns of Wnt8b and Wnt7b in the chicken embryonic brain suggest a correlation with forebrain patterning centers and morphogenesis. *Neuroscience*2002, **113**:689–698.
35. Gaston-Massuet C, McCabe MJ, Scagliotti V, Young RM, Carreno G, Gregory LC, Jayakody SA, Pozzi S, Gualtieri A, Basu B, et al. Transcription factor 7-like 1 is involved in hypothalamo-pituitary axis development in mice and humans. *Proc Natl Acad Sci USA* 2016, **2**: E548-557.
36. Geng X, Speirs C, Lagutin O, Inbal A, Liu W, Solnica-Krezel L, Jeong Y, Epstein DJ, Oliver G. Haploinsufficiency of Six3 fails to activate Sonic hedgehog expression in the ventral forebrain and causes holoprosencephaly. *Dev Cell* 2008, **15**:236–247.
37. Goshu E, Jin H, Lovejoy J, Marion JF, Michaud JL, Fan CM. Sim2 contributes to neuroendocrine hormone gene expression in the anterior hypothalamus. *Mol Endocrinol* 2004, **18**: 1251-1262.
38. Gulacsi AA, Anderson SA. β-catenin-mediated wnt signaling regulates neurogenesis in the ventral telencephalon. *Nat Neurosci* 2008, **11**: 1383-1391.
39. Hagemann AI, Kurz J, Kauffeld S, Chen Q, Reeves PM, Weber S, Schindler S, Davidson G, Kirchhausen T, Scholpp S. In vivo analysis of formation and endocytosis of the Wnt/ß-catenin signaling complex in zebrafish embryos. *J Cell Sci* 2014, **127**: 3970-3982
40. Hagemann AI, Scholpp S. The tale of the three brothers—Shh, Wnt, and Fgf during development of the thalamus. *Front Neurosci* 2012, **6**: 76
41. Hatini V, Tao W, Lai E. Expression of winged helix genes, BF-1 and BF-2, define adjacent domains within the developing forebrain and retina. *J Neurobiol* 1994, **25**:1293–1309.

42. Hoch RV, Rubenstein JL, Pleasure S. Genes and signaling events that establish regional patterning of the mammalian forebrain. *Semin Cell Dev Biol* 2009, **20**:378–386.
43. Hosoya T, Oda Y, Takahashi S, Morita M, Kawauchi S, Ema M, Yamamoto M, Fujii-Kuriyama Y. Defective development of secretory neurons in the hypothalamus of Arnt2-knockout mice. *Genes Cells* 2001, **6**: 361-374.
44. http://www.brain-map.org/
45. Humphreys BD, Valerius MT, Kobayashi A, Mugford JW, Soeung S, Duffield JS, McMahon AP, Bonventre JV. Intrinsic epithelial cells repair the kidney after injury. *Cell Stem Cell* 2008, **2**: 284-291.
46. Ishibashi M, McMahon AP. A Sonic hedgehog-dependent signaling relay regulates growth of diencephalic and mesencephalic primordia in the early mouse embryo. *Development* 2002, **129**:4807–4819.
47. Jeong J, Mao J, Tenzen T, Kottmann AH, McMahon AP. Hedgehog signaling in the neural crest cells regulates the patterning and growth of facial primordia. *Genes Dev* 2004, **18**: 937-951.
48. Jeong Y, Leskow FC, El-Jaick K, Roessler E, Muenke M, Yocum A, Dubourg C, Li X, Geng X, Oliver G, et al. Regulation of a remote Shh forebrain enhancer by the Six3 homeoprotein. *Nat Genet* 2008, **40**:1348–1353.
49. Joksimovic M, Awatramani R. Wnt/β-catenin signaling in midbrain dopaminergic neuron specification and neurogenesis. *J Mol Cell Biol* 2014, **6**: 27-33.
50. Kapsimali M, Caneparo L, Houart C, Wilson SW. Inhibition of Wnt/Axin/β-catenin pathway activity promotes ventral CNS midline tissue to adopt hypothalamic rather than floorplate identity. *Development* 2004, **131**:5923–5933.
51. Kim SH, Shin J, Park HC, Yeo SY, Hong SK, Han S, Rhee M, Kim CH, Chitnis AB, Huh TL. Specification of an anterior neuroectoderm patterning by Frizzled8a-mediated Wnt8b signalling during late gastrulation in zebrafish. *Development* 2002, **129**:4443–4455.
52. Kobayashi D, Kobayashi M, Matsumoto K, Ogura T, Nakafuku M, Shimamura K. Early subdivisions in the neural plate define distinct competence for inductive signals. *Development* 2002, **129**:83–93.
53. Lagutin OV, Zhu CC, Kobayashi D, Topczewski J, Shimamura K, Puelles L, Russell HR, McKinnon PJ, Solnica-Krezel L, Oliver G. Six3 repression of

Wnt signaling in the anterior neuroectoderm is essential for vertebrate forebrain development. *Genes Dev* 2003, **17**:368–379.

54. Lee JE, Wu S, Goering LM, Dorsky RI. Canonical wnt signaling through Lef1 is required for hypothalamic neurogenesis. *Development* 2004, **133**: 4451-4461
55. Lee JE, Wu SF, Goering LM, Dorsky RI. Canonical Wnt signaling through Lef1 is required for hypothalamic neurogenesis. *Development* 2006, **133**:4451–4461.
56. Logan CY, Nusse R. The wnt signaling pathway in development and disease. *Ann Rev Cell Dev Biol* 2004, **20**: 781-810.
57. Lu F, Kar D, Gruenig N, Zhang ZW, Cousins N, Rodgers HM, Swindell EC, Jamrich M, Schuurmans C, Mathers PH, et al. Rax is a selector gene for mediobasal hypothalamic cell types. *J Neurosci* 2013, **33**:259–272.
58. Machluf Y, Gutnick A, Levkowitz G. Development of the zebrafish hypothalamus. *Ann N Y Acad Sci* 2011, **1220**:93–105.
59. Manning L, Ohyama K, Saeger B, Hatano O, Wilson SA, Logan M, Placzek M. Regional morphogenesis in the hypothalamus: a BMP-Tbx2 pathway coordinates fate and proliferation through Shh downregulation. *Dev Cell*2006, **11**:873–885.
60. Markakis EA, Swanson LW. Spatiotemporal patterns of secretomotor neuron generation in the parvicellular neuroendocrine system. *Brain Res Rev* 1997, **24**:255–291.
61. Martinez-Ferre A, Navarro-Garberi M, Bueno C, Martinez S. Wnt signal specifies the intrathalamic limit and its organizer properties by regulating Shh inducation in the alar plate. *J Neurosci* 2013, **33**: 3967-3980.
62. Mathieu J, Barth A, Rosa FM, Wilson SW, Peyrieras N. Distinct and cooperative roles for Nodal and Hedgehog signals during hypothalamic development. *Development* 2002, **129**:3055–3065.
63. Michaud JL, Rosenquist T, May NR, Fan CM. Development of neuroendocrine lineages requires the bHLH-PAS transcription factor SIM1. *Genes Dev* 1998, **12**: 3264-3275.
64. Muñoz Descalzo S, Martinez Arias A. The structure of Wntch signalling and the resolution of transition states in development. *Semin Cell Dev Biol* 2012, **23**: 443-449.
65. Nakai S, Kawano H, Yudate T, Nishi M, Kuno J, Nagata A, Jishage K, Hamada H, Fujii H, Kawamura K. The POU domain transcription factor

Brn-2 is required for the determination of specific neuronal lineages in the hypothalamus of the mouse. *Genes Dev* 1995, **9**: 3109-3121.

66. Ohyama K, Das R, Placzek M. Temporal progression of hypothalamic patterning by a dual action of BMP. *Development* 2008, **135**:3325–3331.
67. Oliver G, Mailhos A, Wehr R, Copeland NG, Jenkins NA, Gruss P. Six3, a murine homologue of the sine oculis gene, demarcates the most anterior border of the developing neural plate and is expressed during eye development. *Development* 1995, **121**: 4045-4055.
68. Orquera DP, Nasif S, Low MJ, Rubinstein M, de Souza F. Essential function of the transcription factor Rax in the early patterning of the mammalian hypothalamus. *Dev Biol* 2016, **416**: 212-224.
69. Padilla SL, Carmody JS, Zeltser LM. Pomc-expressing progenitors give rise to antagonistic neuronal populations in hypothalamic feeding circuits. *Nat Med* 2010, **16**:403–405.
70. Peng G, Westerfield M. Lhx5 promotes forebrain development and activates transcription of secreted Wnt antagonists. *Development* 2006, **133**: 3191-3200.
71. Peukert D, Weber S, Lumsden A, Scholpp S. Lhx2 and Lhx9 determine neuronal differentiation and compartition in the caudal forebrain by regulating Wnt signaling. *PLoS Biol* 2011, **9**: e1001218.
72. Pierrou S, Hellqvist M, Samuelsson L, Enerbäck S, Carlsson P. Cloning and characterization of seven human forkhead proteins: binding site specificity and DNA bending. *EMBO J* 1994, **13**: 5002-5012.
73. Potok MA, Cha KB, Hunt A, Brinkmeier ML, Leitges M, Kispert A, Camper SA. WNT signaling affects gene expression in the ventral diencephalon and pituitary gland growth. *Dev Dyn* 2008, **237**: 1006-1020.
74. Puelles L, Kuwana E, Puelles E, Bulfone A, Shimamura K, Keleher J, Smiga S, Rubenstein JL. Pallial and subpallial derivatives in the embryonic chick and mouse telencephalon, traced by the expression of the genes Dlx-2, Emx-1, Nkx-2.1, Pax-6, and Tbr-1. *J Comp Neurol* 2000, **424**: 409-438.
75. Puelles L, Rubenstein JL. Expression patterns of homeobox and other putative regulatory genes in the embryonic mouse forebrain suggest a neuromeric organization. *Trends Neurosci* 1993, **16**: 472-479
76. Puelles L, Rubenstein JL. Forebrain gene expression domains and the evolving prosomeric model. *Trends Neurosci* 2003, **26**:469–476.
77. Ratié L, Ware M, Barloy-Hubler F, Rome H, Gicquel I, Dubourg C, David V, Dupe V. Novel genes upregulated when NOTCH signalling is disrupted during hypothalamic development. *Neural Dev* 2013, **8**:25.31

78. Rohr KB, Barth KA, Varga ZM, Wilson SW. The nodal pathway acts upstream of hedgehog signaling to specify ventral telencephalic identity. *Neuron* 2001, **29**: 341-351.
79. Rohr KB, Barth KA, Varga ZM, Wilson SW. The nodal pathway acts upstream of hedgehog signaling to specify ventral telencephalic identity. *Neuron* 2001, **29**:341–351.
80. Roy A, de Melo J, Chaturvedi D, Thein T, Cabrera-Socorro A, Houart C, Meyer G, Blackshaw S, Tole S. LHX2 is necessary for the maintenance of optic identity and for the progression of optic morphogenesis. *J Neurosci* 2013, **33**:6877–6884.
81. Rubenstein JL, Martinez S, Shimamura K, Puelles L. The embryonic vertebrate forebrain: the prosomeric model. *Science* 1994, **266**: 578-580.
82. Ryu S, Mahler J, Acampora D, Holzschuh J, Erhardt S, Omodei D, Simeone A, Driever W. Orthopedia homeodomain protein is essential for diencephalic dopaminergic neuron development. *Curr Biol* 2007, **17**: 873-880.
83. Salvatierra J, Lee DA, Zibetti C, Duran-Moreno M, Yoo S, Newman EA, Wang H, Bedont JL, deMelo J, Miranda-Angulo AL, Gil-Perotin S, Garcia-Verdugo JM, Blackshaw S. The LIM homeodomain factor Lhx2 is required for hypothalamic tanycyte specification and differentiation. *J Neurosci* 2014, **10**: 16809-16820.
84. Scholpp S, Wolf O, Brand M, Lumsden A. Hedgehog signalling from the zona limitans intrathalamica orchestrates patterning of the zebrafish diencephalon. *Development* 2006, **133**:855–864.
85. Schonemann MD, Ryan AK, McEvilly RJ, O'Connell SM, Arias CA, Kalla KA, Li P, Sawchenko PE, Rosenfeld MG. Development and survival of the endocrine hypothalamus and posterior pituitary gland requires the neuronal POU domain factor Brn-2. *Genes Dev* 1995, **9**: 3122-3135.
86. Shimada M, Nakamura T. Time of neuron origin in mouse hypothalamic nuclei. *Exp Neurol* 1973, **41**:163–173.
87. Shimogori T, Lee DA, Miranda-Angulo A, Yang Y, Wang H, Jiang L, Yoshida AC, Kataoka A, Mashiko H, Avetisyan M, et al. A genomic atlas of mouse hypothalamic development. *Nat Neurosci* 2010, **13**:767–775.
88. Shinya M, Eschbach C, Clark M, Lehrach H, Furutani-Seiki M. Zebrafish Dkk1, induced by the pre-MBT Wnt signaling, is secreted from the prechordal plate and patterns the anterior neural plate. *Mech Dev* 2000, **98**: 3-17.

89. Siegenthaler JA, Tremper-Wells BS, Miller MW. Foxg1 haploinsufficiency reduces the population of cortical intermediate progenitor cells: effect of increased p21 expression. *Cereb Cortex* 2008, **18**: 1865-1875.
90. Sylvester JB, Rich CA, Loh YH, van Staaden MH, Fraser GJ, Streelman JT. Brain diversity evolves via differences in patterning. *Proc Natl Acad Sci USA* 2010, **107**: 9718-9723.
91. Szabo NE, Zhao T, Cankaya M, Theil T, Zhou X, Alvarez-Bolado G. Role of neuroepithelial Sonic hedgehog in hypothalamic patterning. *J Neurosci* 2009, **29**:6989–7002.
92. Valenta T, Hausmann G, Basler K. The many faces and functions of β-catenin. *EMBO J* 2012, **31**: 2714-2736.
93. VanDunk C, Hunter LA, Gray PA. Development, maturation, and necessity of transcription factors in the mouse suprachiasmatic nucleus. *J Neurosci* 2011, **31**:6457–6467.
94. Vieira C, Martinez S. Sonic hedgehog from the basal plate and the zona limitans intrathalamica exhibits differential activity on diencephalic molecular regionalization and nuclear structure. *Neuroscience* 2006, **143**:129–140.
95. Vieira C, Pombero A, Garcia-Lopez R, Gimeno L, Echevarria D, Martinez S. Molecular mechanisms controlling brain development: an overview of neuroepithelial secondary organizers. *Int J Dev Biol* 2010, **54**:7–20.
96. Virolainen S, Achim K, Peltopuro P, Salminen M, Partanen J. Transcriptional regulatory mechanisms underlying the gabaergic neuron fate in different diencephalic prosomeres. *Development* 2012, **139**: 3795-3805.
97. Wang W, Lufkin T. The murine Otp homeobox gene plays an essential role in the specification of neuronal cell lineages in the developing hypothalamus. *Dev Biol* 2000, **227**: 432-449.
98. Wang X, Kopinke D, Lin J, McPherson AD, Duncan RN, Otsuna H, Moro E, Hoshijima K, Grunwald DJ, Argenton F, Chien C, Murtaugh LC, Dorsky RI. Wnt signaling regulates postembryonic hypothalamic progenitor differentiation. *Cell* 2012, **23**: 624-636.
99. Wang X, Lee JE, Dorsky RI. Identification of wnt-responsive cells in the zebrafish hypothalamus. *Zebrafish* 2009, **6**: 49-58.
100. Wang X, Lee JE, Dorsky RI. Identification of Wnt-responsive cells in the zebrafish hypothalamus. *Zebrafish* 2009, **6**:49–58.
101. Wilson SW, Houart C. Early steps in the development of the forebrain. *Dev Cell* 2004, **6**:167–181.

102. Wrobel CN, Mutch CA, Swaminathan S, Taketo MM, Chenn A. Persistent expression of stabilized beta-catenin delays maturation of radial glial cells into intermediate progenitors. *Dev Biol* 2007, **309**: 285-297.
103. Yu W, McDonnell K, Taketo MM, Bai CB. Wnt signaling determines ventral spinal cord fates in a time-dependent manner. *Development* 2008, **135**: 3687-3696
104. Zeltser M. Shh-dependent formation of the ZLI is opposed by signals from the dorsal diencephalon. *Development* 2005, **132**:2023–2033.
105. Zhang K, Zhang L, Rao F, Brar B, Rodriguez-Flores JL, Taupenot L, O'Connor DT. Human tyrosine hydroxylase natural genetic variation: delineation of functional transcriptional control motifs disrupted in the proximal promoter. *Circ Cardiovasc Genet* 2010, **3**: 187-198.
106. Zhao L, Zevallos SE, Rizzoti K, Jeong Y, Lovell-Badge R, Epstein DJ. Disruption of SoxB1-dependent Sonic hedgehog expression in the hypothalamus causes septo-optic dysplasia. *Dev Cell* 2012, **22**:585–596.

5. BIOGRAPHY

Elizabeth A. Newman was born and raised in Westchester County, New York. She attended Amherst College, in Amherst, MA, where she majored in neuroscience and graduated cum laude in 2009. While at Amherst, she was a laboratory teaching assistant for introductory biology, and was a summer research intern at the Weill Medical College at Burke Rehabilitation Center (summer 2006) and at the University of Alabama at Birmingham (summer 2007). She completed an honors thesis in neuroscience titled, "The Role of GluR2/3-Containing AMPA Receptors in the Plasticity of Horizontal Optokinetic Nystagmus in the Frog (*Rana pipiens*)." After graduating from Amherst, she spent a year at the National Institutes of Health in Bethesda, MD, as part of their Intramural Research Training Award program, in the Laboratory of Mammalian Genes and Development (August 2009-August 2010), where she studied hypothalamic development. Elizabeth began her PhD in neuroscience in the

laboratory of Seth Blackshaw in September, 2010 at Johns Hopkins University. She was a teaching assistant for Neuroscience and Cognition I, and was a member of a student outreach group, Project Bridge.

5.1.1 Publications:

- Howard, K.L., Hall, D.A., Moon, M., Agarwal, P., Newman, E., and Brenner, M. Adult-onset Alexander Disease with Progressive Ataxia and Palatal Tremor, *Movement Disorders* 2008, **23**: 118-122.
- Salvatierra J, Lee DA, Zibetti C, Duran-Moreno M, Yoo S, Newman EA, Wang H, Bedont JL, de Melo J, Miranda-Angulo AL, Gil-Perotin S, Garcia-Verudgo JM, Blackshaw S. *J Neurosci* 2014, **34**: 16809-16820.
- Bedont JL*, Newman EA*, Blackshaw S. Patterning, specification and differentiation in the developing hypothalamus. *Wiley Interdiscip Rev Dev Biol* 2015, **4**: 445-468.